

TISSUE ENGINEERING OF FULL-THICKNESS HUMAN ORAL MUCOSA

A THESIS SUBMITTED TO
ECOLE DOCTORALE INTERDISCIPLINAIRE SCIENCES-SANTE
OF
UNIVERSITE DE LYON
AND
THE GRADUATE SCHOOL OF NATURAL AND APPLIED SCIENCES
OF
MIDDLE EAST TECHNICAL UNIVERSITY

BY

BESTE KINIKOGLU

IN PARTIAL FULFILLMENT OF THE REQUIREMENTS FOR
THE DEGREE OF DOCTEUR
IN
TISSUE ENGINEERING AND CELL BIOLOGY
AND
THE DEGREE OF DOCTOR OF PHILOSOPHY
IN
BIOTECHNOLOGY

DECEMBER 2010

Approval of the thesis:

TISSUE ENGINEERING OF FULL-THICKNESS HUMAN ORAL MUCOSA

submitted by **F. BESTE KINIKOGLU** in partial fulfillment of the requirements for the Degree of **Doctor of Philosophy in Biotechnology Department, Middle East Technical University** by,

Prof. Dr. Canan ÖZGEN
Dean, Graduate School of **Natural and Applied Sciences**

Prof. Dr. İnci EROĞLU
Head of Department, **Biotechnology**

Dr. Odile DAMOUR
Supervisor, **EDISS, Université Lyon I**

Prof. Dr. Vasif HASIRCI
Supervisor, **Biological Sciences Dept., METU**

Examining Committee Members:

Prof. Dr. Pierre BRETON (Head of the Committee)
Hospices Civils de Lyon, Université Lyon I

Dr. Odile DAMOUR
Hospices Civils de Lyon, EDISS

Prof. Dr. Vasif HASIRCI
Biological Sciences Dept., METU

Prof. Dr. Gülay ÖZCENGİZ
Biological Sciences Dept., METU

Assoc. Prof. Dr. İhsan GÜRSEL (Reviewer)
Molecular Biology and Genetics Dept., Bilkent University

Dr. Sylvie SAUVAIGO (Reviewer)
CEA, Université Joseph Fourier Grenoble

Date: 17. 12. 2010

I hereby declare that all information in this document has been obtained and presented in accordance with academic rules and ethical conduct. I also declare that, as required by these rules and conduct, I have fully cited and referenced all material and results that are not original to this work.

Name, Last name : Beste KINIKOGLU

Signature :

ABSTRACT

TISSUE ENGINEERING OF FULL-THICKNESS HUMAN ORAL MUCOSA

Kımkıođlu, Beste

Ph.D., Ecole Doctorale Interdisciplinaire Sciences-Santé (Université de Lyon)

Ph.D., Department of Biotechnology (METU)

Supervisor: Dr. Odile Damour

Supervisor: Prof. Dr. Vasıf Hasırcı

December 2010, 92 pages

Tissue engineered human oral mucosa has the potential to fill tissue deficits caused by facial trauma or malignant lesion surgery. It can also help elucidate the biology of oral mucosa and serve as an alternative to *in vivo* testing of oral care products. The aim of this thesis was to construct a tissue engineered full-thickness human oral mucosa closely mimicking the native tissue. To this end, the feasibility of the concept was tested by co-culturing fibroblasts and epithelial cells isolated from normal human oral mucosa biopsies in a collagen-glycosaminoglycan-chitosan scaffold, developed in our laboratory to construct a skin equivalent. An oral mucosal equivalent closely mimicking the native one was obtained and characterized by histology, immunohistochemistry and transmission electron microscopy. Using the same model, the influence of mesenchymal cells on oral epithelial development was investigated by culturing epithelial cells on lamina propria, corneal stroma and dermal equivalents. They were found to significantly influence the thickness and the ultrastructure of the epithelium. Finally, in order to improve the adhesiveness of conventional scaffolds, an elastin-like recombinamer (ELR) containing the cell adhesion tripeptide, RGD, was used in the production of novel bilayer scaffolds

employing lyophilization and electrospinning. These scaffolds were characterized by mercury porosimetry, scanning electron microscopy and mechanical testing. *In vitro* tests revealed positive contribution of ELR on the proliferation of both fibroblasts and epithelial cells. It was thus possible to construct a viable oral mucosa equivalent using the principles of tissue engineering.

Keywords: Oral Mucosa Engineering, Epithelial Development, Cell Interactions, Collagen Scaffold, Elastin-like Recombinamer

RESUME

INGENIERIE TISSULAIRE DE LA MUQUEUSE ORALE HUMAINE

Kımıkođlu, Beste

Ph.D., Ecole Doctorale Interdisciplinaire Sciences-Santé (Université de Lyon)

Ph.D., Department of Biotechnology (METU)

Superviseur: Dr. Odile Damour

Superviseur: Prof. Dr. Vasıf Hasırcı

Décembre 2010, 92 pages

L'ingénierie de la muqueuse orale humaine (MOH) a pour but le comblement des pertes de substances suite à un traumatisme facial ou à la chirurgie des lésions malignes. Elle a aussi des applications en recherche pour élucider les mécanismes biologiques de la MO et en pharmacotoxicologie comme alternative à l'expérimentation animale. L'objectif de cette thèse était de reconstruire une MOH proche du tissu normal. À cette fin, la faisabilité du concept a d'abord été testée par co-culture de fibroblastes de la lamina propria et de cellules épithéliales de MOH dans le substrat de collagène-chitosan glycosaminoglycane, développé pour la production de peaux reconstruites. La caractérisation de la MOH reconstruite par histologie, immunohistochimie et microscopie électronique à transmission a montré la présence d'une LP équivalente avec un épithélium pluristratifié et non kératinisé très proche du tissu d'origine. Grâce à ce modèle, nous avons ensuite démontré que l'origine des fibroblastes (MO, cornée, peau) influence significativement l'épaisseur et l'ultrastructure de l'épithélium obtenu par culture de cellules épithéliales orales. Enfin, afin d'améliorer les propriétés adhésives du substrat à base collagène, nous avons ajouté au collagène, une élastine-like recombinante (ELR) contenant le tri-

peptide d'adhésion cellulaire, RGD, et produit un nouveau substrat bicouche, poreux par lyophilisation et recouvert d'une couche fibreuse par électrofilage. Ces substrats ont été caractérisés par porosimétrie au mercure, microscopie électronique à balayage et essais mécaniques. Nous avons démontré l'effet stimulant de ELR sur la prolifération des fibroblastes et des cellules épithéliales.

Mots-clés: Ingénierie de la Muqueuse Orale, Développement Epithélial, Interactions Cellulaires, Collagène Substrat, Elastin-like Recombinante

Discipline: Tissue Engineering and Cell Biology

Intitulés et adresses des laboratoires:

- Laboratoire des Substituts Cutanés – UMR 5086/IBCP. Hôpital Edouard Herriot – 69437 Lyon cedex 03, France
- Biotechnology Research Unit, METU, 06531 Ankara, Turkey

ÖZ

TAM KALINLIKLI YAPAY İNSAN AĞIZ MUKOZASI GELİŞTİRİLMESİ

Kımkıođlu, Beste

Ph.D., Ecole Doctorale Interdisciplinaire Sciences-Santé (Université de Lyon)

Ph.D., Biyoteknoloji Bölümü (ODTÜ)

Tez Yöneticisi: Dr. Odile Damour

Tez Yöneticisi: Prof. Dr. Vasıf Hasırcı

Aralık 2010, 92 sayfa

Doku mühendisliđi ürünü insan ađız mukozası, yüz travması ya da kanser dokusuna yönelik cerrahi işlemler sonucunda oluşan doku kayıplarını telafi etme olanađı sağlayabilecektir. Bu yapay ađız mukozası aynı zamanda ađız mukozası biyolojisini biraz daha öğrenmek için olduđu gibi ađız sađlıđı ürünlerinin *in vivo* testlerinin yerine de kullanılabilir. Bu çalışmanın amacı dođal ađız mukozasına çok yakın özellikler taşıyan bir tam kalınlıklı yapay insan ađız mukozası geliştirmektir. Bu amaç dođrultusunda öncelikle bunun yapılabirliđini sınamak amacıyla, insan ađız mukozası biyopsilerinden elde edilmiş fibroblastlar ve epitel hücreler laboratuvarımızda yapay deri yapımı için geliştirilmiş olan bir kollajen-glikozaminoglikan-kitozan doku iskelesi içinde yetiştirilmişlerdir. Histoloji, immunohistoloji ve geçirimli elektron mikroskopisi (TEM) sonuçları dođala çok benzeyen bir yapay ađız mukozasının elde edilebildiđini göstermiştir. Bunun üzerine bu model, mezenkim dokunun ađız epitelyumunun gelişimine etkisini araştırmada kullanılmıştır. Bunun için yapay lamina propria, yapay dermis ve yapay kornea stromaları oluşturulmuş ve ađız epitel hücreleri bunların üzerinde yetiştirilmişlerdir. Oluşan epitel dokuların analizleri sonucunda mezenkim hücre kaynađının

epitelyumun kalınlığına ve ultrastrüktürüne belirgin bir etkisi olduđu gözlemlenmiştir. Son olarak geleneksel doku iskelelerinin hücre uyumluluklarını arttırmak ve böylece bu iskelelere ekilen hücre miktarını da azaltabilmek amacıyla hücre tutunma özelliđi taşıyan tripeptid dizilimi RGD'yi içeren bir elastin benzeri polipeptit (EBP) kullanılarak, liyofilizasyon ve elektroęirme yöntemleri ile özgün, çift katmanlı doku iskeleleri hazırlanmış ve bunlar cıva porozimetresi, taramalı elektron mikroskobu (SEM) ve mekanik testler ile karakterize edilmişlerdir. *In vitro* testler, EBP'nin varlığının hem fibroblastların hem de epitel hücrelerin çođalmasını belirgin bir şekilde arttırdığını göstermiştir.

Anahtar Kelimeler: Yapay Ağız Mukozası, Epitelyum Gelişmesi, Hücreler Arası Etkileşimler, Kollajen Doku İskelesi, Elastin Benzeri Rekombinant

ACKNOWLEDGMENTS

First and foremost, I would like to express my endless thanks and gratitude to my thesis supervisors Dr. Odile Damour and Prof. Vasif Hasırcı. I feel very lucky to have had the opportunity to do my thesis research jointly in their laboratories and under their guidance. This opportunity gave me the chance to enjoy very much the past three years, gaining experience in the two most important areas of Tissue Engineering: biomaterials design and cell biology. They provided me with guidance whenever I needed it and at the same time they let me explore and learn by myself. This thesis has been possible through their guidance, advices and enthusiasm.

I would also like to thank Prof. Pierre Breton, Prof. Gülay Özcengiz, Prof. İhsan Gürsel, and Dr. Sylvie Sauvaigo for serving on my committee, for all their collaboration, suggestions, and useful discussions.

I am grateful to Prof. Pierre Breton and his team at the Centre Hospitalier Lyon-Sud (Chirurgie Maxillo Faciale) for providing me with the human oral mucosa biopsies. Without them this thesis would not be possible. I am also indebted to Prof. Carlos Rodríguez-Cabello (Universidad de Valladolid, Spain) for kindly providing the Elastin-like recombinamer that I had the chance to use in my studies.

I would like to thank all my friends in BIOMAT-METU and Laboratoire des Substituts Cutanés in Lyon for their support, friendship and collaboration.

I gratefully acknowledge the Ph.D. fellowships that I received from the French Government and from the Scientific and Technological Research Council of Turkey (TUBITAK).

Last but definitely not least, I would like to thank my family for their love, support, friendship and guidance which gave me the courage to undertake all I ever did...

PREFACE

Tissue engineering is a sub-branch of the biomaterials field that aims to produce substitutes for the injured or diseased tissues by using a combination of cells and neosynthesized or reconstituted extracellular matrix (ECM) (Langer and Vacanti, 1993). The general approach in tissue engineering is to harvest cells from the tissue, preferably the patient himself, proliferate and seed them on an appropriate biodegradable carrier before implantation into the patient. This carrier is called the scaffold. It should be able to mimic the natural microenvironment of the cells in providing the volume, sites for cell attachment, proliferation, migration, neosynthesis of ECM, and function. Over time, the implanted reconstructed tissue is vascularized, ingrown by the surrounding healthy natural tissue and eventually the carrier degrades in the body, leaving only the seeded and infiltrated cells, the neosynthesized ECM and the blood vessels (Freyman et al., 2001). Construction of oral mucosa is a recent field of tissue engineering that aims to treat and fill the tissue deficits caused by facial trauma or malignant lesion surgery, as well as to study the biology of oral mucosa. It may further serve as a vehicle for gene therapy, and as an alternative to *in vivo* testing of oral care products (Feinberg et al., 2005).

The aim of this research was to construct a tissue engineered full-thickness human oral mucosa closely mimicking the native tissue. In order to achieve this goal, the feasibility of producing a full-thickness oral mucosal equivalent was assessed by co-culturing fibroblasts and epithelial cells isolated from lamina propria and epithelium of normal human oral mucosa biopsies, respectively, in the collagen-glycosaminoglycan (GAG)-chitosan dermal substrate previously developed in our laboratory for the production of a skin equivalent (Collombel et al., 1989). This skin model had been constructed to evaluate cutaneous toxicity (Shahabeddin et al., 1990), safety (Augustin et al., 1997a), and efficiency of cosmetic products (Augustin et al., 1997b). It was also used to develop a hemicornea (Builles et al., 2007). A nonkeratinized oral mucosal equivalent closely mimicking the native one was

obtained and characterized by histology, immunohistochemistry and transmission electron microscopy.

Afterwards, using this oral mucosa model, the influence of mesenchymal cells on oral epithelial development was investigated. For this purpose, lamina propria, corneal stromal, and dermal equivalents were constructed using the collagen-GAG-chitosan scaffolds. On top of these equivalents, oral mucosal epithelial cells were seeded and cultured under the same conditions. The results of histology, immunohistochemistry and transmission electron microscopy showed that the mesenchymal cell source had a significant influence on the thickness and the ultrastructure of the epithelium, but not on the differentiation of oral epithelial cells.

In order to improve the adhesiveness of conventional scaffolds made of collagen, and thus to decrease the initial cell seeding density, which is high for 3-D models, a bioengineered elastin-like recombinamer (ELR) containing the cell adhesion peptide RGD was used as a scaffold material to produce novel bilayer scaffolds for oral tissue engineering. These scaffolds were prepared by blending the ELR with collagen, lyophilization and electrospinning. They were characterized by mercury porosimetry, scanning electron microscopy and mechanical testing.

Finally, the collagen-ELR scaffolds were used to reconstruct full-thickness oral mucosal equivalents using human oral fibroblasts and epithelial cells. The results of the histology, immunohistochemistry and the MTT cell viability assay showed that these equivalents closely mimicked the native oral mucosa both histologically and immunohistologically, and that the presence of the ELR in the scaffold increased the proliferation of both fibroblasts and epithelial cells.

To better understand the experimental sections of the present research, in the next “Introduction” section, the structure of human oral mucosa, literature on the influence of the mesenchymal tissue on oral epithelial development, strategies developed to reconstruct oral mucosal defects, cells and biomaterials used in oral mucosa engineering, and finally scaffold production techniques are presented.

TABLE OF CONTENTS

ABSTRACT	iv
RESUME	vi
ÖZ	viii
ACKNOWLEDGMENTS	x
PREFACE	xi
TABLE OF CONTENTS	xiii
CHAPTER	
1. INTRODUCTION	1
1.1. Normal Oral Mucosa	1
1.1.1. Ultrastructure and Composition of Oral Mucosa	2
1.1.2. Patern of Keratinization in Oral Mucosal Epithelia	4
1.1.3. Influence of the Mesencymal Tissue on Epithelial Development	4
1.2. Reconstruction of Oral Mucosal Defects	6
1.2.1. Oral Mucosal Grafts	6
1.2.2. Oral Mucosal Epithelial Cell Sheets	7
1.2.3. Full-thickness Oral Mucosa Equivalents	9
1.3. Tissue Engineering of Oral Mucosa	11
1.3.1. Cell Types and Sources Used in Oral Mucosa Engineering	11
1.3.2. Scaffolds Used in Oral Mucosa Engineering	13
1.3.2.1. Natural Scaffolds	13
1.3.2.2. Synthetic Scaffolds	16
1.3.2.3. Recombinant Polymers: Elastin-like Recombinamer	16
1.3.3. Scaffold Production Techniques Used in Oral Mucosa Engineering	20
1.3.3.1. Freeze-drying	21
1.3.3.2. Electrospinning	22

2. MATERIALS AND METHODS	26
2.1. Materials	26
2.2. Methods	27
2.2.1. Scaffold Preparation	27
2.2.1.1. Preparation of MIMEDISC® Scaffolds	27
2.2.1.2. Preparation of Collagen-Elastin-like Recombinamer Scaffolds	28
2.2.1.3. Characterization of Collagen-ELR Scaffolds	32
2.2.2. In vitro Studies	34
2.2.2.1. Origin, Isolation and Culture of Human Oral Epithelial Cells	34
2.2.2.2. Origin, Isolation and Culture of Human Oral Fibroblasts	34
2.2.2.3. Origin, Isolation and Culture of Human Dermal Fibroblasts ...	35
2.2.2.4. Origin, Isolation and Culture of Human Stromal Keratocytes	35
2.2.2.5. Preparation of Lamina Propria, Dermal and Stromal Equivalents	35
2.2.2.6. Preparation of Epithelialized Equivalents	36
2.2.2.7. Assessment of Cell Viability	36
2.2.3. Characterization of Tissue Equivalents	37
2.2.3.1. Histology	37
2.2.3.2. Immunohistochemistry	37
2.2.3.3. Transmission Electron Microscopy	38
2.2.4. Statistical Analysis	38
3. RESULTS AND DISCUSSION	39
3.1. Reconstruction of a Full-thickness Human Oral Mucosal Equivalent Based on a Collagen-Glycosaminoglycan-Chitosan Substrate	39
3.1.1. Histology	39
3.1.2. Immunohistochemistry	40
3.1.3. Transmission Electron Microscopy	43
3.1.4. Discussion	45
3.2. Study of the Influence of the Mesenchymal Cell Source on Oral	

Epithelial Development	49
3.2.1. Histology	49
3.2.2. Immunohistochemistry	50
3.2.3. Transmission Electron Microscopy	52
3.2.4. Discussion	53
3.3. Preparation and Characterization of Novel Scaffolds of Elastin-like Recombinamer and Collagen for Soft Tissue Engineering	57
3.3.1. Characterization and Purity of Collagen Type I Isolated from Rat Tails	57
3.3.2. Structural Properties of the Scaffolds	58
3.3.3. Compressive Mechanical Properties of the Scaffolds	65
3.3.4. Discussion	66
3.4. Development of a Full-thickness Tissue Engineered Human Oral Mucosa Based on a Novel Bilayer Protein Scaffold	69
3.4.1. Cell Proliferation in Collagen-ELR Scaffolds: MTT Assay	69
3.4.2. Histology	70
3.4.3. Immunohistochemistry	71
4. CONCLUSION	73
GLOSSARY	74
REFERENCES	76
CURRICULUM VITAE	91

CHAPTER 1

INTRODUCTION

1.1. Normal Oral Mucosa

Oral mucosa represents the barrier between the mouth and the oral cavity, and functions to protect the underlying tissue from mechanical damage and from entry of microorganisms and toxic materials (Squier and Kremer, 2001). Its structure is similar more to skin than to any other mucosa in the body, and just like skin, with which it forms a junction at the lips, it is basically composed of a stratified epithelium and an underlying dense connective tissue, i.e. lamina propria. The two are attached to each other at the basement membrane region. Epithelium consists of tightly packed epithelial cells. Lamina propria is composed of fibroblasts, connective tissue, small blood vessels (capillaries), inflammatory cells (macrophages) and extracellular matrix (ECM) (Sonis, 2004). The physiological features that distinguish oral mucosa from skin are its pink color due to extensive blood supply, its moist surface, higher permeability due to its lipid content, absence of appendages (such as hair follicles, sebaceous glands, sweat glands; oral mucosa contains on the other hand only minor salivary glands) and its pattern of keratinization (Winning and Townsend, 2000; Squier and Kremer, 2001; Izumi et al., 2003). Oral mucosa has distinct regions, some require more strength like hard palate and gingiva, and some require more elasticity like cheek, lips and floor of the mouth. According to the function of the region in the oral cavity, the epithelium of oral mucosa may be keratinized (masticatory mucosa), nonkeratinized (lining

mucosa) or both (specialized mucosa) as in the case of dorsum of the tongue, which consists of both keratinized and nonkeratinized regions. On the other hand, epithelium of skin is keratinized regardless of its location in the body (Squier, 1991).

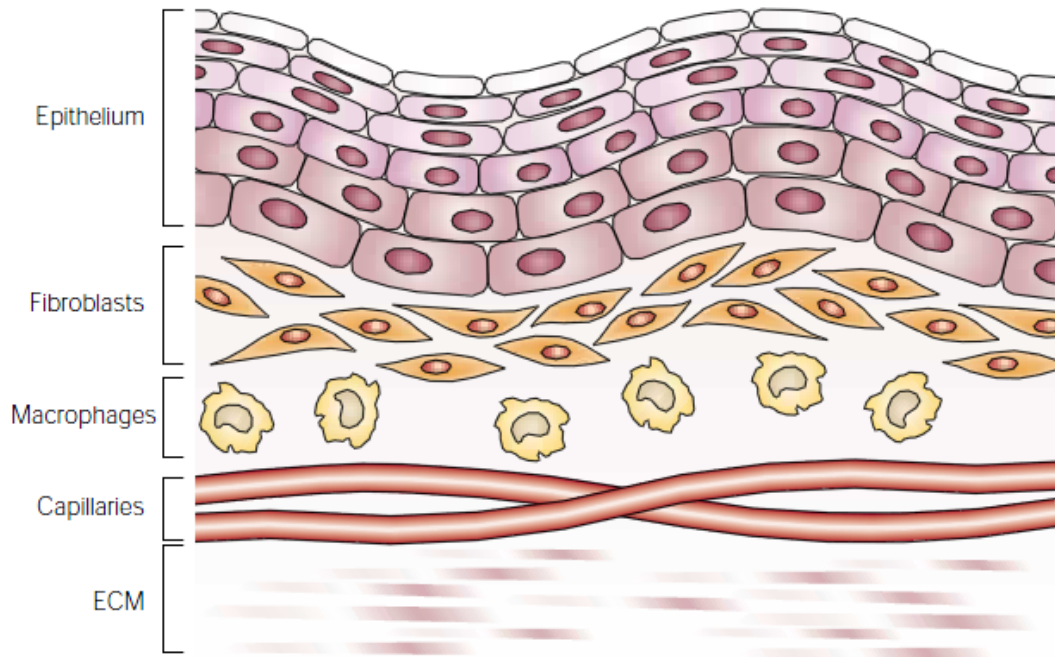


Figure 1.1. General structure of oral mucosa (Sonis, 2004)

1.1.1. Ultrastructure and Composition of Oral Mucosa

Epithelium of oral mucosa is composed of various cell layers with different degrees of differentiation; namely, the basal layer, spinous layer, granular (keratinized epithelium) or intermediate layer (nonkeratinized epithelium), and the keratinized (keratinized epithelium) or superficial layer (nonkeratinized epithelium) (Winning and Townsend, 2000). In the basal layer of the epithelium, the cells are responsible for cell division and production; they are the least differentiated and smallest ones and form two to three layers in the epithelium. As these cells move and differentiate into the spinous layer, they increase in size, change in shape, and there are more desmosomes and keratin filaments. In the next layer, granular

(keratinized epithelium) or intermediate layer (nonkeratinized epithelium), the cells become flattened with an increasing percentage of keratin filaments. In the keratinized layer (keratinized epithelium), the cells either retain their nuclei (parakeratinization, common in gingival epithelium), or they have no nuclei (orthokeratinization) (Winning and Townsend, 2000). On the other hand, in nonkeratinized oral mucosa, the cells in the superficial layer retain their nuclei and the number of desmosomes is decreased. Due to the presence of the keratinized layer in keratinized oral mucosa, it has less permeability than the nonkeratinized oral mucosa, but still it is 10 times more permeable than skin. Besides epithelial cells; melanocytes, Langerhan cells, Merkel cells, and lymphocytes also exist in the epithelium (Winning and Townsend, 2000). The thickness of the epithelium in oral mucosa varies according to its location in the oral cavity. Cheek mucosa has a thicker epithelium ($580 \pm 90 \mu\text{m}$), compared to the epithelium in the floor of mouth, which is very thin ($190 \pm 40 \mu\text{m}$). The thickness of the hard palate epithelium is somewhere in between these two regions ($310 \pm 50 \mu\text{m}$). The epidermis of the skin is the thinnest of all, 100 to 120 μm (Schroeder, 1981). This might be due to the fact that nonkeratinized oral lining tissue turns over more rapidly than does the keratinized mucosa (Rowat and Squier, 1986).

The basement membrane is the region which attaches the epithelium to the underlying lamina propria. This attachment involves hemidesmosomal attachment of basal epithelial cells to a basal lamina, which in turn is attached via anchoring fibrils (collagen VII) to collagen fibers of the underlying lamina propria. The latter is composed of cells and fibers embedded in ground substance composed of proteoglycans and glycoproteins. Many fibroblasts are present, but only very occasional macrophages, plasma cells, mast cells, and lymphocytes are found in the lamina propria (Moharamzadeh et al., 2007). Fibroblasts are responsible for producing collagen fibers, types I, III, V and VI, which are more organized and thicker in keratinized oral mucosa than nonkeratinized one (Winning and Townsend, 2000). The average collagen fiber diameter range in human lamina propria is reported as 20-40 nm. This 20 nm range is due to the fact that the average fibril diameter varies with the region in the mouth, or for the same region with their location in the lamina propria (Susi et al., 1967; Ottani et al., 1998). Collagen fibrils

in native human skin are of larger diameter (53–82 nm) compared to those in oral mucosa (Stewart, 1995).

1.1.2. Pattern of Keratinization in Oral Mucosal Epithelia

Keratinized and nonkeratinized epithelia of oral mucosa are derived from the same germ layer and as their names imply they show variation with respect to the extent and type of keratinization due to their location in oral cavity. All epithelial cells contain keratins, which are proteins that form intermediate filaments of the cytoskeleton. It was demonstrated that the keratins expressed in keratinized hard palate epithelium are similar to that of epidermis and that the nonkeratinized epithelium expressed a distinctly different set of keratins (Table 1) (Clausen et al., 1986; Winning and Townsend, 2000; Moharamzadeh et al., 2007).

Table 1.1. Keratin expression profile in oral epithelia

Tissue	Basic, Type II Subfamily				Acidic, Type I Subfamily				
	K1,2	K4	K5	K6	K10	K13	K14	K16	K19
Nonkeratinized oral mucosa	-	+(sb)	+(b)	-	-	+(sb)	+(b)	-	+(b)
Keratinized oral mucosa	+(sb)	-	+(b)	+(sb)	+(sb)	-	+(b)	+(sb)	-
Epidermis	+(sb)	-	+(b)	-	+(sb)	-	+(b)	-	-

(b): expressed in basal layer, (sb): expressed in suprabasal layers

1.1.3. Influence of the Mesenchymal Tissue on Epithelial Development

Different types of epithelia have evolved to provide the optimal form of protection for their specific location. For example, epidermis is dry, constantly exposed to changing humidity and great variability of temperatures, mainly lower than 37°C, whereas oral epithelium is exposed to heavy abrasion, 100% humidity and mainly a temperature of 37°C (Gibbs and Ponec, 2000). On the other hand, corneal surface must be extremely smooth and transparent in order to allow the formation of a sharp image on the retina (Dohlman, 1971).

Oral cavity has distinct regions, some require more strength, e.g. hard palate and gingiva, and some require more elasticity like cheek, lips and floor of the mouth. According to the function of the region in the oral cavity, the epithelium of oral mucosa is keratinized (masticatory mucosa), nonkeratinized (lining mucosa) or both, e.g. specialized mucosa of the dorsum of the tongue, which consists of both keratinized and nonkeratinized regions (Squier, 1991). Since keratinized and nonkeratinized epithelia of oral mucosa, that represent the extremes of differentiation of stratified squamous epithelia, are derived from the same germ layer, they provide a unique material to study epithelial differentiation (Clausen et al., 1986).

Mesenchymal tissue, mainly composed of extracellular matrix and also of cells and soluble factors which are released when needed, is known to influence the morphogenesis, proliferation and differentiation of a variety of embryonic epithelia (Sharpe and Ferguson, 1988). Potential of epithelial development is gradually restricted as a consequence of influence from inductive tissues and other environmental factors as the developmental fate is progressively determined (Cunha et al., 1983). On the other hand, whether the commitment to a particular epithelial differentiation is an irreversible process or not is still debated. The first study to demonstrate the possibility to reverse the epithelial differentiation was published in 1983 by Cunha and colleagues, who successfully induced the adult epithelium of urinary bladder to form glandular structures resembling prostate by culturing mesenchyme of the urogenital sinus on it.

Even if for some scientists epithelial differentiation is an intrinsic property of epithelial cells, independent of the underlying mesenchymal tissue (de Luca et al., 1990; Gibbs and Ponec, 2000), others found influence of mesenchymal tissue on epithelial cell differentiation. Indeed, using cross-combination of normal tissues after epithelial-connective tissue separation, it has been shown that adult epithelia could be influenced by extrinsic mesenchymal factors, which caused changes in patterns of keratinization (Mackenzie et al., 1979), in morphogenesis and cytodifferentiation (Schweizer et al., 1984) and in cytokeratin expression (Merne and Syrjänen, 2003). In addition, a recent study interestingly revealed that only alveolar fibroblasts have an effect on epithelial differentiation among gingival,

palatal and dermal fibroblasts, stimulating skin keratinocytes to express keratins typical of nonkeratinized oral mucosal epithelium instead of those encountered in normal epidermis (Chinnathambi et al., 2003). Not only the mesenchymal tissue but the environment of the oral cavity is also thought to influence the epithelial differentiation. Nicotine (Kwon et al., 1999) and wet environment (Holle and Kunstfeld, 2004) were suggested to stimulate the differentiation of oral mucosal keratinocytes. Indeed, in some studies medium was added on top of oral mucosal equivalents during the air-liquid interface phase of culture and helped mimic oral cavity conditions and to prevent differentiation (Tomakidi et al., 1998).

Abnormalities in epithelial-mesenchymal interactions lead to a variety of pathologies such as premalignant lesions, e.g. leukoplakia, epithelial dysplasia or even malignancy (Sharpe and Ferguson, 1988). Elucidation of the mechanisms of epithelial-mesenchymal interactions should be of relevance for controlling normal as well as pathologic growth and development (Cunha et al., 1982). As shown in the literature presented, past research on the influence of mesenchymal tissue on epithelial development has raised questions, indicating that this subject still needs further investigation.

1.2. Reconstruction of Oral Mucosal Defects

Oral tissue reconstruction is required after tissue deficits due to tumor excision, cleft palate repair, trauma, repair of diseased tissue (such as gingivitis and other gum diseases) and for generating soft tissue around teeth and dental implants. Approaches developed for reconstruction of oral cavity can be broadly grouped as: oral mucosal grafts, oral mucosal epithelial cell sheets and tissue-engineered three-dimensional (3D) full-thickness oral mucosal equivalents.

1.2.1. Oral Mucosal Grafts

For the reconstruction of oral mucosal defects, the main sources for the transplants are the inner cheek and the palate (Lauer, 2009). Palatal mucosal grafts are routinely used to cover mucosal defects caused by vestibuloplasty (Raghoobar et

al., 1995). But oral tissues are limited in size and quantity. Therefore, either skin transplants or intestinal mucosa were used to cover extensive defects (Lauer, 2009). However, this approach has serious disadvantages; one is donor site morbidity and the other is the different characteristics of skin, such as hair growth (Ueda et al., 2001), and different pattern of keratinization which results in negligible assimilation even years after transplantation (Lauer, 2009). These facts brought about the need to use regenerative medicine and tissue engineering to develop oral mucosal equivalents.

1.2.2. Oral Mucosal Epithelial Cell Sheets

Driven by the problems associated with oral mucosal grafts and by the success of epidermal cell sheets, which had been applied to skin defects caused by severe burns, ulcers, etc., researchers in the recent years started to grow autologous oral epithelial cells in sheets in the laboratory from small oral biopsies. Cell sheet engineering makes use of several techniques such as culturing on temperature-responsive culture dishes (Okano et al., 1993), on human amniotic membranes (Nakamura et al., 2003) and on collagen membranes (Imaizumi et al., 2004). The former is the oldest and the most established method, where temperature-responsive culture dishes are created by the covalent grafting of the temperature-responsive polymer poly(*N*-isopropylacrylamide) (PNIPAM) on to ordinary tissue culture dishes of polystyrene (Yamada et al., 1990; Okano et al., 1993). Under normal culture conditions at 37°C, the dish surfaces are relatively hydrophobic and cells attach, spread, and proliferate as on typical tissue culture dishes. However, upon decrease of temperature below the polymer's lower critical solution temperature (LCST) of 32°C, the polymer surface graft of PNIPAM becomes hydrophilic and swells, forming a hydration layer between the dish surface and the cultured cells, leading to their spontaneous detachment without the need for enzymatic treatments such as trypsinization. By avoiding proteolytic treatment, critical cell surface proteins such as ion channels, growth factor receptors and cell-to-cell junction proteins remain intact, and cells can be non-invasively harvested as intact sheets along with their deposited extracellular matrix (ECM) (Yang et al., 2005).

The advantage of oral mucosal epithelium is its high regenerative capacity allowing the site of removal to heal very rapidly and without scar formation (Murakami et al., 2006). In addition, oral mucosal epithelial cell sheets were proven to be superior to epidermal cell sheets in some other respects: it took 12 days to form an epithelial sheet from small epithelial segments as compared to 14 days in the case of a skin epithelial sheet. Furthermore, viability of mucosal epithelial sheets was maintained for 30 days *in vitro* as opposed to 22 days for skin epithelial sheets (Ueda, 1995). Clinical results were good, accelerated healing of oral mucosal defects and a smooth and keratinized grafted site, without infection or scar contraction, was observed (Langdon et al., 1991; Raghoobar et al., 1995; Ueda et al., 2001; Bodner and Grossman, 2003). The oral mucosal epithelial cell sheets were used not only for oral cavity reconstruction but also for ocular surface reconstruction in bilateral cases (Inatomi et al., 2008) and for treatment of oesophageal ulcerations (Ohki et al., 2006).

On the other hand, there was one major problem with the oral epithelial cell sheets used for oral mucosal reconstruction: they were not only fragile and difficult to handle but also had low engraftment rates (Feinberg et al., 2005). It was also found that the presence of a mesenchymal tissue assisted in epithelial graft adherence and epithelial maturation, and minimized wound contraction while encouraging the formation of a basement membrane (Gallico and O'Conner, 1995). This led the scientists to reconstruct 3D, full-thickness oral mucosal equivalents consisting of both an epithelium and an underlying lamina propria to provide support for the former.



Figure 1.2. Oral mucosa epithelial cell sheet
(<http://www.dentistry.bham.ac.uk/admissions/page1.asp>)

1.2.3. Full-thickness Oral Mucosa Equivalents

To overcome the problems associated with epithelial cell sheets, 3D models of oral mucosa were recently developed. The advantages of these models are: they are easier to handle and able to fill deep defects, they resemble more the native tissue due to their more complex structure with both an epithelium and a lamina propria, and a basement membrane between them, possibility to incorporate different cell types, high degree of differentiation, and finally, potential for histological assessment of the process under study and potential for monitoring tissue growth or damage, together with the expression of tissue proteins or mRNA *in situ* (Dongari-Bagtzoglou and Kashleva, 2006). The difference between an oral epithelial cell sheet and a 3D full-thickness oral mucosal equivalent in terms of their tensile strengths can be seen by comparing Figures 1.2 and 1.3.

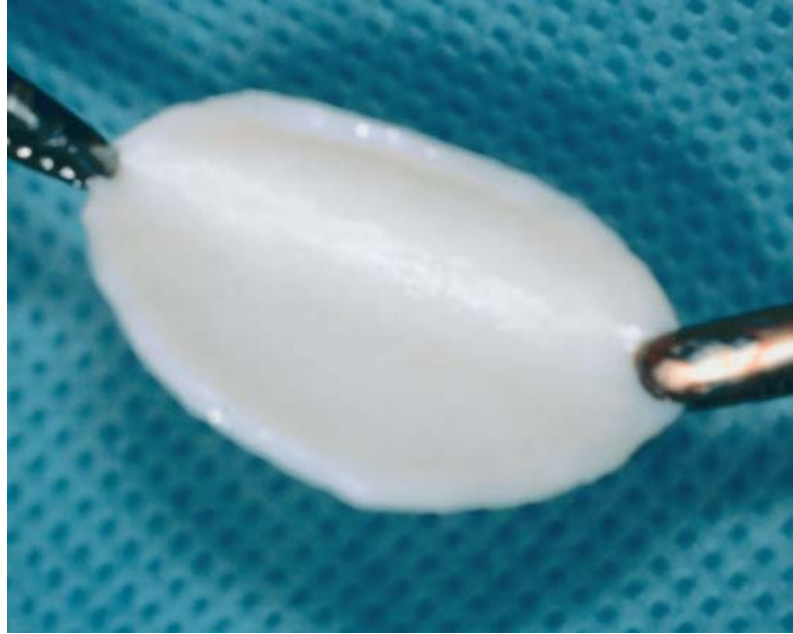


Figure 1.3. EVPOME (ex vivo produced human oral mucosa equivalent)
(Izumi et al., 2003)

Recently 3D models of full-thickness oral mucosa were reconstructed using acellular cadaver/animal dermis (Yoshizawa et al., 2004; Nakanishi et al., 2007; Xiong et al., 2008) and polymer-based scaffolds (Alaminos et al., 2007; Luitaud et al., 2007; Moharamzadeh et al., 2008). The constructs containing a cadaver/animal dermis lack fibroblasts. Fibroblasts are the most important cells of a lamina propria equivalent. They promote the growth and differentiation of epithelial cells, and the formation of a basement membrane (Gallico and O'Conner, 1995; Dongari-Bagtzoglou and Kashleva, 2006). There is only one *in vivo* study of the implantation of a full-thickness oral mucosal equivalent reported in the literature. This equivalent is composed of an acellular dermis and autologous epithelial cells, and was transplanted in dogs, but it did not result in better healing compared to the control incisions, probably due to insufficient vascularization after implantation of the equivalent (Ophof et al., 2008). The only clinically successful full-thickness oral mucosal equivalent reported in the literature is EVPOME (ex vivo produced oral mucosa equivalent). It is composed of AlloDerm® (allogenic human acellular dermis) and autologous epithelial cells, and it resulted in better healing (Izumi et al., 2003).

1.3. Tissue Engineering of Oral Mucosa

Oral epithelial cell sheets and full-thickness oral mucosa equivalents are regenerative medicine and tissue engineering approaches which aim to reconstruct oral tissue using cells with or without biodegradable scaffolds, respectively. Oral tissue engineering is a very recent field and until now, no human oral tissue-engineered products have been available for clinical applications.

1.3.1. Cell Types and Sources Used in Oral Mucosa Engineering

Cell lines and primary cells are the two main groups of cells used in oral mucosal tissue engineering. Buccal carcinoma cell line TR146 was used in the reconstruction of oral mucosal equivalents but mostly primary cells isolated from normal oral mucosa biopsies are preferred due to the fact that carcinoma cell lines may not always accurately represent normal epithelial cells and they are not suitable for clinical use (Dongari-Bagtzoglou and Kashleva, 2006; Moharamzadeh et al., 2007). Stem cells are highly proliferative cells with a capacity to differentiate into various cell types and for this reason they seem to be very promising for tissue engineering but have not been used in the reconstruction of oral mucosal equivalents so far. When the concept of oral epithelial cell sheet transplantation was successful, this was attributed to the healing potential of the progenitor cells among the oral epithelial cells that contain stem cells (Igarashi et al., 2008). Indeed, epidermis of skin and limbus of cornea were shown to contain stem cells. However, the localization of stem cells in the oral epithelium is not fully understood, but a pure population of oral epithelial stem cells had to be isolated for application to tissue engineering (Igarashi et al., 2008). The stem cells of the human oral mucosal epithelium have been thought to be in the basal layer. The basal cells were reported to express stem/progenitor cell-related markers, PCNA, Ki-67, cytokeratins K5/14, K19, integrins ($\alpha 2$, $\alpha 3$, $\alpha 6$, $\beta 1$ and $\beta 4$), neurotrophin receptor p75 but not differentiation markers, K1/10, K4/13 (Igarashi et al., 2008). Recently, a progenitor/stem-cell-enriched population was successfully isolated from cultured primary oral mucosal keratinocytes (Izumi et al., 2007). However, there is little

indirect evidence that stem cells might also exist in the lamina propria of oral mucosa. There are reports about stem cell populations associated with hair follicles within the skin, but the hairless oral mucosa is deprived of these structures. Still the structural and cellular resemblance between oral mucosa and skin, and more importantly the ability of oral tissue to heal without scar in a fetal-like manner indicated that this possibility was worth investigating (Stephens and Genever, 2007).

Tissue engineered oral mucosal equivalents contain epithelial cells either alone or with fibroblasts. The presence of fibroblasts is important considering the influence of their interactions with epithelial cells on the development of the developing tissue, as explained in the previous sections. In fact, besides epithelial cells; melanocytes, Langerhans cells, Merkel cells, and lymphocytes also exist in the epithelium of the native oral mucosa (Winning and Townsend, 2000). In the lamina propria, fibroblasts constitute the vast majority of the cells, only very occasional macrophages, plasma cells, mast cells, and lymphocytes are found (Moharamzadeh et al., 2007). Skin equivalents comprising Langerhans cells, melanocytes, adipose cells and endothelial cells (forming tubular capillaries in the dermis) were reported (Auxenfans et al., 2009). Considering the similarities between skin and oral mucosa, a similar approach may be undertaken to reconstruct such oral mucosal equivalents, i.e. immunocompetent, pigmented, adipose or endothelialized.

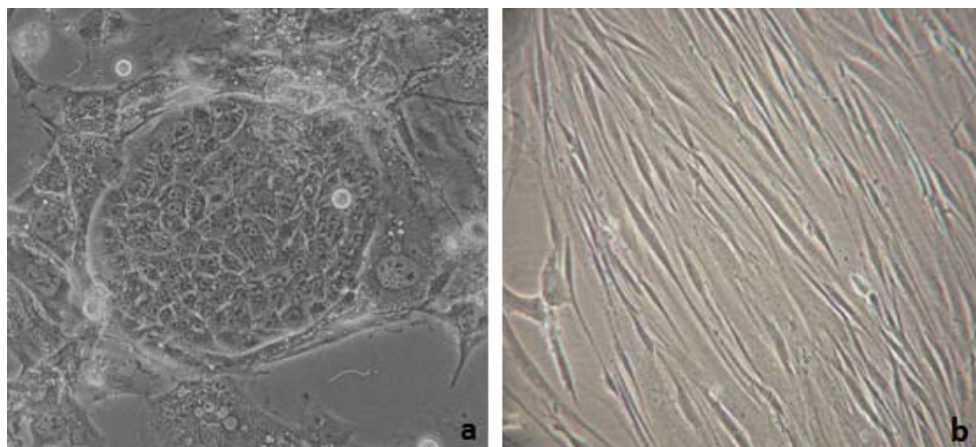


Figure 1.4. Morphology of oral mucosa cells in cell culture flasks. a) Small and rounded epithelial cells forming clones, and b) larger and elongated fibroblasts.

1.3.2. Scaffolds Used in Oral Mucosa Engineering

Any 3D oral mucosal equivalent should contain a scaffold which, when seeded with fibroblasts, would form the lamina propria equivalent. The choice for the scaffold material is a crucial one since the success of the tissue-engineered implant depends mostly on it. The ideal scaffold to be used in oral mucosa engineering must not induce a toxic or immune response or result in excessive inflammation. It should have an acceptably low level of disease risk, be slowly biodegradable, support the reconstruction of normal tissue and have similar mechanical and physical properties to the oral mucosa it replaces. In addition, it should be readily available and capable of being prepared and stored with a long shelf life (MacNeil, 2007). Porosity is also a very important property of the scaffold, because a lamina propria scaffold should possess an optimum pore size and distribution to allow fibroblast infiltration and proliferation, and also cell communication and medium perfusion. A scaffold suitable for intrinsic vascularization must have a high porosity (>40–60%), and an interconnected pore structure (Will et al., 2008). Scaffolds used in oral mucosa engineering can be broadly grouped as natural scaffolds and synthetic scaffolds according to the origin of the polymeric material used.

1.3.2.1. Natural Scaffolds

Natural scaffolds are either cadaver or animal derived de-epithelialized acellular matrices or they are mostly constructed using natural polymers extracted from animals. Porcine skin (Xiong et al., 2008), de-epithelialized human cadaver dermis (Cho et al., 2000; Ophof et al., 2002; Bhargava et al., 2004; Yoshizawa et al., 2004; Iida et al., 2005; Nakanishi et al., 2007), AlloDermTM (also a human cadaveric dermis) (Izumi et al., 1999; Izumi et al., 2000; Ophof et al., 2002; Izumi et al., 2003), human amniotic membrane (Nakamura et al., 2003) and de-epithelialized bovine tongue (Hildebrand et al., 2002) have been used so far as acellular matrices for oral mucosa engineering. Natural polymers have the advantage of responding to the environment via degradation and remodeling

through the action of the enzymes. They are also generally non-toxic, even at high concentrations (Dang and Leong, 2006), which should be of relevance especially in oral mucosa engineering. Among natural polymers, collagen is the most commonly used in scaffold design due to its high biocompatibility and biodegradability. In addition, it is adhesive, fibrous, cohesive, and can be used in combination with other materials. On the other hand, it might be antigenic through telopeptides, though it is possible to remove these small telopeptides proteolytically before use (Glowacki and Mizuno, 2008). The lamina propria of native oral mucosa itself is also composed mainly of collagen, mainly collagen type I with some collagen type III in the deeper layers (Moharamzadeh et al., 2007). Collagen scaffolds gave promising results in oral mucosa engineering (Masuda et al., 1996; Moriyama et al., 2001; Navarro et al., 2001; Rouabhia and Deslauriers, 2002; Mostefaoui et al., 2002; Ophof et al., 2002; Andrian et al., 2004; Claveau et al., 2004; Tardif et al., 2004; Luitaud et al., 2007; Moharamzadeh et al., 2008), but other natural materials such as fibrin (Alaminos et al., 2007), elastin (Ophof et al., 2002) and glycosaminoglycan (Navarro et al., 2001; Ophof et al., 2002) were also used, alone or in combination with collagen, for the same purpose.

1.3.2.1.1. Collagen

Collagen is the most abundant protein in all animals. One third of total protein in humans and three-quarters of the dry weight of skin is collagen. It is the predominant component of the extracellular matrix (Shoulders and Rainers, 2009). The superfamily of collagens can be divided into 19 groups according to their fiber-to-fiber relations and organization. Collagen type I is the most abundant collagen type found in various tissues and belongs to the family of collagens that form fibrils along with types II, III, V and XI. All fibril forming collagens are similar in size and they all contain large triple helical domains with about 1000 amino acids or 330 Gly-X-Y- repeats per chain. Moreover, they are first synthesized as larger precursors which are later on processed to collagens by cleavage of N-propeptides and C-propeptides by specific proteinases. Another common property of these collagens is that they all assemble into cross-striated fibrils in which each

molecule is displaced about one-quarter of its length relative to its nearest neighbor along the axis of the fibril (Prockop and Kivirikko, 1995). Collagen type I contains $\alpha 1$ and $\alpha 2$ chains and forms a $\alpha 1[I]_2\alpha 2[I]$ triple helix (Bornstein and Sage, 1980). Besides the lamina propria of oral mucosa, it is also found in dermis, bone, tendon and ligament (Shoulders and Rainers, 2009). Network-forming collagens include type IV collagens found in basement membranes, and type XIII and X collagens. Compared to fibril-forming collagens, type IV collagen has a longer collagenous domain which consists of about 1400 amino acids in –Gly-X-Y- repeats that are frequently interrupted by short noncollagenous sequences. The molecules self assemble to form net-like structures in which monomers associate at the C-termini to form dimers and at the N-termini to form tetramers. Besides these end-to-end interactions, the triple-helical domains intertwine to form supercoiled structures (Prockop and Kivirikko, 1995).

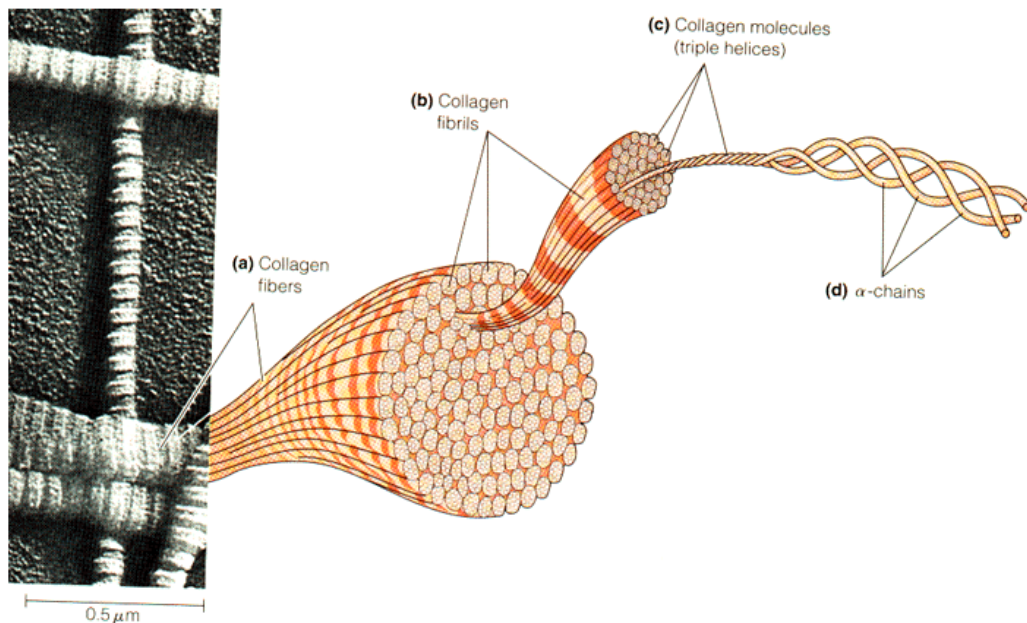


Figure 1.5. Structure of collagen fibers
(<http://course1.winona.edu/sberg/ILLUST/fig11-2.gif>)

1.3.2.2. Synthetic Scaffolds

Synthetic polymers such as poly(glycolic acid), poly(lactic acid) and their copolymers, poly(p-dioxanone), and copolymers of trimethylene carbonate and glycolide are popular in tissue engineering due to the researcher's ability to tailor mechanical properties and degradation kinetics to suit various applications and the possibility to fabricate them into various shapes with desired morphologic features and chemical groups (Gunatillake and Adhikari, 2003). They have not been used in oral mucosa engineering so far.

1.3.2.3. Recombinant Polymers: Elastin-like Recombinamer

Recombinant polymers are proteins designed using recombinant DNA technology and contain desired peptide sequences for advanced applications in biotechnology. Recently researchers started to use them as another category of materials for tissue engineering.

All the properties displayed by biological materials and systems are entirely determined by the physical and chemical properties of their monomers and their sequence. Materials science began to take advantage of the power of new techniques in molecular biology and genetic engineering such as recombinant DNA technology, which allows the introduction a synthetic gene in the genetic content of a microorganism, plant or other eukaryotic organisms and induce the production of its encoded protein-based polymer as a recombinant protein (Rodriguez-Cabello et al., 2007). These macromolecules are generically named as "recombinamers" (Rodriguez-Cabello et al., 2009). This technology is superior to any other polymer synthesis technology in terms of the control, complexity and fine-tuning possibility that it offers. Using this technology, it is possible to bioengineer protein-based polymers (PBPs) of more complex and well defined structure. Elastin-like recombinamers (ELRs) form a class of these biocompatible PBPs. They are composed of the pentapeptide repeat Val-Pro-Gly-Xaa-Gly (VPGXG), which is derived from the hydrophobic domain of tropoelastin and where X represents any natural or modified amino acid, except proline (Chilkoti et al., 2006). At low

temperatures, ELRs are soluble in aqueous solutions, but as the solution temperature is raised, they become insoluble and aggregate at a critical temperature, termed the inverse transition temperature (T_t). This process is reversible meaning that when the temperature is lowered below T_t , the ELR aggregate resolubilizes. ELRs can also be designed to respond to other physical stimuli such as redox, pH, light, etc. by incorporation of suitable guest residues in the polypeptide chain at the fourth position (Chilkoti et al., 2006). After the finding of the extraordinary biocompatibility of the (VPGVG)-based ELRs, their *in vitro* capabilities for tissue engineering were tested (Rodriguez-Cabello et al., 2009). When the simple crosslinked matrices of poly(VPGVG)s were tested for cell adhesion, it was found that cells did not adhere at all to this matrix and no fibrous capsule formed around it when implanted (Urry et al., 1993). Soon after, these polypeptide molecules were enriched with short peptides having specific bioactivity, which were easily inserted into the polymer sequence. The first active peptides inserted in the polymer chain were the well-known general-purpose cell adhesion tripeptide RGD (R = L-arginine, G = glycine and D = L-aspartic acid) and the REDV (E = L-glutamic acid and V = L-valine), which is specific to endothelial cells. The resulting bioactivated (VPGVG) derivatives, especially those based on RGD, showed a high capacity to promote cell attachment (Rodriguez-Cabello et al., 2007).

ELRs have been used as coatings (Ozturk et al., 2009) and films (Martínez-Osorio et al., 2009) for improved cell attachment, as hydrogels to promote chondrogenesis (Betre et al., 2006; Martín et al., 2009; Nettles et al., 2010) or as polymer injections (Urry et al., 1998; Adams et al., 2009). They could also be shaped into fibers in pure form (Huang et al., 2000). The first ELR candidates for tissue engineering applications were simple polymers, to which the cells did not attach. Soon after, they were enriched with short peptides having specific bioactivity (Rodríguez-Cabello et al., 2007). Recently, a scaffold containing an ELR with substrate amino acids for mTGase, recognition sequences for endothelial cell adhesion (REDV), elastic mechanical behavior (VPGIG), and for targeting of specific elastases for proteolytic reabsorption (VGVAPG), was found to be suitable for vascular tissue engineering (Garcia et al., 2009). To our knowledge, ELR

functionalized with cell adhesion peptide RGD has not been used as scaffold material for the reconstruction of a tissue equivalent so far.

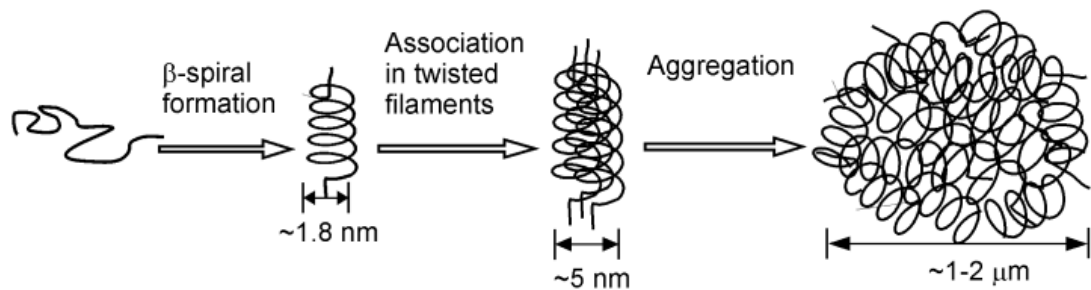


Figure 1.6. Aggregation of elastin-like recombinamers at the inverse transition temperature (Rodriguez-Cabello et al., 2007).

1.3.2.3.1. The H-RGD6 Elastin-like Recombinamer

The elastin-like recombinamer H-RGD6 contains 6 monomers of RGD, a histidine-tag, 6 aspartic acids, 24 lysines and 7 histidines, which are charged residues (Figure 1.7).

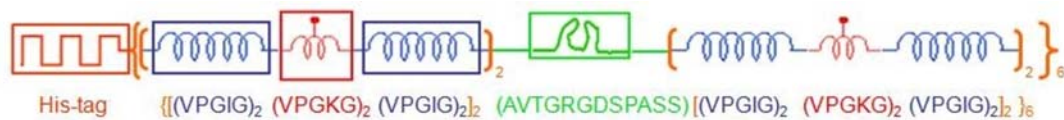


Figure 1.7. Schematics of the featured elastin-like recombinamer, H-RGD6.

ELRs are soluble in water below their transition temperature (T_t) and segregate from the solution above that temperature. This temperature-responsive behavior has been exploited to purify the polymer from the bacterial lysate. Figure 1.8 shows the results of the MALDI-TOF and SDS-PAGE tests. These tests were performed to verify the purity of the sample and correctness of the molecular weight of H-RGD6 after expression and purification protocols (Costa et al., 2009).

The experimental molecular weights found by both techniques match well with the theoretical molecular weight of the polymer (60661 Da). MALDI-TOF spectrum shows a high intensity peak at 60543 Da, which is approximate to the theoretical value of H-RGD6. SDS-PAGE also permits to identify an intense

band corresponding to the biopolymer, with the same molecular weight. In conclusion, the characterization tests point to the bioproduction of a polymer with the desired composition, sequence, molecular weight and purity (Costa et al., 2009).

The stimuli-responsive nature of H-RGD6 in PBS (pH 7.4) was studied by measuring the temperature dependence of the aggregate size of the biopolymer chains. The results are presented in Figure 1.9, and reflect the segregation of ELPs and formation of larger aggregates in suspension above T_t , which causes an abrupt increase in turbidity (Costa et al., 2009).

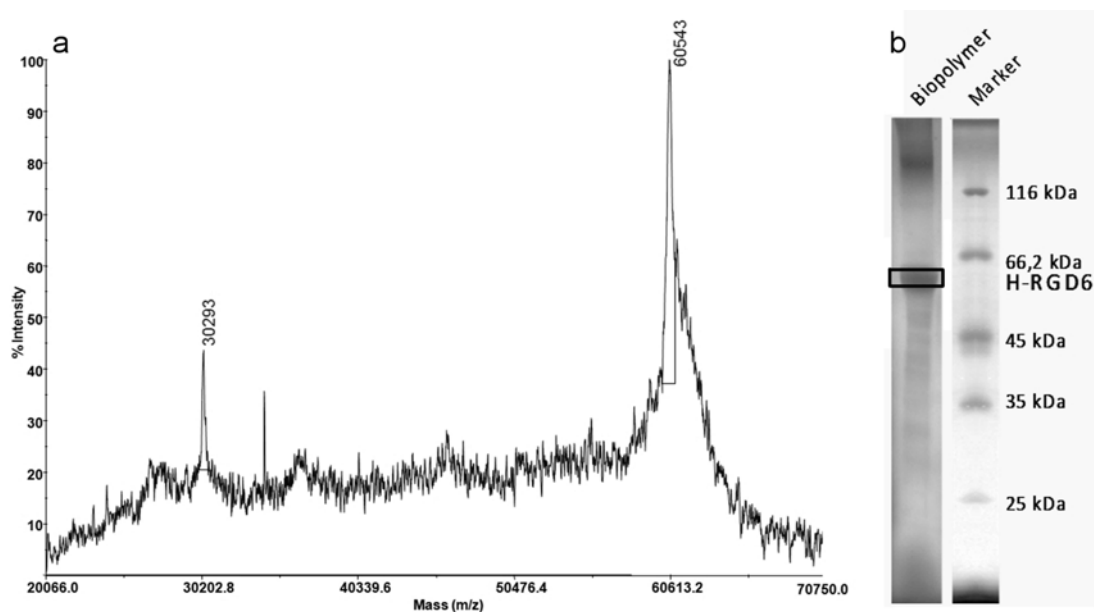


Figure 1.8. Assessment of H-RGD6 purity and molecular weight. The expected mass of the polypeptide was 60611 Da. (a) MALDI-TOF of the biopolymer. Signal at 30293 Da is assigned to doubly charged species. (b) Analysis of biopolymer extract by SDS-PAGE (Costa et al., 2009).

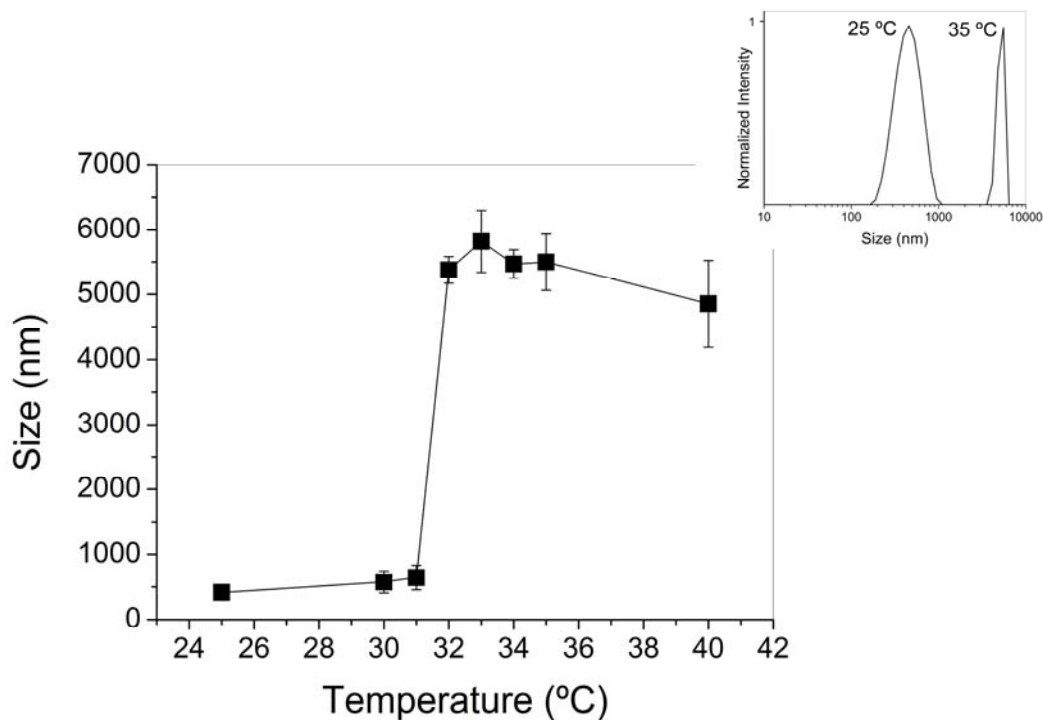


Figure 1.9. Aggregate size profile for a 1 mg/mL H-RGD6 solution in PBS (pH 7.4) in the temperature range 25-40°C. Error bars represent one standard deviation. The inset graphics present representative size distribution profiles at temperatures below and above the T_t (Costa et al., 2009).

The aggregate size measurement indicated a T_t around 32°C with this particular polymer. Across this temperature, a 9-fold increase in the aggregate size from around 650 nm to 5400 nm was found. Figure 1.9 insert also shows the representative size distribution at 25 and 40°C, indicating a quite narrow and monomodal distribution of the size of the objects in solution below and above the T_t (Costa et al., 2009).

1.3.3. Scaffold Production Techniques Used in Oral Mucosa Engineering

Several techniques have been developed to fabricate scaffolds for tissue engineering such as solvent-casting and particulate-leaching, gas foaming, fiber meshes/fiber bonding, phase separation, melt molding, emulsion freeze drying, solution casting and freeze-drying (Buckley and Kelly, 2004). For oral mucosa

engineering, in most cases, freeze drying has been employed as the fabrication method to create porous scaffolds.

1.3.3.1. Freeze-drying

Scaffolds for tissue engineering may be produced by a multitude of different and novel techniques which aim to mimic the natural ECM. As a result, the spectrum of scaffold types available with very different properties has expanded (Weigel et al., 2006). Freeze-drying of aqueous solutions of natural biopolymers such as collagen has been reported for the production of well-defined porous matrices, pore sizes and orientation, achieved by the controlled growth of ice crystals during the freeze-drying process (Chen et al., 2002). In this process, the solution to be frozen contains the polymer such as collagen and the solvent, freezing traps the polymer in the spaces between the growing ice crystals and forms a continuous interpenetrating network of ice and the polymer. A reduction in the chamber pressure causes the ice to sublime, leaving behind the polymer as highly porous foam (Freyman et al., 2001) (Figure 1.10).

Freezing temperature, solute and polymer concentration were shown to strongly influence the porous structure of the scaffold obtained by freeze-drying. Freezing of a collagen solution in a -20°C freezer resulted in larger pore sizes than fast freezing using a mixture of dry ice and ethanol (-80°C), and the most rapid freezing procedure, using liquid nitrogen, lead to the smallest pores (-196°C) (Faraj et al., 2009). When the freezing temperature was kept constant, and the collagen was dissolved either in water or in acetic acid, it was observed that the morphology of a scaffold from a collagen suspension in water displayed more thin thread-like structures than a scaffold from a collagen suspension in diluted acetic acid. The walls of the pores and lamellae were more compact and smoother in the diluted acetic acid scaffold (Faraj et al., 2009). The same authors showed that the addition of ethanol (2.8%) in a collagen solution resulted in closed surfaced foams. Solute concentration was also shown to influence the pore size in scaffolds produced by freeze-drying. An inverse relationship was found between collagen concentration and pore size (Madaghiele et al., 2008).

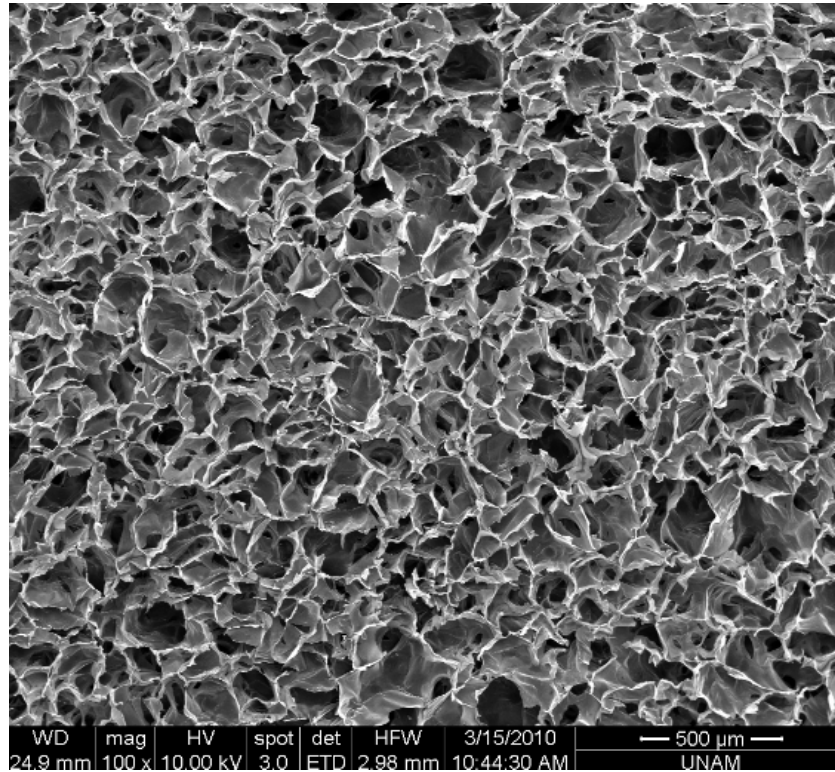


Figure 1.10. Collagen foam obtained via freeze drying of collagen solution

1.3.3.2. Electrospinning

Cells cultured in 3D environments behave differently than those cultured in a 2D environment, adopting more *in vivo* like morphologies. The environment affects the cell-receptor ligation, intercellular signaling, cellular migration and also the diffusion and adhesion of proteins, growth factors and enzymes needed for cell survival and function (Nisbet et al., 2009). The 3D fibrous scaffolds composed of nanoscale multifibrils prepared with the aim of mimicking the supramolecular architecture and the biological functions of the natural ECM as much as possible, have attracted a great deal of attention especially in the field of tissue engineering. Electrospinning is a technique to produce ultrafine fibers in the nanometer or micrometer range by electrically charging a suspended droplet of polymer melt or solution. A high-voltage electrostatic field created between a metallic nozzle of a syringe and a metallic collector is used to generate sufficient surface charge to overcome the surface tension in a pendent drop of the polymer fluid. Nanofibers are

formed by the narrowing of the ejected jet stream as it undergoes increasing surface charge density due to the evaporation of the solvent (Weigel et al., 2006) (Figure 1.11). Work on electrospinning of collagen type I indicated the ability to electrospin reproducibly nanostructured scaffolds that retain their biological and structural properties (Matthews et al., 2002). The concentration of the collagen solutions used in this study ranged in from 0.03 to 0.10 g/mL in hexafluoropropanol (HFP) and resulted in mats and scaffolds consisting of 100 nm to 5 μ m diameter fibers. Calf skin type I collagen electrospun in this study has been analyzed with transmission electron microscopy and revealed the 67 nm banding that is characteristic of native collagen. The authors therefore concluded that an electrospun collagen mat might be a true biomimetic scaffold, because sub-micron diameter fibers retaining their natural collagen ultrastructure could be created.

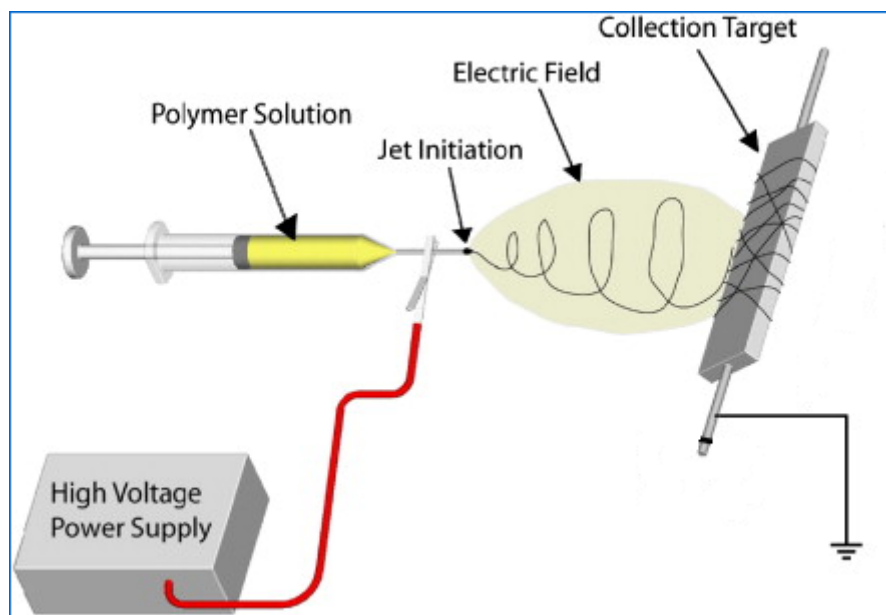


Figure 1.11. Basic electrospinning setup (Barnes et al., 2007)

HFP is widely accepted as the solvent of choice for electrospinning collagen. HFP is an organic, volatile solvent with a boiling point of 61°C. Such a low boiling point is a desirable characteristic in electrospinning applications because it promotes the evaporation of the solvent in the jet under conventional atmospheric conditions and results in the deposition of polymer fibers reaching the

collector in a dry state (Matthews et al., 2002). Since most of HFP evaporates during electrospinning, the trace amount which might remain in the electrospun mats was found not to be toxic to cells even without any further treatment of the scaffold prior to cell seeding (Yang et al., 2009). Others incubated the electrospun mats in a vacuum for 2 days at room temperature to eliminate the remaining HFP (Han et al., 2007).

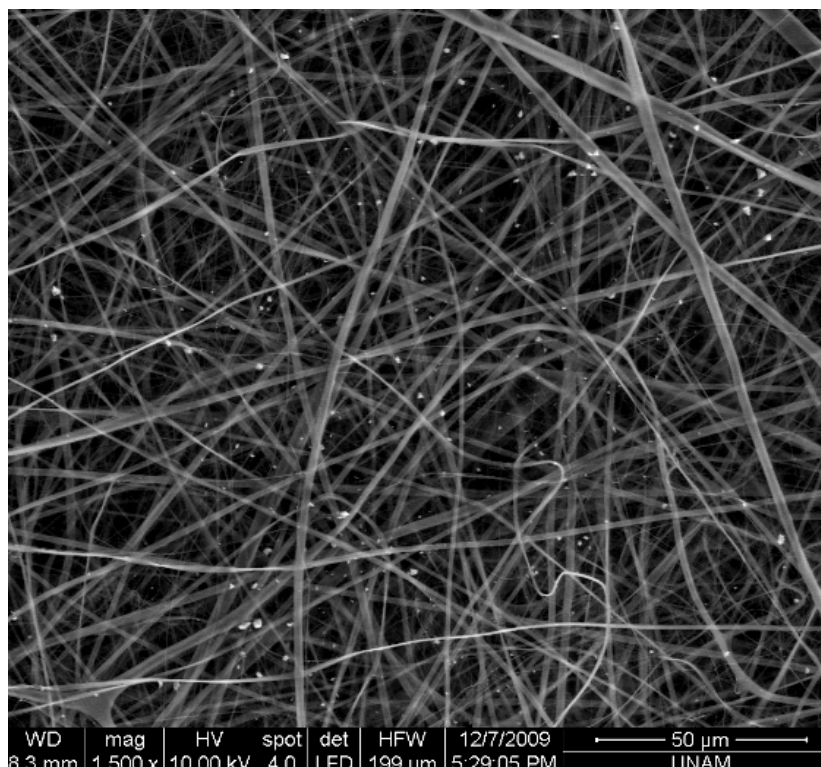


Figure 1.12. Collagen fibers obtained via electrospinning of collagen solution

It should be noted that cells cultured on electrospun scaffolds may not always penetrate into the scaffold and may accumulate at the surface due to short distances between the fibers of these scaffolds. But even this may be acceptable because the cells may receive nutrients and growth cues from the three-dimensional structure whereas the cells on 2D surfaces do not have this opportunity (Nisbet et al., 2009). Besides it is possible to increase the porosity of these scaffolds whereas it is not possible to do it on 2D scaffolds.

The majority of skin equivalents and almost all oral mucosal equivalents are based on freeze-dried biopolymer foams with random but interconnected pores. Fiber-based scaffolds can have advantages over foams such as greater homogeneity, higher porosity, higher interconnectivity and reproducibility (Tuzlakoglu and Reis, 2009).

The studies on skin equivalents based on electrospun scaffolds gave promising results indicating their potential for oral mucosa engineering. In a very recent study, skin substitutes were fabricated using either freeze-dried (FD) or electrospun (ES) collagen scaffolds (Powell et al., 2008). The results indicate that ES scaffolds can be used to fabricate skin substitutes with optimal cellular organization and have more potential to reduce wound contraction than FD scaffolds. These advantages are expected to lead to reduced morbidity in patients treated with such skin substitutes (Powell et al., 2008). Another recent study found that collagen nanofibrous matrices were very effective as wound-healing accelerators in early-stage wound repair (Rho et al., 2006). The authors report that crosslinked collagen nanofibers coated with ECM proteins, particularly type I collagen, may be a good candidate for biomedical applications, such as wound dressings and scaffolds for tissue engineering (Rho et al., 2006). Other non-collagenic nanofibrous materials were also shown to be effective as skin substitutes. Indeed, high cell attachment and spreading of human oral mucosal keratinocytes and fibroblasts were observed on nanofibrous chitin scaffolds, and the cellular response was even higher when the scaffold was treated with collagen type I (Noh et al., 2006). PLGA-PLLA electrospun scaffolds were able to support keratinocyte, fibroblast and endothelial cell growth and extracellular matrix production (Blackwood et al., 2008). Other nanofibrous materials such as collagen/silk fibroin (Yeo et al., 2008), carboxyethyl chitosan/poly(vinyl alcohol) (Zhou et al., 2008), gelatin (Powell et al., 2008), PLGA/chitosan (Duan et al., 2007), poly(ϵ -caprolactone) (Kim et al., 2007) were also found to promote keratinocyte and/or fibroblast attachment and proliferation, indicating the potential of nanofibrous mats as future wound dressings for oral mucosa and skin regeneration.

CHAPTER 2

MATERIALS AND METHODS

2.1. Materials

Dispase, trypsin-EDTA (0.05%), Dulbecco's Modified Eagle Medium (DMEM) and F12 nutrient mixture were purchased from GIBCO® Invitrogen (USA), triiodo thyronine, bovine serum albumin, methylthiazolyldiphenyl-tetrazolium bromide (MTT) and 1,1,1,3,3,3 hexafluoro-2-propanol (HFIP) were supplied by Sigma (USA). Fetal calf serum and bovine calf serum were obtained from (Hyclone), hydrocortisone was from Upjohn (USA), insulin (Umuline) from Lilly (France), selenium from Laboratoire Aguetant (France), isoprenaline hydrochloride (Isuprel) from Sterling Winthrop (USA), epidermal growth factor (EGF) from Austral Biologicals (USA) and ascorbic acid from Bayer (Germany). Penicillin G and streptomycin were purchased from Panpharma (France) and amphotericin B from Bristol Myers Squibb (USA). Collagenase A was supplied by Roche Diagnostics (Switzerland), cell strainer by BD Biosciences (USA), and type III bovine collagen, chitosan (95% deacylated) and chondroitin 4,6 sulfates by LPI (France). Optimal cutting temperature (OCT) compound Sakura (Japan) and buffered formalin were purchased from LABOnord (France). The SuperFrost® Plus slides were obtained from Menzel-Gläser (Germany). Anti-filaggrin, anti-cytokeratin 10 and anti-Ki67 were supplied by Novocastra (UK), anti-cytokeratin 13, anti-laminin 5 and normal goat serum (NGS) from Chemicon (USA), anti-cytokeratin 12 from SantaCruz (USA) and anti-cytokeratin 3 from Progen

(Germany). Diaminobenzidine (DAB) enzyme substrate and AlexaFluor 488 IgG were purchased from Dako (Denmark) and Invitrogen (USA), respectively. Propidium iodide (PI) and Hoechst 33258 stains were obtained from Vector Laboratories (USA). Acetic acid and ethanol were purchased from Merck (USA), syringes and needles from Ayset AS (Turkey). Genipin was supplied by Wako Chemicals (Germany).

Human oral mucosa biopsies were obtained from Hospices Civils de Lyon (HCL) (France) with informed consent from patients undergoing oral surgery. Collagen type I was either purchased (LPI, Lyon, France) or isolated from Sprague Dawley rat tails. MIMEDISC® foams were provided by BASF-BCS (France). Elastin-like recombinamer containing RGD amino acid sequences (complete amino acid sequence is MESLLP [(VPGIG) 2 (VPGKG) (VPGIG) 2] 2AVTGRGDSPASS [(VPGIG) 2 (VPGKG) (VPGIG) 2] 2] 8V) was a kind gift of Prof. Carlos Rodríguez-Cabello, and was produced and isolated from *Escherichia coli* (*E. coli*) at the University of Valladolid (Spain).

2.2. Methods

2.2.1. Scaffold Preparation

Collagen-glycosaminoglycan (GAG)-chitosan MIMEDISC® scaffolds were prepared and provided by BASF-BCS (France) and collagen-elastin-like recombinamer scaffolds were designed and prepared at METU (Turkey).

2.2.1.1. Preparation of MIMEDISC® Scaffolds

Collagen-GAG-chitosan MIMEDISC® substrates were prepared by BASF-BCS (France) as previously described (Collombel et al., 1989). Briefly, bovine collagens type I and III, chitosan (95% deacylated) and chondroitin-4,6-sulfates were dissolved in water and mixed. The gel, which contained 72% collagen, 20% chitosan and 8% GAG, was poured into Snapwell inserts and frozen overnight at -70°C. The frozen plates were then lyophilized, submerged in 70%

ethanol for 24 h, rinsed and equilibrated in 5 mL of DMEM, and incubated at 37°C with 5% CO₂ for a minimum of 24 h.

2.2.1.2. Preparation of Collagen-Elastin-like Recombinamer Scaffolds

2.2.1.2.1. Collagen

In the present studies, type I collagen isolated from rat tails according to the following procedure was used as the scaffold material.

2.2.1.2.1.1. Isolation

Type I collagen was isolated from male Sprague-Dawley rats after terminating the rats by ether inhalation. Rat tails were dissected and tendons were placed in cold acetic acid (0.5 M) for several days at 4°C with stirring to dissolve the tendons and after that the solution was filtered to remove any insoluble material. Then the collagen solution (500 mL) was dialyzed against a buffer (5 L, 12.5 mM NaH₂PO₄, 11.5 mM Na₂HPO₄, pH 7.2) at 4°C. After the collagen precipitated out of the solution as a white solid it was centrifuged at 16000 x g for 10 min at 4°C. Pellet was dissolved in cold acetic acid (500 mL, 0.15 M) at 4°C overnight. NaCl (25 g, solid) was added to give a final concentration of 5% and this was incubated at 4°C overnight to dissolve the salt. Collagen was precipitated after this step. Final pellet was dissolved in cold acetic acid (500 mL, 0.15 M) at 4°C overnight and dialyzed for 5 consecutive days at 4°C. Collagen solution was centrifuged again and the pellet was stirred in 70% EtOH for 48 h. After a final centrifugation step, final pellet was frozen at – 80°C and lyophilized for 12 h.

2.2.1.2.1.2. SDS-PAGE Analysis of Isolated Collagen Type I

Purity of the isolated type I collagen was determined by SDS-PAGE. Separating (10 % acrylamide/bisacrylamide) and stacking (4.2 % acrylamide/bisacrylamide) gels were prepared and the isolated collagen was loaded

in 0.2 % (in 0.15 M acetic acid) concentration after denaturing at 95° C for 5 min. Samples were run at 30 mA for 2.5 h. Later the gel was stained with 0.2 % Coomassie Brilliant Blue by incubating overnight on a shaker and destained in a solution of 40 % water, 50 % methanol and 10 % acetic acid.

2.2.1.2.2. Elastin-like Recombinamer

The elastin-like recombinamer (ELR) used in the preparation of the scaffolds was produced by and isolated from *Escherichia coli* (*E. coli*) and characterized at the University of Valladolid (Spain) according to the following procedures. The ELR contains 6 monomers of RGD, a histidine-tag, 6 aspartic acids, 24 lysines and 7 histidines, which are charged residues, being designated as H-RGD6 (Costa et al., 2009). Expression conditions and purification protocols were adapted from McPherson et al. (1992) and Girotti et al. (2004). Gene expression of a recombinant *Escherichia coli* strain BLR (DE3) containing the expressing gene of H-RGD6 was induced in a 12 L Applikon fermentor, in terrific broth medium (TB) with 0.1% of carbenicilin and 0.1% of glucose, under controlled conditions of temperature (37°C) and pH (7.00). The fermentation was stopped after registering an optical density variation, at 600 nm inferior to 0.25, in a time frame of 1 h. Subsequent to fermentation, the culture was harvested by centrifugation, resuspended and lysed by ultrasonic disruption. Insoluble debris was removed by centrifugation and the cleared lysate was subjected to several cycles of cold and warm centrifugations, (4 and 40°C). All the purification steps were carried out in a sodium chloride (NaCl) solution at 0.5 M. The polymer solution was then frozen at -24°C and lyophilized.

SDS-PAGE was performed to assess H-RGD6 purity after purification. For this test, 5 µL of a H-RGD6 solution at 1 mg/mL were loaded in a polyacrylamide gel. The identification of an intense band around 60 kDa was expected to confirm the presence of the polymer and its purity.

To further assess H-RGD6 purity and molecular weight, Matrix-Assisted Laser Desorption/Ionization Time-of-Flight (MALDI-TOF) mass spectroscopy was

performed in a Voyager STR, from Applied Biosystems, in linear mode and with an external calibration using bovine serum albumin (BSA).

H-RGD6 aggregate size in solution was measured using a Nano-ZS from Malvern (United Kingdom), for a range of temperatures between 25 and 40°C, with a stabilization time of 5 minutes. H-RGD6 samples were prepared at 1 mg/mL in phosphate buffer solution (PBS, pH 7.4). Twelve runs were performed for each sample to determine the particle/aggregate size, in order to obtain a final average value at constant temperature.

2.2.1.2.3. Preparation of ELR-Collagen Foams

Macroporous ELR containing collagen scaffolds were prepared in two ways: by either incorporating the ELR into the scaffold by adding it to collagen solution, or by adsorbing it onto the surface of the collagen foams after formation. According to the final approach, to incorporate it in the scaffold, 13.5 mg/mL collagen and ELR were dissolved in acetic acid (0.5 M) and phosphate buffered saline (PBS, pH 7.2), respectively and three volumes of collagen solution were vigorously mixed with one volume of ELR solution. The mixture was then frozen at -20°C for 24h and lyophilized for 13 h.

According to the second approach, to adsorb the ELR onto collagen foam surface, collagen solutions (1.35%) in acetic acid (0.5 M) were lyophilized as above. The resulting foams were then immersed in the ELR solution (0.1% in PBS) at 37°C for 2 h. Collagen foams (1.35%) without ELR were prepared as controls.

To obtain closed surfaced foams, 10% ethanol (v/v) was present in the protein solution during foam preparation and the foams were frozen at -80°C for 24 h prior to lyophilization, instead of -20°C, to close the pores on the surface. Addition of ethanol in foam solution before lyophilization was previously shown to result in closed surfaced scaffolds, and lower freezing temperatures to yield smaller pores (Faraj et al., 2007).

2.2.1.2.4. Preparation of ELR-Collagen Fibrous Mats

ELR containing fibrous mats were prepared via electrospinning collagen and collagen-ELR solutions to investigate the influence of ELR incorporation on fibrous scaffold properties. Collagen (9.3%) and ELR (13.2%) were prepared in 1,1,1,3,3,3-hexafluoro-2-propanol and PBS (pH 7.2), respectively; and four volumes of collagen solution were mixed with one volume of ELR solution so that the final total protein concentration was 10% and the collagen/ELR ratio was always 3:1 (w/w) as in the foams.

Pure collagen fibrous mats, having the same protein concentration (10%), were also prepared as controls. Electrospinning was performed by loading the solution in a 10 mL syringe fitted with a 3 cm 18 G blunt-end needle and dispensing at a rate of 20 μ L/min, applying a voltage of 22.5 kV and the fibers were collected on a flat plate at a distance of 10 cm.

2.2.1.2.5. Preparation of ELR-Collagen Foam-Fiber Bilayer Scaffolds

ELR containing foam-fiber bilayer scaffolds were prepared by electrospinning the above described ELR-collagen solutions directly onto the foams which were attached to the collector. In this way, the upper part of the resulting bilayer scaffold was fibrous and the lower part was porous. The fibers were collected onto two types of foams: porous and closed surfaced ones.

2.2.1.2.6. Crosslinking of the ELR-Collagen Scaffolds

Collagen and collagen-ELR scaffolds were crosslinked in various ways: chemically by using genipin, physically via dehydrothermal treatment (DHT) or by the combination of both. For genipin crosslinking, genipin was dissolved in either 70% ethanol as commonly reported in literature, or in PBS to prevent closing of the pores on the surface of the foams. Genipin solution was added to the collagen-ELR solution, vigorously mixed to have a final concentration of 0.1% w/v and the mixture was incubated at room temperature (RT) for 48 h before lyophilization.

Addition of the crosslinker before lyophilization, instead of afterwards, was reported to better conserve the foam dimensions (Vrana et al., 2008). To crosslink fibrous mats, genipin was either added to the collagen solution prior to electrospinning, or afterwards (0.1% w/v, 48 h, RT). For DHT crosslinking, foams and fibrous mats were incubated at elevated temperatures in a vacuum oven under 27 in.Hg pressure. Different temperatures and incubation times (105°C for 24 h, 105°C for 72 h, 150°C for 24 h, 150°C for 48 h) were tested. The two methods were also combined; DHT (150°C, 24 h) was followed by genipin crosslinking (0.1%, 48 h, RT).

To determine whether the scaffolds would maintain their integrity during tissue culture, crosslinked scaffolds were incubated in PBS at 37°C for 1 month.

2.2.1.3. Characterization of Collagen-ELR Scaffolds

2.2.1.3.1. Foam Thickness

Thicknesses of the scaffolds were measured using a standard micrometer with a sensitivity of 0.1 μm .

2.2.1.3.2. Pore Size and its Distribution

Pore size and its distribution in the foams were determined with a mercury porosimeter (Poremaster 60; Quantachrome) under low pressure (50 psi) at METU Central Lab.

2.2.1.3.3. Morphology and Microstructure of Scaffolds

Morphology, the surface and inner microstructures of the foams and fibrous scaffolds were studied with a FEI Quanta 200F (USA) scanning electron microscope (SEM) at UNAM (Bilkent Univ.) after sputter-coating (12 nm) with gold-palladium. Fiber diameters and pore sizes were measured using the image

processing program NIH ImageJ using 4 different areas of the image to obtain the average values.

2.2.1.3.4. Mechanical Properties under Compression

A mechanical testing system (LRX 5K, Lloyd Instruments Ltd, UK), controlled by a computer running program (WindapR), was used to perform compression tests on the scaffolds. The cell load was 5 kN and the crosshead displacement rate was 10 mm/min. Elastic modulus (E^*), flexibility ($1/E^*$), elastic collapse stress and strain (σ_{el}^* , ϵ_{el}^*), and the collapse plateau modulus ($\Delta\sigma/\Delta\epsilon$) of the scaffolds were calculated from the load-strain graphs as previously described for low-density, open-cell foams (Harley et al., 2007).

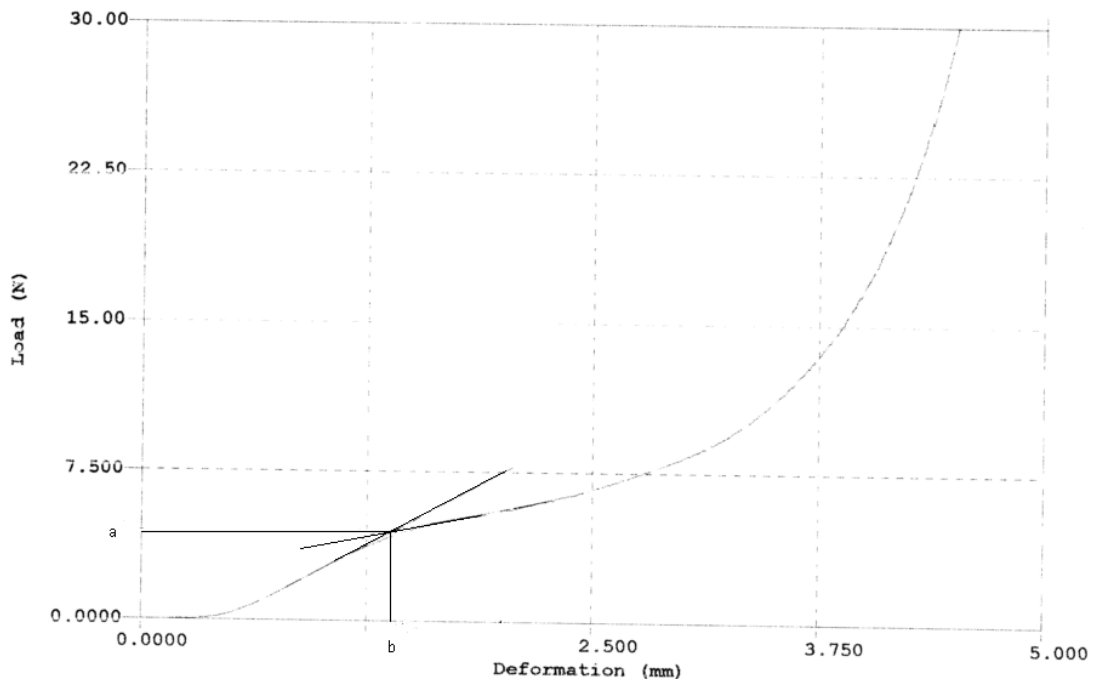


Figure 2.1. Characteristic stress-strain curve observed for a dry collagen-based scaffold under compression. Elastic collapse stress (σ_{el}^*) and strain (ϵ_{el}^*) were denoted as a and b on the graph, respectively.

2.2.2. *In Vitro* Studies

All cells were isolated from human biopsies which were obtained with informed consent from patients.

2.2.2.1. Origin, Isolation and Culture of Human Oral Epithelial Cells

Epithelial cells were isolated from human oral mucosal biopsies removed from the nonkeratinized cheek region of the mouth, and obtained from patients undergoing oral surgery. The biopsies were first measured, and then cut into small pieces in order to increase the effectiveness of the enzymes used. The separation of the epithelium from the lamina propria was performed by incubation with dispase (10 mg/mL, 3 h, 4°C). After separation, epithelium was treated with trypsin (0.5 g/L) - EDTA (0.2 g/L) for 20 min to extract the cells, which were collected every 10 min. Epithelial cells were grown at 6000-8000 cells/cm² on a feeder layer of irradiated human fibroblasts in a specially designed medium as follows: DMEM-Ham-F12 2.78/1, 10% fetal calf serum, 0.4 µg/mL hydrocortisone, 0.12 UI/mL insulin (Umuline), 0.033 µg/mL selenium, 0.4 µg/mL isoprenaline hydrochloride (Isuprel), 2 x 10⁻⁹ M triiodo thyronine, 10 ng/mL epidermal growth factor, and antibiotics. The cells were trypsinized at confluence and seeded on the foams at passage 2 or 3.

2.2.2.2. Origin, Isolation and Culture of Human Oral Fibroblasts

Oral fibroblasts were isolated from the same human oral mucosa biopsies as epithelial cells. After epithelium-lamina propria separation, isolation was performed by treating with collagenase A (0.1 U/mL, 20 min, 37°C) with continuous stirring. The digest was purified by filtering through a 70 µm cell strainer. This procedure was repeated 6 times, and then the digest was immediately placed in a monolayer culture. Fibroblasts were seeded at a density of 10000 cells/cm² and cultured in fibroblast medium composed of DMEM, 10% newborn

calf serum (NCS), and antibiotics. The medium was changed every two days until cell confluence was reached. At confluence, cells were resuspended using trypsin 0.5 g/L - EDTA 0.2 g/L, then amplified over three passages (from P₀ to P₂) and seeded onto the matrix at P₃.

2.2.2.3. Origin, Isolation and Culture of Human Dermal Fibroblasts

Dermal fibroblasts which had been isolated from human foreskin biopsies according to Black et al., 2005 were used in the *in vitro* studies. They were seeded at a density of 10 000 cells/cm² and cultured in fibroblast medium composed of DMEM, 10% newborn calf serum (NCS), and antibiotics. The media were changed every two days until cell confluence was reached. At confluence, cells were resuspended using trypsin 0.5 g/L - EDTA 0.2 g/L, then amplified over three passages and seeded into the substrate foam at passage 3.

2.2.2.4. Origin, Isolation and Culture of Human Stromal Keratocytes

Stromal keratocytes which had been isolated from human cornea biopsies as reported earlier (Builles et al., 2007) were used in the *in vitro* studies. They were seeded at a density of 10000 cells/cm² and cultured in keratocyte medium designed by Builles et al., 2007 and composed of DMEM–Ham-F12 1/1, 10% newborn calf serum (NCS), 5 ng/ml b-FGF, and antibiotics. The media were changed every two days until confluence was reached. At confluence, cells were resuspended using trypsin 0.5 g/L - EDTA 0.2 g/L, then amplified over three passages and seeded onto the substrate foam at passage 3.

2.2.2.5. Preparation of Lamina Propria, Dermal and Stromal Equivalents

Lamina propria, dermal and corneal stromal equivalents (LPE, DE and CSE) consisted of collagen-based foams in which human oral mucosa fibroblasts, human dermal fibroblasts and human corneal stroma keratocytes were cultured, respectively. These constructs were prepared by adding a cell suspension of 2.5 x

$10^5/\text{cm}^2$ onto the foams. LPEs and DEs were cultured for 21 days in a medium composed of DMEM, 10% fetal calf serum, 10 ng/mL epidermal growth factor, 50 $\mu\text{g}/\text{mL}$ ascorbic acid, and CSEs in keratocyte medium supplemented with ascorbic acid. Culture medium was changed daily until the seeding of oral epithelial cells.

2.2.2.6. Preparation of Epithelialized Equivalents

Human oral epithelial cells were seeded on lamina propria, dermal and stromal equivalents at a concentration of $2.5 \times 10^5/\text{cm}^2$. The resulting constructs were cultured in the epithelial cell medium supplemented with 50 $\mu\text{g}/\text{mL}$ ascorbic acid under submerged conditions for 7 days. They were then elevated at the air-liquid interface for the remaining 14 days in another medium with DMEM-Ham-F12 2.2/1, 8 mg/mL bovine serum albumin, 0.4 $\mu\text{g}/\text{mL}$ hydrocortisone, 0.12 UI/mL insulin (Umuline), 50 $\mu\text{g}/\text{mL}$ ascorbic acid, and antibiotics. As a result, three epithelialized models were obtained: oral epithelial cells cultured on (a) lamina propria equivalent (OLPE), (b) dermal equivalent (ODE), and (c) corneal stromal equivalent (OCSE).

2.2.2.7. Assessment of Cell Viability

Cell viability on collagen-based scaffolds was assessed by using the MTT cell viability assay. Human oral fibroblasts were seeded on scaffolds as presented in the earlier sections. On days 7 and 14, the cell-seeded scaffolds were briefly rinsed with PBS and incubated in freshly prepared MTT solution (1 mg/mL in PBS) for 2 h at 37°C. The formazan produced by live cells was extracted using acidified isopropanol by transferring the cell seeded scaffolds into 15 mL tubes containing 2 mL acidified isopropanol and incubating for 30 min at room temperature on a mechanical stirrer. Samples of 100 μL were taken from the solution containing the cell seeded scaffolds and put into the wells of a 96-well plate. The optical density (OD) values at 550 were determined spectrophotometrically.

2.2.3. Characterization of Tissue Equivalents

2.2.3.1. Histology

Tissue equivalents were fixed in 4% formaldehyde solution and embedded in paraffin. Sections, 5 µm thick, were cut and stained using hematoxylin-phloxin-saffron (HPS).

2.2.3.2. Immunohistochemistry

The primary antibodies used in these studies were anti-filaggrin (dilution 1:25), anti-cytokeratin 3 (dilution 1:100), anti-cytokeratin 10 (dilution 1:50), anti-cytokeratin 12 (dilution 1:100), anti-cytokeratin 13 (dilution 1:75), anti-laminin 5 (dilution 1:100) and anti-Ki67 (dilution 1:25). For the detection of K3, K10, K12, K13 and laminin 5, tissue equivalents were embedded in optimum cutting temperature compound (OCT) and frozen at -20°C. Then, sections of 5 µm thickness were fixed in acetone for 10 min at -20°C and blocked in phosphate buffered saline containing 4% bovine serum albumin and 5% normal goat serum. All primary antibodies were incubated for 90 min at room temperature. The secondary antibody was AlexaFluor 488 IgG (dilution 1:100). For the detection of filaggrin and Ki67, tissue constructs were fixed in buffered formalin and embedded in paraffin. Five µm thick sections were dewaxed, rehydrated, pretreated at high temperature (95°C) for antigen retrieval. They were then incubated with the primary antibody followed by the secondary antibody AlexaFluor 488 IgG (for Ki67) or the secondary antibody coupled to peroxidase (for filaggrin). In case of the latter, a brown precipitate indicating the distribution of the target protein was obtained with diaminobenzidine (DAB) enzyme substrate. Counterstaining was done with Harris hematoxylin. Propidium iodide or Hoechst 33258 stain was used to counterstain the cell nuclei. In all immunofluorescence stainings, native nonkeratinized human oral mucosa, native human skin and native cornea were used as either positive or

negative controls. Specimens were analyzed with a Zeiss LSM 510 Confocal Laser Scanning Microscope and a Nikon Eclipse Fluorescence Microscope.

2.2.3.3. Transmission Electron Microscopy

Tissue equivalents were fixed with 2% glutaraldehyde-0.1 M sodiumcacodylate/HCl, pH 7.4 for 2 h and postfixed with 1% osmium tetroxide-0.15 M sodiumcacodylate/HCl, pH 7.4 for 1 h. After dehydration in a growing gradient of ethanol, the samples were embedded in Epon and finally polymerized at 60°C for 48 or 72 h. The blocks were cut using an ultramicrotome and sections of 60-80 nm thickness were contrasted with uranyl acetate and lead citrate. Observations were done with transmission electron microscopy (JEM JEOL 1400 and Philips CM 120). Images were recorded using an Orius Gatan camera and 20 fibril diameters were measured using a digital micrograph by two observers on three different regions of lamina propria, and average values were calculated.

2.2.4. Statistical analysis

Numbers of cell layers in the epithelia of the 3 models were counted by 3 people using HPS micrographs of 3 samples for each model and 3 different areas of each image. The statistical analysis of the data was done by Student's *t*-test. The results were expressed as mean \pm standard error of the mean.

CHAPTER 3

RESULTS AND DISCUSSION

3.1. Reconstruction of a Full-thickness Human Oral Mucosal Equivalent Based on a Collagen-Glycosaminoglycan-Chitosan Substrate

In this study, oral fibroblasts and oral epithelial cells isolated from normal human oral mucosa biopsies (cheek region), were co-cultured in a collagen-glycosaminoglycan-chitosan (CGC) foam to construct full-thickness human oral mucosa equivalents.

3.1.1. Histology

Histological analysis showed that the fibroblasts seeded into the collagen-GAG-chitosan foam were able to proliferate, migrate within the substrate, and synthesize new extracellular matrix filling the pores of the substrate, and forming a lamina propria equivalent (LPE) (Figure 3.1a). At the top of this LPE were epithelial cells that proliferated during 7 days of culture under submerged conditions and for 14 days of culture at the air-liquid interface, forming a nonkeratinized multilayered (9 to 10 layers thick) epithelium and giving rise to a full-thickness oral mucosal equivalent (OME). The epithelial cells in the superficial layer were seen to retain their nuclei and stratum corneum was absent as in native nonkeratinized oral mucosa (Figure 3.1c), whereas the skin equivalent cultured under the same conditions (our control of differentiation) is completely

differentiated with a basal layer, a stratum spinosum, a stratum granulosum and a well-developed stratum corneum (Figure 3.1b), as in native skin (Figure 3.1d).

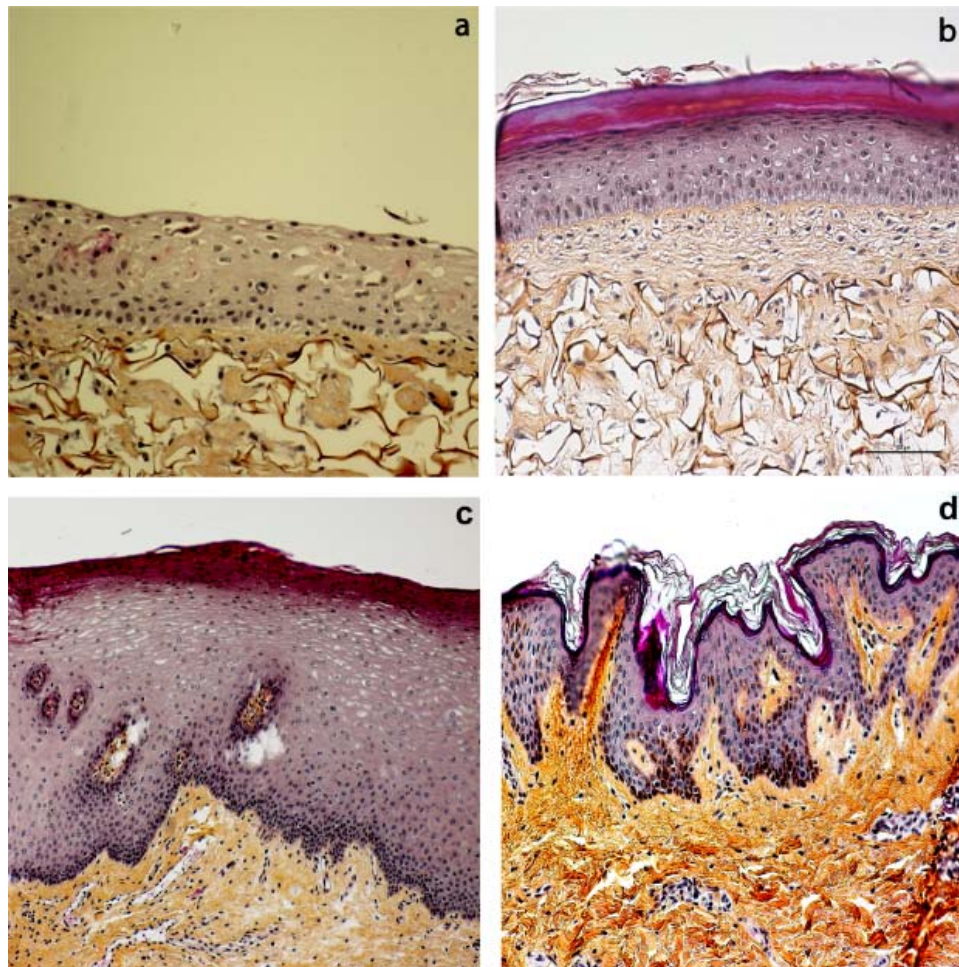


Figure 3.1. Histological analysis of various artificial and natural tissues. a) human oral mucosal equivalent (x200), b) human skin equivalent (x200), c) native human oral mucosa (x100) and d) native human skin (x200). Cell nuclei were stained in blue by hematoxylin, cytoplasm in pink by phloxine and extracellular matrix of connective tissue in orange/yellow by saffron.

3.1.2. Immunohistochemistry

Keratin 3/76 (K3/76, clone AE5), which recognizes both K3 in cornea and K76 in oral mucosa, was strongly expressed in the OME and the native human OM, especially in suprabasal layers (Figure 3.2a and b). It was, however, found to be completely absent in the native human skin (Figure 3.2c) (Table 3.1).

Keratin 10 (K10), marker of keratinized epithelium, was found to be completely absent in both our OME and native oral mucosa (Figure 3.2d and e), but expressed in native human skin (Figure 3.2f) (Table 3.1).

Keratin 13 (K13), the major differentiation-associated marker of nonkeratinized oral mucosa, was very strongly expressed in both OME and native OM (Figure 3.2g and h) but not in skin (Figure 3.2i). Its expression was restricted to suprabasal layers of our construct (basal cells did not express it) (Figure 3.2g) (Table 3.1).

The basement membrane protein laminin 5, the major component of anchoring filaments, was strongly expressed all along the interface between lamina propria and epithelium in the reconstructed oral mucosa, as well as in native oral mucosa and skin (Figure 3.2j,k,l; Table 3.1).

Ki67 antigen, a marker of proliferative cells, was detected in basal cells of the OME as in native oral mucosa and skin. The number of proliferating cells labelled using anti-Ki67 was highest in native oral mucosa, followed by native skin and OME (Figure 3.2m,n,o; Table 3.1).

Table 3.1. Immunohistochemical staining of the human oral mucosal equivalent, native human oral mucosa and native human skin

Markers	Intensity of staining ^a		
	Human oral mucosal equivalent	Native human oral mucosa	Native human skin
K3	++	++	-
K13	+++	+++	-
K10	-	-	+++
Laminin5	+++	+++	+++
Ki67	+	+++	++

a. +++: very strong, ++: strong, +: moderate, -: no expression

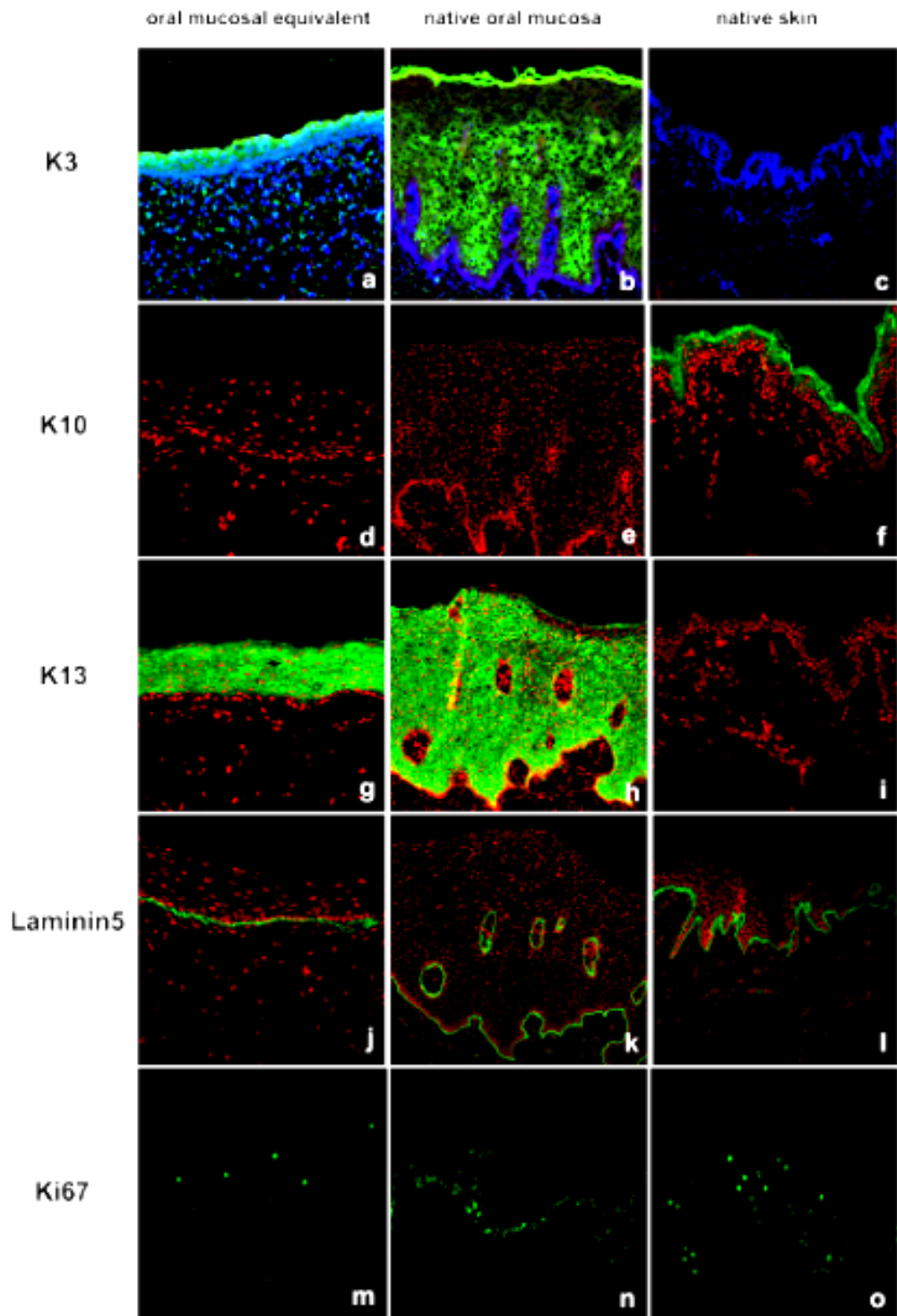


Figure 3.2. Immunofluorescence labelling of keratins 3, 10 and 13; basement membrane protein laminin 5; and proliferating cell antigen Ki67 in the oral mucosal equivalent, native oral mucosa and native skin. Immunolabelling is shown in green, cell nuclei are shown either in blue (K3) or in red (K10, K13, laminin5) (for K3: OME, OM, skin: x100; for K10, K13, laminin5: OME, skin: x200, OM: x100; for Ki67: OME, OM, skin: x200).

3.1.3. Transmission Electron Microscopy

Transmission electron microscopy analysis of the reconstructed oral mucosa showed the ultrastructural organization of the epithelium, lamina propria and basement membrane (Figure 3.3). In the epithelium, the size and shape of the cells changed with location; the cells became larger and flattened as they moved and differentiated towards the oral surface (Figure 3.3a). Observation of numerous desmosomes between adjacent epithelial cells was encouraging (Figure 3.3e and f). No stratum corneum and stratum granulosum were observed, as in the case for nonkeratinized native oral mucosa. A continuous and ultrastructurally well-organized basement membrane was formed on the lamina propria equivalent all along the interface between the epithelium and the lamina propria (Figure 3.3c and d). In the subepithelial layer and in the deep layer of lamina propria of the reconstructed oral mucosa, large amounts of newly synthesized collagen was detected by transmission electron microscopy (Figure 3.3g); striations of the collagen fibrils were visible at higher magnifications (Figure 3.3h). The connective tissue was represented by fibrils of collagen which were straight in some regions and wavy in others. Some of them oriented parallel to the oral surface and some did not (Figure 3.3g). The average collagen fibril diameter in the reconstructed oral mucosa was measured as 28.4 nm.

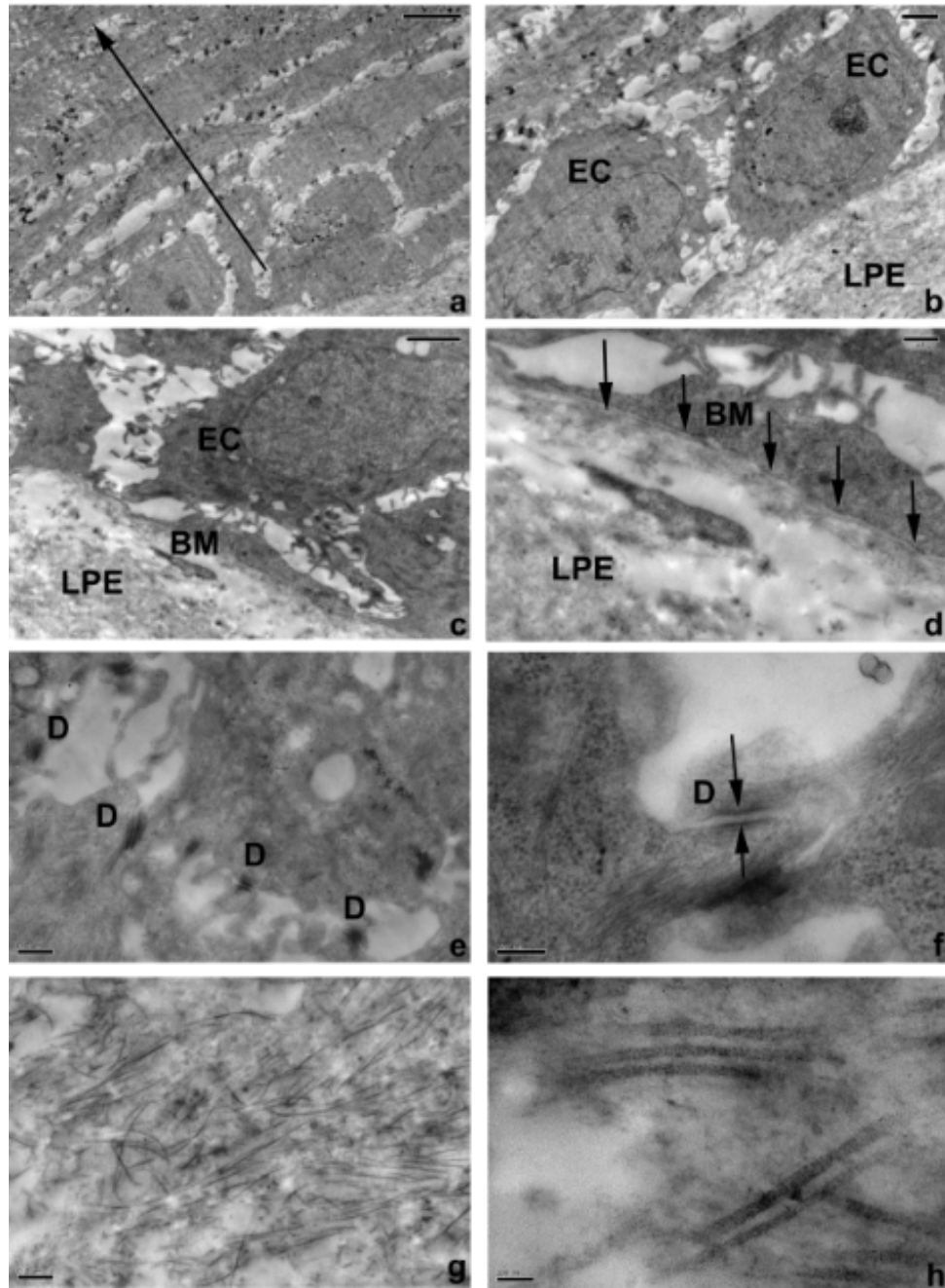


Figure 3.3. Ultrastructural analysis of the oral mucosal equivalent by transmission electron microscopy a) different cell layers and differentiation in the epithelium (arrow: basal to superficial layer direction) (bar = 5 μm), b) two adjacent basal epithelial cells (ECs) residing on the lamina propria equivalent (LPE) (bar = 2 μm), c) basement membrane (BM) formed between the LPE and the epithelium (bar = 2 μm), d) the continuous and well-organized BM at higher magnification (bar = 0.5 μm), e) numerous desmosomes were detected between adjacent epithelial cells (bar = 0.5 μm), f) a desmosome at higher magnification (bar = 200 nm), g) newly synthesized collagen I fibrils in the LPE (bar = 0.5 μm), h) collagen fibril striations visible at higher magnification (bar = 100 nm).

3.1.4. Discussion

The 3-D model constructed of collagen-GAG-chitosan allowed us to reproduce an OME comprising a pluristratified epithelium firmly anchored to a LPE through an ultrastructurally well-organized epithelial/LP junction mimicking native nonkeratinized human oral mucosa. This is the first case where a nonkeratinized epithelium is obtained under optimal conditions for differentiation, with complete exposure of the equivalent's surface to air at the air-liquid interface for a 2 week period in a medium poor in growth factors and serum. Earlier studies on tissue engineered oral mucosa had mostly focused on keratinized OMEs. There is only one study where a nonkeratinized OME was reconstructed using gingival cells and adding medium on the epithelium to mimic oral cavity conditions (Tomakidi et al., 1998). The humidity is known to inhibit differentiation (Régnier et al., 1992). The fact that the epithelial cells are nonkeratinized may be due either to their interaction with fibroblasts of lamina propria, or to their genetic programming. To elucidate this, we decided to compare the differentiation of epithelial cells on dermal, stromal and lamina propria equivalents.

In the epithelium of our model, epithelial cells retained their nuclei and stratum corneum was absent, as revealed by HPS staining (Figure 3.1a). The very strong expression of K13, which is the major differentiation-associated marker of nonkeratinized epithelium in oral mucosa, and the absence of keratin 10, which is expressed only by keratinizing epithelial cells, supported the nonkeratinizing differentiation of the epithelium of the reconstructed oral mucosa even after two weeks at the air-liquid interface (Figure 3.2d and g). The expression of K13 was restricted to suprabasal layers (Figure 3.2g) in accordance with its expression profile reported in literature (Moharamzadeh et al., 2007). Epithelial cells of nonkeratinizing oral epithelium follow a different differentiation pathway than epidermal keratinocytes and keratinocytes in keratinizing oral epithelium (Winning et al., 2000). First, it was argued that the differentiation pathway followed by the epithelial cells was an intrinsic property of the epithelium, and later on it was suggested that both inherent and extrinsic factors play a role in the determination of the differentiation pathway of oral epithelium and that the expression of some

keratins, such as K13, are determined extrinsically by factors derived from the underlying connective tissue (Winning et al., 2000). Here, it was found that epithelial cells of oral mucosa, when seeded on stroma equivalents (collagen-GAG-chitosan scaffold populated with keratocytes of corneal stroma), they nevertheless expressed K13 strongly (Figure 3.4). This means that strong expression of K13 by OM epithelial cells is independent of fibroblast-epithelial cell interactions. However, the results demonstrate the influence of fibroblast-epithelial cell interactions on the thickness of the epithelium. Indeed, if we compare the thickness of the epithelia formed by culturing the same oral mucosal epithelial cells under the same conditions either on stroma equivalents (SEs) or on LPEs, the resulting epithelium was very thin (1-2 layers) on stroma equivalents as in native cornea; whereas, the epithelium formed on lamina propria equivalents was thicker (9-10 layers) resembling more the native OM (Figure 3.4). These results indicate that cell interactions interfere with the thickness of the epithelium. It has also been suggested that nonkeratinized oral lining tissue turns over more rapidly than does the keratinized mucosa and this higher rate of proliferation probably results in thicker epithelium (Rowat and Squier, 1986). In order to demonstrate this, it would be interesting to culture limbic cells both on a SE and a LPE. The fact that higher number of cells expressing Ki67 were found in native nonkeratinized oral mucosa compared to native skin, which is a keratinized tissue, supports this suggestion (Figure 3.2n and o). Ki67 antigen, a marker of proliferative cells, was detected in the basal cells of the OME as in native oral mucosa and skin, indicating that the OME was capable of self-renewal (Figure 3.2m). However, although the spatial distribution of proliferating cells in the OME was very similar to native tissues; their number was found to be higher in native tissues. The progressive decrease in the number of cells expressing Ki67 has already been shown in the course of kinetics of proliferation in an oral mucosa model (Tomakidi et al., 1998), passing from a maximum proliferative state in the first week to a few cells at the end of third week, as was observed in this study. This is due to the fact that the highest proliferation rate in a developing oral mucosa is at the early stage of epithelial formation (1 week after epithelial cell seeding) and it decreases progressively as time passes (Tomakidi et al., 1998). In the present model, Ki67 antigen detection

was performed at the end of epithelial formation (3 weeks after epithelial cell seeding), revealing lower number of cells retaining proliferative capacity. What we wanted to show was that even after such a longtime, the cells were still able to proliferate, so that if we transplant this oral mucosal equivalent *in vivo*, the epithelium will still be able to self-renew.

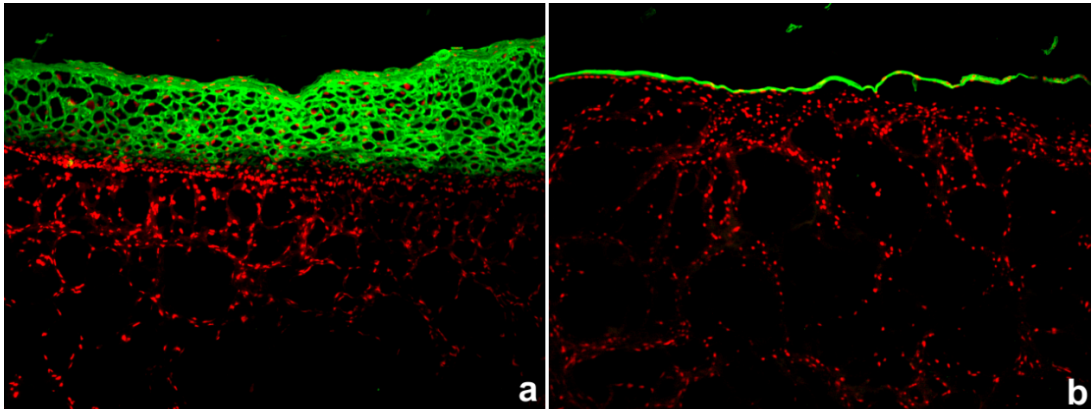


Figure 3.4. Oral epithelial cells cultured under same conditions on mesenchymal tissue equivalents. a) on a lamina propria equivalent forming a thick epithelium (x100), b) on a stromal equivalent forming a thin epithelium (x100). However, expression of K13 strongly in both cases was observed. Immunolabeling for K13 is shown in green and cell nuclei are stained in red with PI.

Keratin 3/76 is the most commonly used antibody prepared from AE5 clone (K3/76, AE5). It was expressed in native oral mucosa and in the OME. The present results are in accordance with a previous study where the expression of keratin 3 has been shown in oral mucosal epithelial cell sheets (Hayashida et al., 2005), suggesting that keratin 3, which is known as a specific marker of corneal epithelia cells, is also a marker of oral mucosa. Here, the results of the present study show for the first time the expression of K3/K76 in an oral mucosal equivalent (Figure 3.2a). In fact, it was recently reported that this antibody from the AE5 clone detects not only the expression of K3, but also that of the related K76 (formerly K2p), which is specifically expressed in suprabasal layers of oral masticatory epithelium (Moll et al., 2008). So, it is possible that the labelling observed in our OME was due to the reaction of the antibody with K76 and not with K3.

On the other hand, using TEM several desmosomes could be observed at the epithelium level (Figure 3.3e), these intercellular junctions are crucial for epithelial adhesion and barrier function in stratifying epithelia (Niessen 2007).

The basement membrane formed in the present model was continuous and ultrastructurally well-organized all along the interface between epithelium and the LPE, as shown by both immunolabeling for the classical basement membrane marker laminin 5 (Figure 3.2j), and TEM (Figure 3.3d). This ultrastructural organization was previously shown to be the result of the interaction between fibroblasts and keratinocytes (Sahuc et al., 1996). Only models allowing contact between fibroblasts of extracellular matrix and keratinocytes present this organization. So, our results indicate that our scaffold permitted a dialogue to occur between epithelial cells and fibroblasts, as would be the case *in vivo*. The basement membrane is an important feature a reconstructed oral mucosa should possess, it is the attachment zone necessary to withstand sheer stress in oral mucosa (Feinberg et al., 2005), and also has an important role in wound healing and disease (Winning et al., 2000).

Deeper, in the LPE, large amounts of newly synthesized collagen were detected by TEM (Figure 3.3g). Some of the collagen fibrils were straight and parallel to the oral surface, and some were wavy and less organized (Figure 3.3g). In fact, the collagen fibres in the lamina propria of the nonkeratinized oral mucosa were reported to be loosely and less regularly organized compared to keratinized mucosa where they are arranged in bundles (Winning et al., 2000). The average collagen fibril diameter in the reconstructed oral mucosa (28.4 nm) was similar to that in native human oral mucosa, for which the collagen fibril diameter range has been reported as 20-40 nm. This 20 nm range is due to the fact that the average fibril diameter varies with the region in the mouth, or in the same region with their location in the lamina propria (Susi et al., 1967; Ottani et al., 1998). Collagen fibrils in native human skin are of larger diameter (53-82 nm) compared to oral mucosa (Stewart 1995). Because this oral mucosa 3-D model is very close to human tissue, we propose the use of this OME as a model to test the efficiency or toxicity of oral care products, or it may be further tested *in vivo* for potential clinical applications.

The main challenge for success *in vivo* is to secure the attachment and survival of cultured cells on the wound beds. For this purpose, future strategies to accelerate vascularization are needed, such as reconstruction of endothelialized oral mucosal substitutes by incorporation of endothelial cells and vascular endothelial growth factor (VEGF).

3.2. Study of the Influence of the Mesenchymal Cell Source on Oral Epithelial Development

In this section, oral fibroblasts, dermal fibroblasts and corneal stromal keratocytes, isolated from normal human oral mucosa, foreskin and cornea biopsies, were cultured in CGC foams to obtain lamina propria, dermis and stroma equivalents, respectively. Oral epithelial cells isolated from normal human oral mucosa biopsies were cultured on these equivalents under the same conditions. The resulting epithelia formed on these equivalents containing mesenchymal cells of different origins were studied and compared to elucidate the influence of the mesenchymal cell source on oral epithelial development.

3.2.1. Histology

Histological analysis showed that the fibroblasts of lamina propria, dermal fibroblasts and keratocytes of corneal stroma seeded into the collagen-GAG-chitosan foams were able to proliferate, migrate within the thickness of the substrate, and synthesize new extracellular matrix filling the pores of the substrate, thus giving rise to a lamina propria equivalent (LPE), a dermal equivalent (DE) and a corneal stromal equivalent (CSE), respectively (Figures 3.5a, 3.5b and 3.5c). As the top layer of these mesenchymal tissue equivalents, epithelial cells of oral mucosa were seeded and cultured for 7 days under submerged conditions and 14 days at an air-liquid interface. They formed nonkeratinized multilayered epithelia on the LPEs, DEs and CSEs with the following average number of cell layers: 11.3 ± 0.4 , 5.3 ± 0.3 and 2.1 ± 0.3 , respectively. The differences between the number of epithelial cell layers of the three models were statistically significant ($p < 0.001$).

Native cornea itself has a relatively thin epithelium of a few layers (Figure 3.5f). Epithelial cells in the superficial layers of the different epithelia were seen to retain their nuclei and stratum corneum was absent as in native oral mucosa (Figure 3.5d), whereas native skin was completely differentiated with an orthokeratotic stratum corneum (Figure 3.5e).

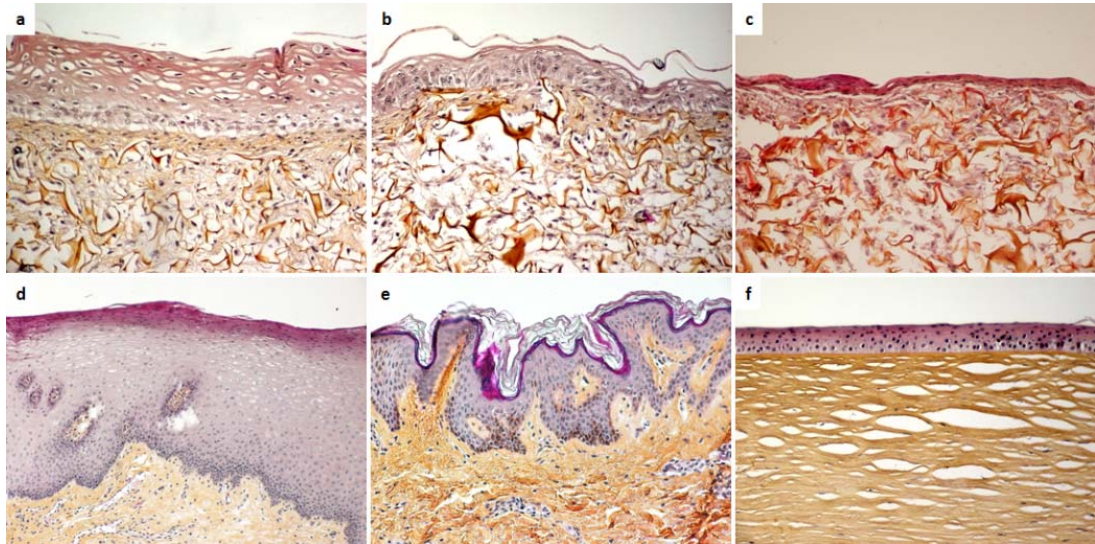


Figure 3.5. Histological analysis of the various models. (a) OLPE model (x200), (b) ODE model (x200), (c) OCSE model (x200), (d) native human oral mucosa (x100), (e) native human skin (x200), and (f) native human cornea (x200). Cell nuclei were stained blue with hematoxylin, cytoplasm pink with phloxine and extracellular matrix of connective tissue orange/yellow with saffron. In the LPE, DE and CSE, oral fibroblasts, dermal fibroblasts and stromal keratocytes seeded in the collagen-GAG-chitosan foams have migrated, proliferated and populated the foams. The pores are filled with newly synthesized extracellular matrix (a, b and c). On the LPE, DE and CSE, oral epithelial cells form nonkeratinized multilayered pluristratified epithelia of 11, 5 and 2 layers, respectively, and are seen to retain their nuclei in the superficial layer (a, b and c), as in the native oral mucosa (d). In contrast, the native skin is completely differentiated with an orthokeratotic stratum corneum (e).

3.2.2. Immunohistochemistry

Filaggrin, a marker of terminal epidermal differentiation, and keratin 10 (K10), marker of keratinized epithelium, were completely absent in all models. On the other hand, native skin, which has a keratinized and fully differentiated

epithelium, was stained positive for both of them (Figure 3.6). Keratin 12 (K12), a marker of corneal epithelial differentiation, was absent from all models, although it was expressed strongly in the epithelium of native cornea (Figure 3.6). Keratin 13 (K13), the major differentiation-associated marker of nonkeratinized oral mucosa, was expressed very strongly in OLPE and ODE models as was in the native oral mucosa. It was also present in the thin epithelium of OCSE (Figure 3.6). The basement membrane protein laminin 5, the major component of anchoring filaments, was strongly and continuously expressed in all models (Figure 3.6).

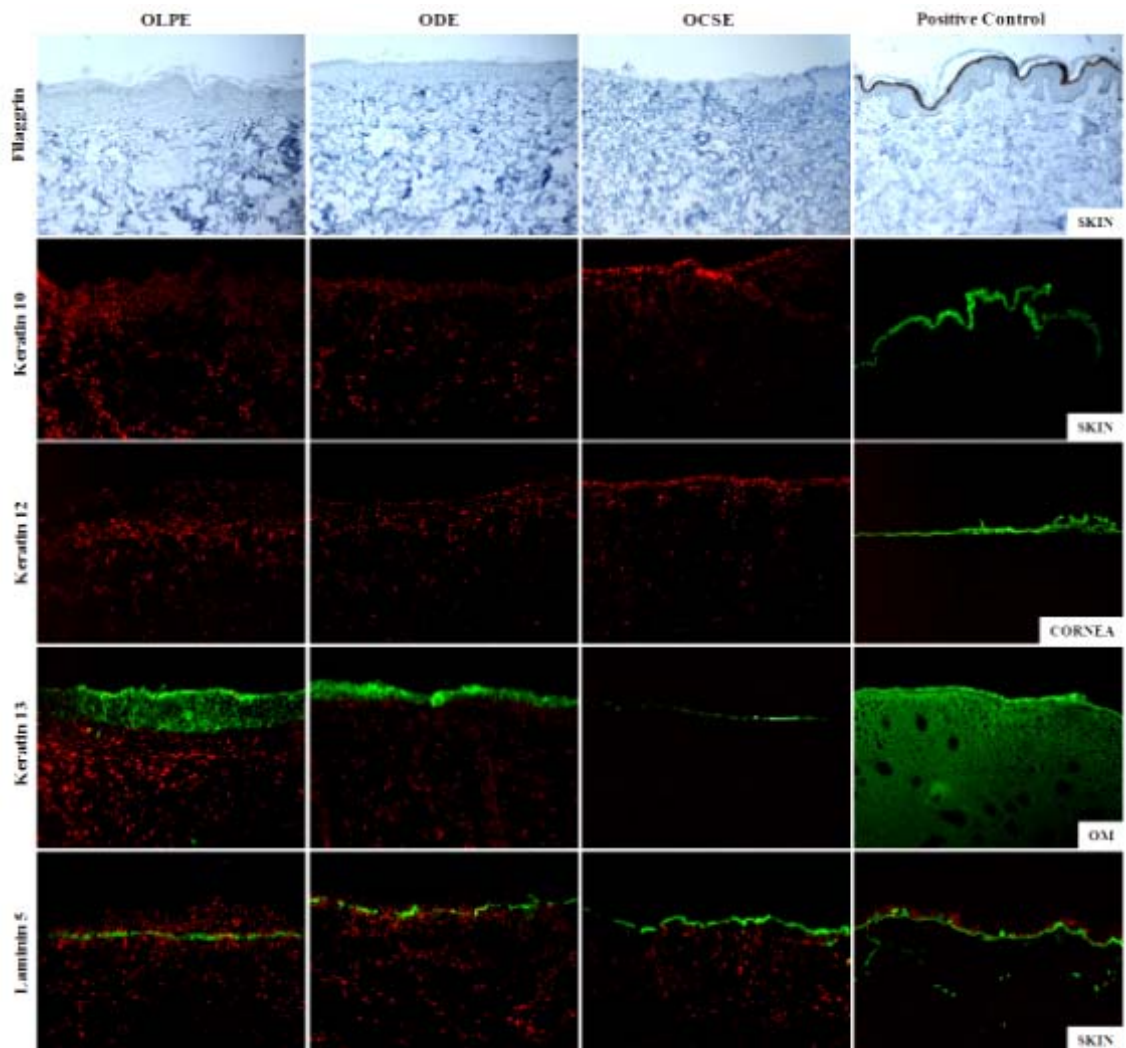


Figure 3.6. Immunolabelling of filaggrin, keratins 10, 12 and 13; and the basement membrane protein laminin 5 in the three constructs, OLPE, ODE and OCSE. Immunolabelling is shown in green (fluorescence) or brown (DAB), cell nuclei are shown in red (x100).

3.2.3. Transmission Electron Microscopy

The ultrastructural organization in the tissue engineered models was examined by transmission electron microscopy (TEM). TEM analysis confirmed the histological findings: the epithelium formed on the DE had 5 layers, whereas the one on the LPE was much thicker (11 layers) and stratified, and neither had stratum corneum (Figures 3.7a and 3.7b). In both models, cells had several organelles and mitochondria. Their morphology changed, becoming flattened with elongated nuclei, as they moved towards the culture surface,. As a result, the basal cells were very different in size and shape compared to the superficial ones; they were more voluminous, rounder, with distinct keratin bundles. Numerous intercellular junctions of different types, namely keratin-associated desmosomes with clearly visible desmosomal plaques and gap junctions were detected in these two models (Figure 3.7c). The number of intercellular junctions was higher in the basal and suprabasal layers compared to the superficial layer. Apart from the difference in their thickness and number of layers in their epithelia, the most characteristic feature of the OLPE model that distinguished it from the ODE, was the presence of abundant microvilli in the epithelium of the former (Figure 3.7a). In that model, density of microvilli was remarkably higher in the superficial layers compared to basal layer (Figure 3.7a). In the stromal part of the OCSE model, keratocytes were observed to express signs of intense metabolic activity (Figure 3.7d).

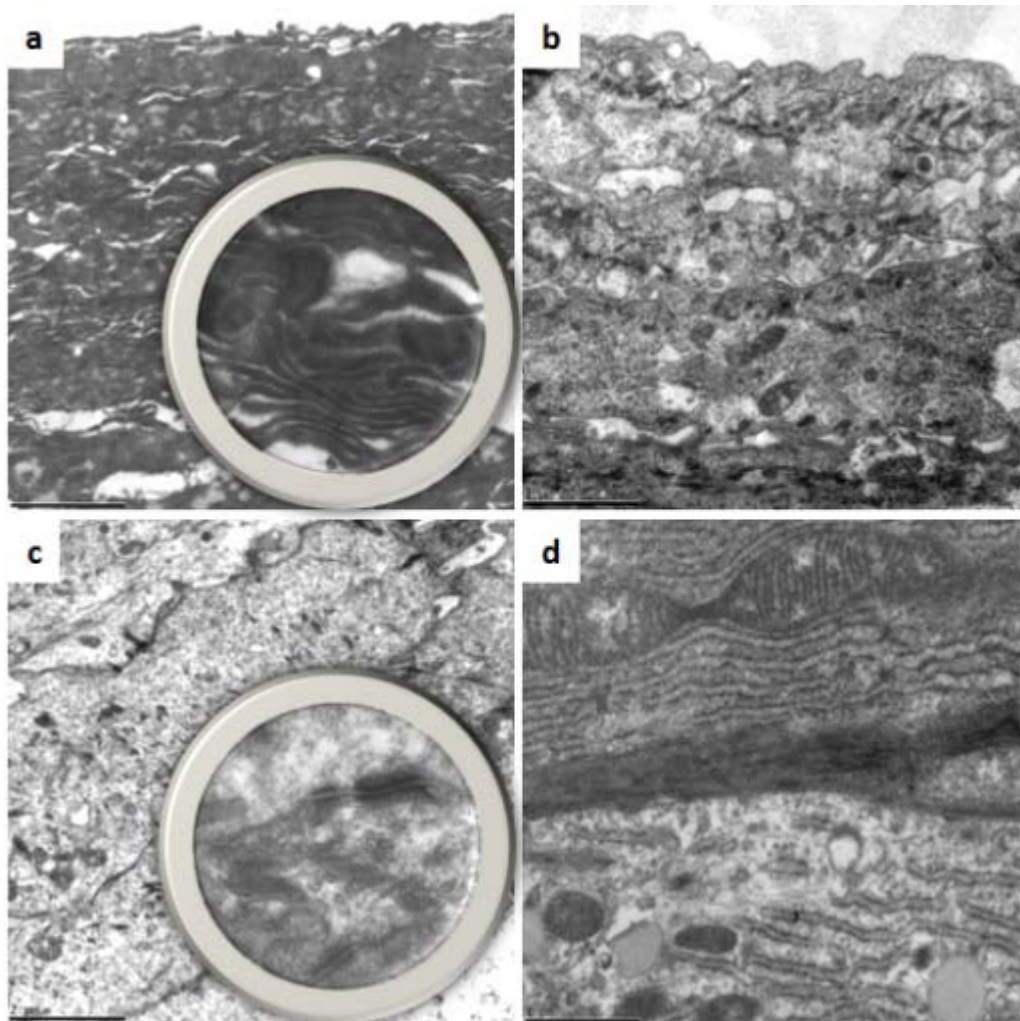


Figure 3.7. Transmission electron microscopic analysis of the models. (a) the OLPE model where an epithelium of 11 layers without a stratum corneum had formed. A number of microvilli were present in the superficial layers of the epithelium (bar = 2 μ m), (b) the ODE structure where an epithelium of 5 layers with numerous intercellular junctions and without any stratum corneum or any microvilli was observed (bar = 1 μ m), (c) several types of intercellular junctions such as desmosomes and GAP junctions (insert) were detected. Their number was very high especially in the suprabasal and basal layers (bar = 2 μ m), (d) the keratocytes in the OCSE model were observed to be highly active (bar = 1 μ m).

3.2.4. Discussion

The results of the analyses of the three types of constructs composed of mesenchymal cells of different sources (oral, dermal and corneal fibroblasts) and of the same oral epithelial cells clearly showed that the mesenchymal cell source had a

significant influence on the thickness and the ultrastructure of the epithelium, but not on the differentiation of oral epithelial cells. Histological analysis showed that the epithelium of the OLPE model was significantly thicker containing up to 11 cell layers compared to the epithelium formed on dermal equivalents which contained only 5 layers. This situation was comparable to the differences observed in native tissues, whose epithelia also differed in thickness. The epithelium of the OCSE model was the thinnest of all, as in native cornea. These results suggest that our models allowed interaction between epithelial cells and the underlying mesenchymal cells, and that the latter had an effect on the thickness of the epithelium formed. Oral fibroblasts favoured epithelial cell proliferation more than the dermal and corneal fibroblasts did.

Signalling between oral mucosal epithelial cells and mesenchymal tissue involves a bifurcating action of a combination of soluble growth factors. These factors were suggested to stimulate synthesis of specific extracellular matrix molecules by oral mesenchymal cells, and the appearance of receptors for such molecules on epithelial cells (Sharpe and Ferguson, 1988). In this way, a combination of mesenchymal soluble factors and extracellular matrix molecules was thought to direct epithelial differentiation. These signals act on epithelial basal (stem) cells, causing them to synthesize unique proteins, which may direct subsequent differentiation of daughter cells (Sharpe and Ferguson, 1988). In our study, oral epithelial cells developed the thinnest epithelium in the OCSE model, where they were cocultured with corneal stromal keratocytes. Keratocytes and fibroblasts are known to induce changes through soluble factors, and some of these factors are secreted in very high amounts by corneal keratocytes, whereas they are secreted in lesser amounts by dermal fibroblasts and in trace amounts by oral fibroblasts (Carrier et al., 2009; Szpaderska et al., 2003). For instance, the very low secretion of one soluble factor, interleukin 6, by oral fibroblasts was thought to be the reason for diminished inflammation and faster healing of oral mucosa (Szpaderska et al., 2003), and for the difference in the thickness of corneal and skin epithelia (Carrier et al., 2009). In the present study, TEM analysis showed that the stromal keratocytes, in the OCSE model, were extremely active metabolically and thus, potentially capable of producing large quantities of soluble factors. Hence, the

presence of such soluble factors might have affected oral epithelial development in that model.

In terms of differentiation, epithelial cells cocultured in three different models with oral fibroblasts, dermal fibroblasts or corneal stromal keratocytes preserved their oral mucosal phenotype, staining positive for keratin 13, the major differentiation-associated marker of nonkeratinized oral mucosa. They were not stained with antibodies to keratin 10 and filaggrin, which are markers for keratinized and terminally differentiated epidermis, and keratin 12, marker of corneal epithelial differentiation. Considering that the effect of wet environment was eliminated (all three types of constructs were cultured at an air-liquid interface for 2 weeks), it may be concluded that keratin expression and differentiation are not modulated by environmental conditions or by the fibroblasts, but are more likely to be an intrinsic property of the oral epithelial cells resulting from their genetic programming. However, it should be noted that the mesenchymal tissue is composed not only of fibroblasts, but also of fibrous connective tissue, capillaries, macrophages and extracellular matrix (ECM). This might be the reason why some studies, mostly *in vivo*, have found influence of mesenchymal tissue on epithelial differentiation. Indeed, in the clinical trials of oral mucosal epithelial cell sheet transplantation on corneal stroma to restore the ocular surface in case of bilateral limbal epithelial deficiency, we observed that some oral epithelial cells expressed keratin 13, some keratin 12, and others both keratin 12 and 13, suggesting a possible transdifferentiation (manuscript in preparation).

Laminins are a family of multifunctional molecules with a central role in the organization and the physiology of basement membranes (Tunggal et al., 2002). Laminin 5 (alpha3 beta3 gamma2) is specifically present in the basal lamina underneath epithelia and plays an essential role for anchoring basal epithelial cells to the underlying extracellular matrix by contributing to the formation of hemidesmosomes, junction structures that serve to attach cells to underlying substrata (El-Ghannam et al., 1998). In all of the three models of the present study, OLPE, ODE and OCSE, laminin 5 was expressed strongly and continuously at the basement membrane level, regardless of the source of the mesenchymal cell type. Laminin 5 is known to be a product of epithelial cells, but fibroblasts were shown to

contribute to its integration into the extracellular matrix architecture (Elkhal et al., 2004).

The presence of abundant surface microvilli in the OLPE model, and their absence in the ODE, was the most striking feature of this model when analysed by TEM. Microvilli, which are villus-like projections, along with other features such as pits and ridge-like folds called microprojections, were reported in both keratinized and non-keratinized epithelia of oral mucosa (Grossman et al., 1987). The microvilli found in nonkeratinized epithelium were observed to be more linear in morphology, resembling very much the ones observed in the epithelium of our OLPE model, compared to the ones present in the keratinized oral epithelium (Grossman et al., 1987). The microvilli found on the absorptive mucosal cells of the small intestine present an enormous surface area to the intestinal contents, thereby facilitating absorption (Gropper et al., 2009). In oral mucosa, their role is less evident. In the literature it was suggested that these surface features of epithelial cells of oral mucosal have a role in cell stretching as initially proposed by Wassersug and Johnson (1976), and possibly as a means of intercellular adhesion (Cleaton-Jones, 1975). In another study (Landay and Schroeder, 1977), microvilli were suggested as a means of interdigitation between adjacent cell surfaces in the epithelium of normal human oral mucosa. It was later argued that this surface arrangement in oral mucosal epithelium might also result as a consequence of packing large areas of cell membrane into a confined space (Hiscott et al., 1996). In the present study, it was interesting to find that the same oral epithelial cells cultured on dermal equivalents did not form any microvilli, as in native skin; whereas, the ones cultured on the LPEs had formed an epithelium with a large number of microvilli, as in native oral mucosa. The obvious reason might be the influence of the mesenchymal cell source, which affects microvilli formation and controls the thickness of the epithelium developed on it.

To conclude, our results demonstrated that the mesenchymal cell source significantly influences the thickness and the ultrastructure of the epithelium developed by the oral epithelial cells, but not their differentiation, which might be an intrinsic property of these cells due to their genetic programming.

3.3. Preparation and Characterization of Novel Scaffolds of Elastin-Like Recombinamer and Collagen for Soft Tissue Engineering

In this study, an elastin-like recombinamer, bioengineered to contain the cell adhesion peptide RGD, was blended with collagen to produce foams, fibers and a combination of them (foam-fiber bilayer structures) in order to mimic the natural structure of soft tissues composed predominantly of collagen and elastin and at the same time to improve the adhesive properties of conventional scaffolds made of collagen. The resulting scaffolds were assessed for their structural, mechanical and crosslinking capacities (they were crosslinked by two methods: physically via dehydrothermal treatment or chemically by using genipin) for use in soft tissue engineering.

3.3.1. Characterization and Purity of Collagen Type I Isolated from Rat Tails

Purity of the isolated type I collagen was confirmed by SDS-PAGE (Figure 3.8). Column 1 shows the protein marker, where the bands are at 260 kDa, 140 kDa, 100 kDa and 70 kDa (top to bottom). The isolated collagen (RTC, column 2) had doublets at apparent molecular weights of 115 and 130 kDa, and at 215 and 235 kDa which is the typical band pattern for type I collagen. The absence of any other bands indicates that the collagen isolated from rat tails is pure type I collagen.

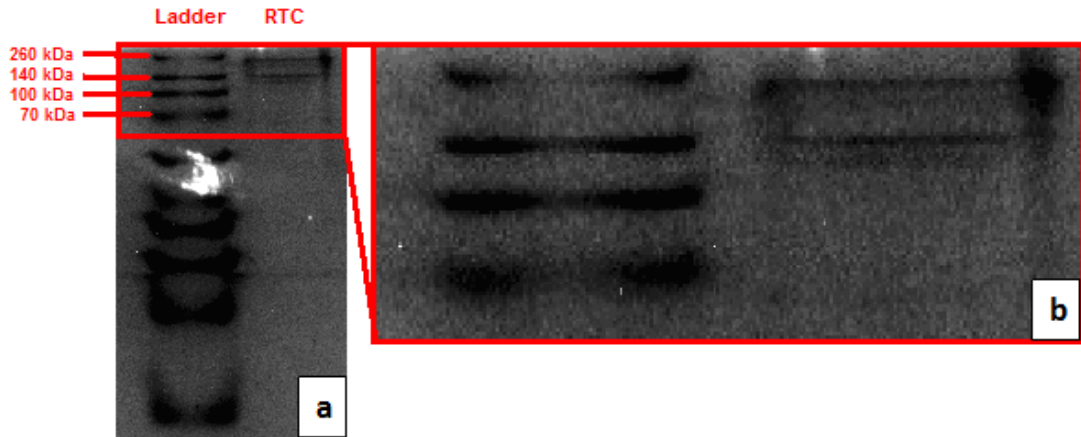


Figure 3.8. Purity of collagen isolated from rat tail tendons. (a) SDS-PAGE analysis of type I collagen isolated from rat tail tendons. First column shows the protein marker (ladder) and second column the isolated rat tail collagen (RTC). (b) Magnified version of (a).

3.3.2. Structural Properties of the Scaffolds

Structural properties of all scaffolds (foams and fibers) depended strongly on ELR presence and the crosslinking method. When ELR was adsorbed onto the collagen foam surface, the resulting scaffold had semi-closed pores on the surface (Figure 3.9E); whereas, when it was mixed with collagen solution before lyophilization, the resulting scaffold had open, porous surface (Figures 3.9A and 3.9B). When pure and ELR incorporated collagen foams were compared (Figures 3.9A and 3.9C), the former had thicker pore walls and larger pore sizes, whereas, the latter had thinner pore walls and smaller pores (Figure 3.9, Table 3.2). The pore size distribution was broaden in ELR containing foams (Table 3.2).

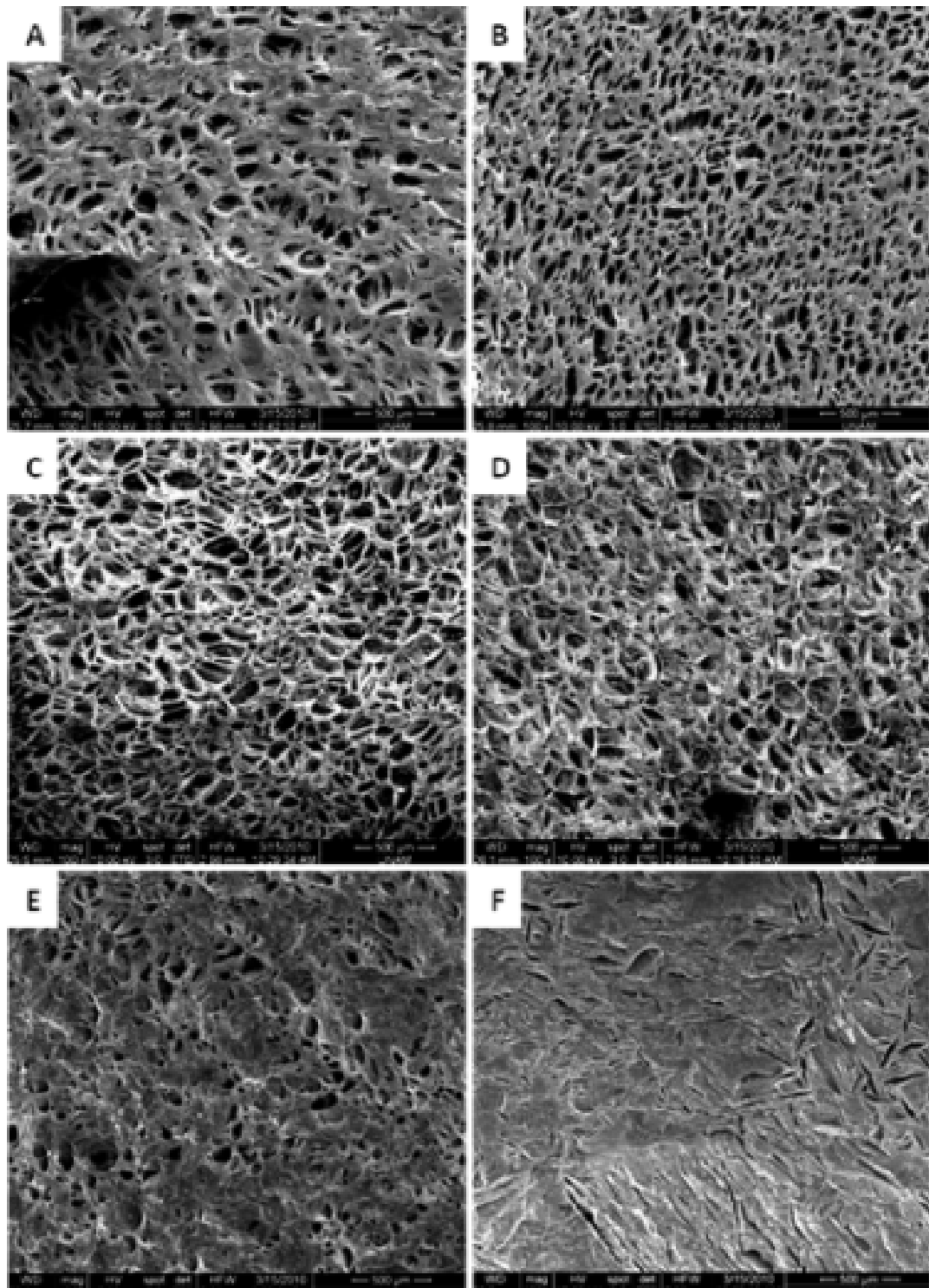


Figure 3.9. SEM micrographs of collagen-based foams. (A) uncrosslinked collagen foam, (B) DHT crosslinked collagen foam, (C) uncrosslinked ELR-collagen foam, (D) DHT crosslinked ELR-collagen foam, (E) collagen foam with ELR adsorbed on its surface, (F) collagen foam prepared with ethanol addition (10% v/v). DHT crosslinking: 150°C, 48 h.

Table 3.2. Changing of thickness, pore size and pore size distribution of collagen and ELR-collagen foams with crosslinking type.

Scaffold	Thickness (mm)	Pore size (μm) ^a	Pore size range (μm)
Uncrosslinked collagen foam	5.00	200	70 – 200
Uncrosslinked collagen+ELR foam	4.00	20	4 – 200
DHT-crosslinked collagen foam	5.30	200	80 – 200
DHT-crosslinked collagen+ELR foam	4.30	20	4 – 200
GP-crosslinked collagen foam	4.67	30	4 – 200
GP-crosslinked collagen+ELR foam	3.83	15	4 – 200

a. the most abundant pore size in a foam, given in the porosimetry. DHT: dehydrothermal treatment, ELR: elastin-like recombinamer, GP: genipin.

Genipin crosslinking significantly decreased the pore size; whereas, DHT did not affect the pore size, or its distribution (Figures 3.9 and 3.10, Table 3.2). DHT crosslinked scaffolds had highly porous surface, bottom and inner microstructure (Figure 3.10).

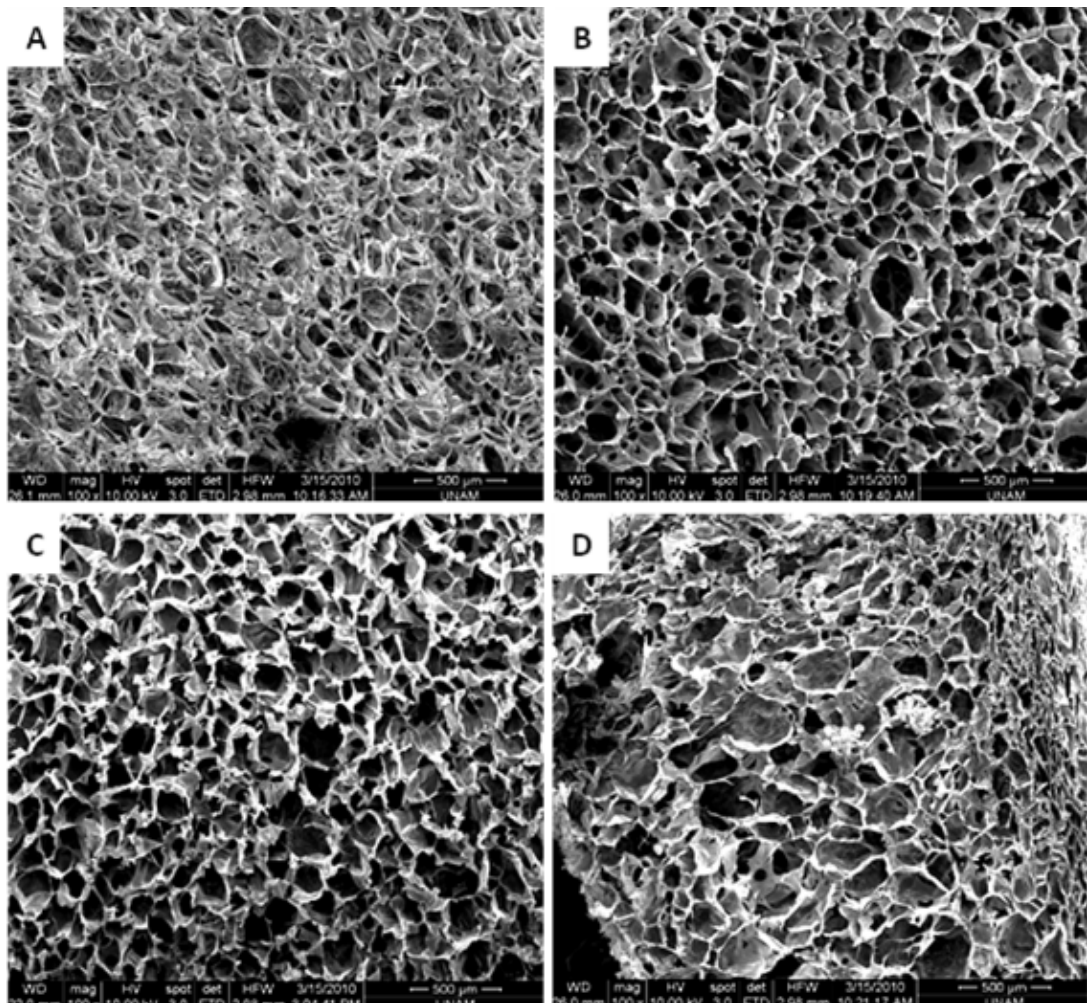


Figure 3.10. SEM analysis of (A) the surface, (B) the inner middle plane, (C) the bottom and (D) the cross section of the porous collagen-ELR foams crosslinked via DHT (150°C 48 h).

Addition of ethanol (10% v/v) into the ELR-collagen or pure collagen solution resulted in closed surface foams (Figure 3.9F). Similarly, when genipin was dissolved in 70% ethanol and added to the protein solution, the resulting foam had closed surface as opposed to the open surfaced one prepared using genipin in PBS (Figure 3.11).

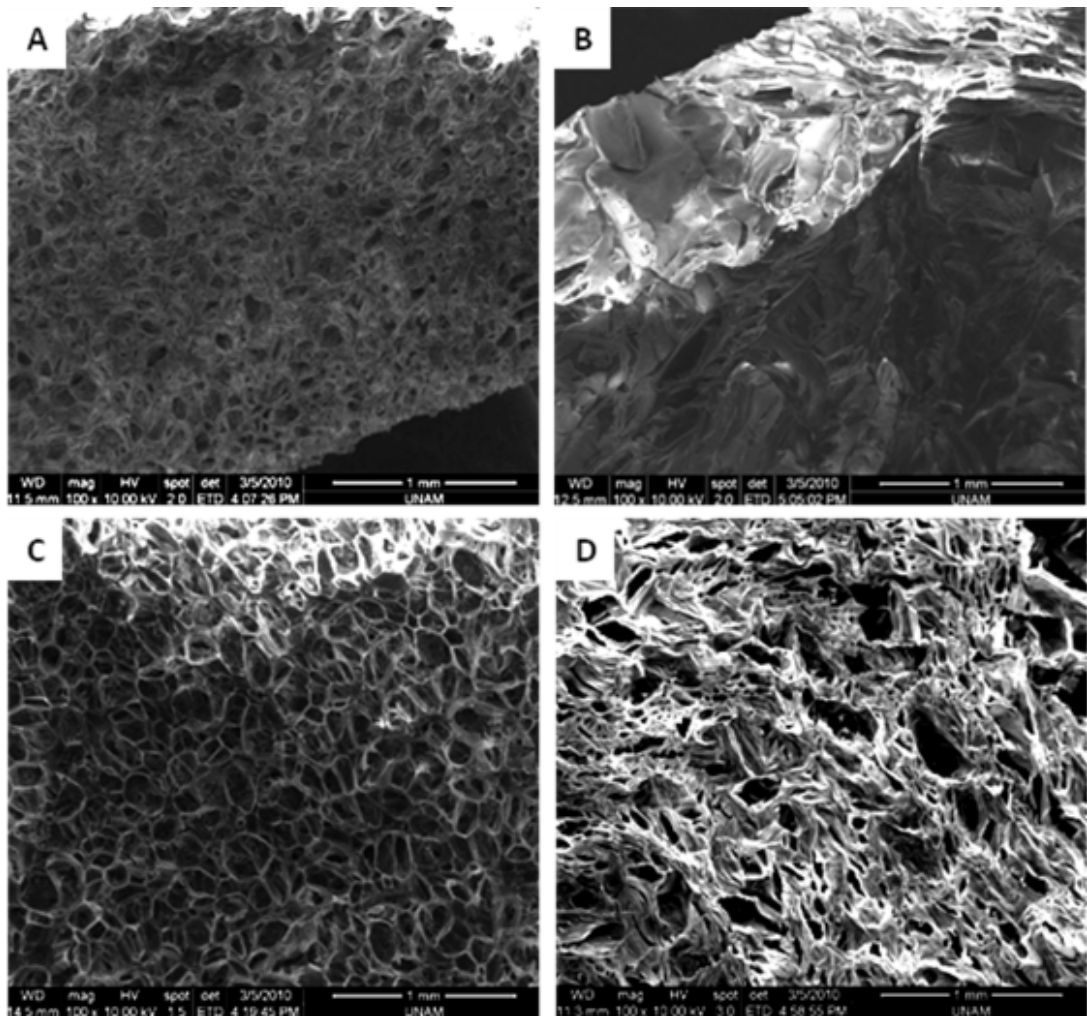


Figure 3.11. SEM micrographs of collagen foams and ELR-collagen foams crosslinked by genipin. Collagen dissolved in (A) PBS, (B) 70% ethanol, ELR-collagen crosslinked by genipin dissolved in (C) PBS, (D) 70% ethanol.

Incorporation of ELR decreased the diameter of the collagen fibers significantly, from micron to nanoscale. DHT was also found to cause a decrease in the diameter of both pure collagen and ELR-collagen fibers, but this reduction was not as large as the one caused by ELR (Figure 3.12). Crosslinking with genipin destroyed the fibrous structure, regardless of whether genipin was added to the protein solution prior to electrospinning or afterwards (Figure 3.13). On the other hand, all dehydrothermal treatments (105°C for 24 h, 105°C for 72 h, 150°C for 24 h, 150°C for 48 h) appeared to preserve the fibrous structure. However, after 24 h incubation in distilled water, only fibers treated at 150°C for 48 h or by the

combination of two methods: DHT (150°C, 24 h) followed by genipin crosslinking (0.1%, 48 h, RT) persisted.

A	Scaffold	Fiber diameter (μm)
	Uncrosslinked pure collagen (10%)	1.179
	Uncrosslinked collagen+ELR (10%)	0.306
	DHT crosslinked pure collagen (10%)	1.007
	DHT crosslinked collagen+ELR (10%)	0.263

Figure 3.12. Uncrosslinked and DHT crosslinked collagen and collagen-ELR (3:1, w/w) fibrous mats. (A) Average fiber diameters. (B) Pure collagen fibers, collagen concentration 10% (1000x). (C) Collagen-ELR (3:1) fibers, the same total protein concentration 10% (1000x).

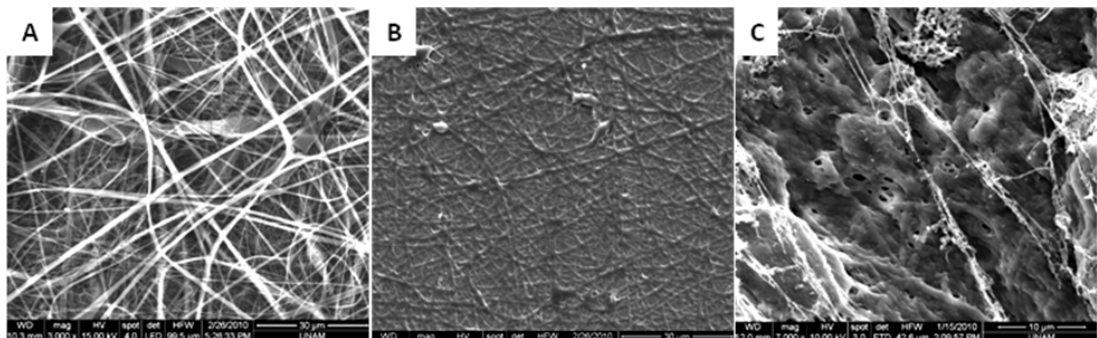


Figure 3.13. SEM of collagen fibers. (A) uncrosslinked, (B) crosslinked using genipin by adding into collagen solution before electrospinning, (C) crosslinked by incubating the electrospun fibers in genipin solution (0.1 w/v, 48 h, RT).

To obtain bilayer scaffolds, protein solution was electrospun directly onto foam, surfaces of which were either closed or open pore type (Figure 3.14A). In these bilayer constructs, the upper (fibrous) layer either separated from the lower spongy part by a closed pore layer (Figure 3.14B), or the two parts were in close contact with each other through the pores (Figure 3.14C). In the former, although the surface of the foam was totally closed, the inner microstructure was porous and the inner pores were flattened and had lamellar structure (Figure 3.14B). Thus, it formed a two-compartment construct with individual fibrous and macroporous regions.

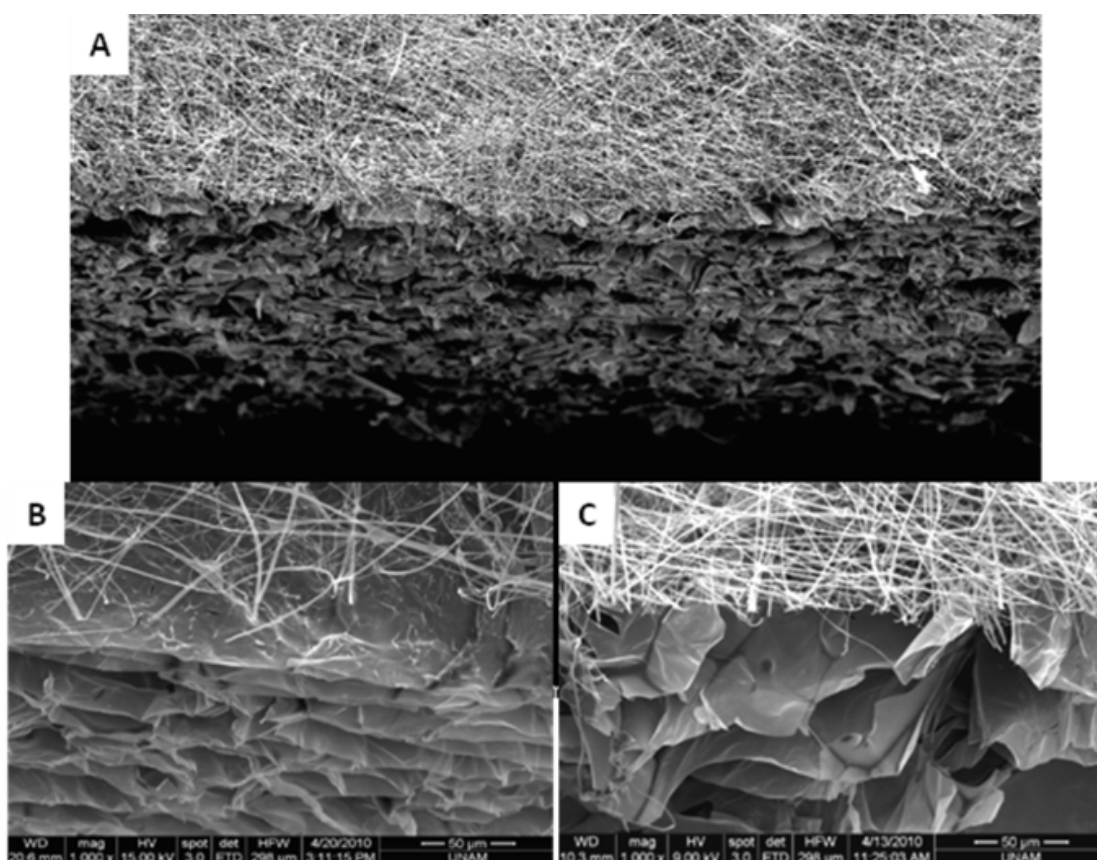


Figure 3.14. SEM micrographs of foam-fiber bilayer scaffolds. A) The upper layer of the scaffold is fibrous, while the lower, spongy, part is porous. B) Fibers on closed surfaced foam; the porosity of the inner structure was retained although the pores were flattened and lamellar. C) Fibers deposited on open surfaced foam.

3.3.3. Compressive Mechanical Properties of the Scaffolds

Except for closed surfaced foams, all pure and ELR containing collagen foams exhibited stress-strain behavior characteristics of low density, open cell foams with distinct linear elastic, collapse plateau and densification regimes. Both ELR incorporation and crosslinking affected the mechanical properties. ELR incorporation decreased the compressive strength (σ_{el}^*) and stiffness (E^*) of both uncrosslinked and crosslinked (genipin and DHT) scaffolds (Table 3.3). On the other hand, crosslinking increased the stiffness and compressive strength of both pure and ELR containing scaffolds, where the effect of crosslinking with genipin was more pronounced than that with DHT.

Table 3.3. Pure and ELR incorporated collagen scaffolds under compressive forces

Scaffold	E^* (kPa)	$1/E^*$ (kPa ⁻¹)	σ_{el}^* (kPa)	ε_{el}^*	$\Delta\sigma/\Delta\varepsilon$ (kPa)
Uncrosslinked collagen foam	139.5	0.007	29.5	0.341	53.7
Uncrosslinked collagen+ELR foam	87.3	0.011	13.5	0.272	47.0
DHT crosslinked collagen foam	155.6	0.006	44.2	0.367	77.7
DHT crosslinked collagen+ELR foam	115.0	0.008	39.8	0.327	63.0
Genipin crosslinked collagen foam	385.8	0.002	72.1	0.284	130.3
Genipin crosslinked collagen+ELR foam	140.7	0.007	42.5	0.399	47.4

a. E^* : linear elastic modulus, $1/E^*$: flexibility, σ_{el}^* : elastic collapse stress, ε_{el}^* : elastic collapse strain, $\Delta\sigma/\Delta\varepsilon$: collapse plateau modulus

3.3.4. Discussion

In soft tissues, collagen and elastin are the predominant components of the extracellular matrix (Shoulders and Raines, 2009). In this study, to mimic this natural structure and at the same time to improve the conventional scaffolds made of collagen, a bioengineered elastin-like recombinamer containing the cell adhesion peptide RGD was blended with collagen to produce foams, fibers and a combination of them (foam-fiber bilayer structures). In the bilayer structure, the protein solution was electrospun onto two types of foams: with surfaces with closed or open pores. In the former, the fibrous top part was literally separated from the spongy bottom part by a closed pore skin layer. In this structure, the foam part was expected to serve as a support for the fragile fibers and to facilitate their handling during culture. The closed pore surface would prevent the cells seeded on the fibers from migrating into the foam. On the other hand, in the latter bilayer structure, the fibrous part was attached to the foam with open pores; this was expected to make this structure suitable for coculture studies where different cell types on different sides of the construct could communicate with each other more freely. For instance, in skin tissue engineering, as well as in oral mucosa and cornea, epithelial cells and mesenchymal cells should reside in two distinct layers: a relatively thin epithelium and a thicker extracellular matrix, but should nevertheless be able to communicate with each other for proper epithelial development (Kinikoglu et al., 2009).

Incorporation of ELR was found to have a profound effect on the structural and mechanical properties of both the foams and the fibrous mats. In foams, the pore size was significantly decreased upon incorporation of ELR whether the collagen and ELR were uncrosslinked, or dehydrothermally or chemically crosslinked with genipin. ELR also increased the pore size distribution, causing smaller pores to form. This drastic decrease in pore size (from 200 μm to 20 μm) and increase in its distribution (from 70-200 μm to 4-200 μm) might be beneficial in tissue culture, considering that the size of a human dermal fibroblast, the major cell type of the dermis, varies between 10-100 μm (Zhu et al., 2008) and that fibroblast migration decreases as scaffold pore size increases above 90 μm (Harley et al., 2008). It was also reported that scaffolds used for studies of skin

regeneration were inactive when the mean pore size was either lower than 20 μm or higher than 120 μm (Yannas et al., 1989). Therefore, incorporation of ELR decreased the pore size to a suitable range for cell migration. When the ELR was added after the collagen foam was formed, instead of before, the surface of the foam was rather closed, probably because the ELR filled the pores on the surface during adsorption. Therefore, when, not only cell attachment to the surface, but population of the foam by the cells is important, incorporation of ELR in the foam before it is formed should be the approach. In fibrous mats, ELR led to significantly smaller diameters (>3 fold, a decrease from micron to nanoscale) even when the same total protein concentration (10%) was used. ELR was previously shown to bind to collagen, and is thought that it might interfere with incorporation of more collagen molecules into the fibers (Garcia et al., 2009).

Except for foams with closed pores, all pure and ELR containing collagen foams under compression exhibited stress-strain behavior that is characteristic of low density, open cell foams with distinct linear elastic, collapse plateau and densification regimes. Incorporation of ELR decreased the stiffness and compressive strength, but increased the flexibility. Therefore, pure collagen scaffolds might be advantageous in applications requiring high strength, such as hard tissue engineering, but for soft tissue engineering, the elasticity that the ELR brings to the scaffold is very useful.

In order to find an effective crosslinking method for ELR-collagen structures, genipin and dehydrothermal treatments, both non-toxic, were tested. Both scaffolds had good physical stability and remained insoluble for over 1 month in PBS at 37°C. When genipin was introduced before foam or fiber formation, foams preserved their form better (data not shown); otherwise they tended to deform and dissolve during incubation. When compared to DHT, genipin crosslinking significantly decreased the pore size and the flexibility of both pure and ELR containing collagen foams, but it significantly increased their compressive strength. Therefore, for hard tissue engineering, where compressive strength is crucial, genipin crosslinking should be preferred over DHT, either alone or combined with DHT.

As has been reported in the literature, following crosslinking collagen with genipin, the normally opaque collagen turns blue with a strong fluorescence at 630 nm when excited at 590 nm (Sundararaghavan et al., 2008). With ELR the color was even darker. DHT did not lead to such color changes. It is possible that in the (immuno)fluorescence analyses of tissue equivalents, the genipin-induced strong autofluorescence of the ELR-collagen scaffolds might cause problems by interfering with the specific fluorescent stainings.

Crosslinking of ELR-collagen fibrous mats with genipin disrupted their fibrous nature, probably by dissolving or swelling them. Uncrosslinked collagen and ELR readily dissolve in aqueous media; therefore, crosslinking in an aqueous medium was not appropriate. Crosslinking of collagen fibers by glutaraldehyde vapor was also reported to disrupt the fibrous structure (Rho et al., 2006), although not as extensively as 1-ethyl-3-(3-dimethylaminopropyl)-carbodiimide (EDC) (Rho et al., 2006) or genipin (present study). In this study, DHT was used to crosslink fibers at several temperatures and for various durations, and it was found out that when the fibers were incubated at 150°C for 48 h or for 24 h followed by genipin crosslinking (0.1 w/v in PBS, 48 h, RT), they preserved their fibrous structure even after 24 h incubation in distilled water. When uncrosslinked and crosslinked fibers were compared, it was found that DHT crosslinking decreased the diameter of both pure collagen and ELR-collagen fibers slightly; as opposed to glutaraldehyde crosslinking, which caused an increase in collagen fiber diameter (Bhardwaj and Kundu, 2010).

Scaffolds act as both physical support structures and also as regulators of cell activity. Microstructural and mechanical properties of scaffolds have been shown to significantly affect cell behavior such as adhesion, growth, and differentiation, and to influence the bioactivity of scaffolds used for *in vivo* regeneration applications of various tissues, such as cartilage, skin, and peripheral nerves (Harley et al., 2008). Here, the foam-fiber bilayer scaffolds designed using ELR and collagen and crosslinked by genipin or DHT were assessed for their microstructural and mechanical capacities, and DHT crosslinked structures proved their potential for use in soft tissue engineering due to their continuous and interconnected pore network, appropriate pore size and its distribution, neat fibrous

structure, high flexibility and adequate mechanical stability. In the following section, these scaffolds were tested *in vitro*, coculturing epithelial cells and fibroblasts for the reconstruction of full-thickness oral mucosa equivalents.

3.4. Development of a Full-Thickness Tissue Engineered Human Oral Mucosa Based on a Novel Bilayer Protein Scaffold

In this study, elastin-like recombinamer (ELR) - collagen bilayer scaffolds were used to construct full-thickness human oral mucosal equivalents by co-culture of fibroblasts and epithelial cells isolated from normal human oral mucosa biopsies. The porous, thicker, bottom layer of the scaffold served as a support to the fragile upper nanofibrous layer to facilitate handling especially during air-liquid interface phase of culture. The nanofibrous upper layer served as the substrate for fibroblasts. Oral epithelial cells were seeded on the top.

3.4.1. Cell Proliferation in Collagen-ELR Scaffolds: MTT Assay

The proliferation of oral fibroblasts in ELR-collagen and control collagen scaffolds were assessed and compared using the MTT assay at days 0, 7 and 14 of culture. The results of the assay showed that fibroblasts initially seeded at the same density on both types of scaffolds continued to proliferate over the course of 14 days, and that the number of cells on ELR-collagen scaffolds exceeded that of cells on control collagen scaffolds by day 7. The difference became significant by day 14 (Figure 3.15).

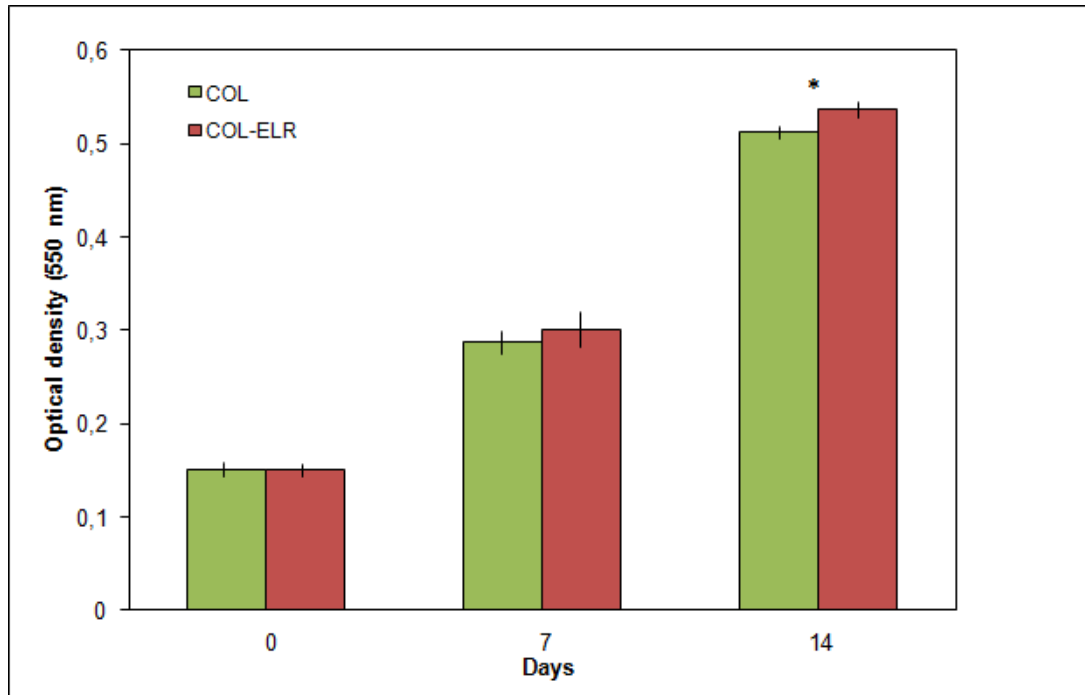


Figure 3.15. Comparison of human oral mucosal fibroblast proliferation on collagen and collagen-ELR scaffolds determined by the MTT assay. The initial cell density (day 0) and the culture conditions were the same for both scaffolds. *Statistical significance of $p < 0.05$.

3.4.2. Histology

It is reported in literature that cells cultured on electrospun scaffolds may not always penetrate into the scaffold and may accumulate at the surface due to short distances between the fibers of these scaffolds (Nisbet et al., 2009). Therefore, techniques such as porogen addition and salt leaching were used in several studies to increase the porosity of these scaffolds (Nisbet et al., 2009). In the present study, the results of the histology showed that in the oral mucosal equivalent, fibroblasts seeded onto the ELR-collagen nanofibrous scaffold migrated through the whole thickness of the scaffold which was produced without any additional porogen or salt leaching application to increase porosity. They proliferated and populated the scaffold by synthesizing new extracellular matrix. Epithelial cells formed a nonkeratinized multilayered pluristratified epithelium on the surface and were seen to retain their nuclei in the superficial layer. The epithelium they formed was firmly

anchored to the underlying lamina propria equivalent by a continuous and well-organized basement membrane (Figure 3.16).

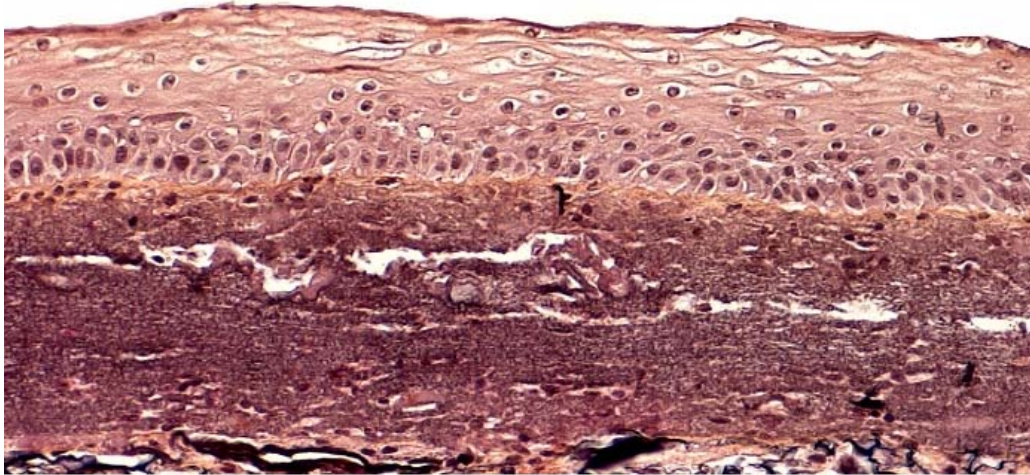


Figure 3.16. Histological analysis of the full-thickness human oral mucosal equivalent based on the nanofibrous collagen-ELR scaffold (x200). Cell nuclei were stained in blue by hematoxylin, cytoplasm in pink by phloxine and extracellular matrix of connective tissue in orange/yellow by saffron.

3.4.3. Immunohistochemistry

ELR-collagen nanofibrous scaffold, the control collagen nanofibrous scaffold and the native human oral mucosa were immunostained for keratin 13, the major differentiation marker of nonkeratinized oral mucosa epithelium, and the basement membrane protein laminin 5. The results showed that the oral mucosal equivalent reconstructed using the collagen-ELR scaffold had a much thicker epithelium compared to the control collagen scaffold. There was a strong expression of the K13 in the epithelium of the oral mucosal equivalent, as well as a strong and continuous expression of laminin 5 at the epithelium-lamina propria junction, as in native human oral mucosa (Figure 3.17).

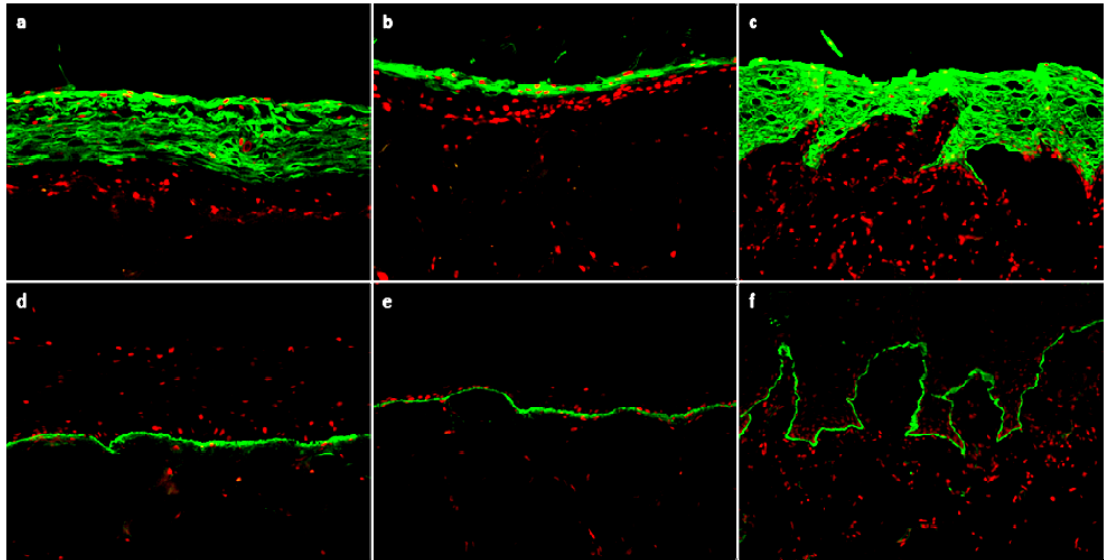


Figure 3.17. Immunofluorescence labelling of keratin 13 (a,b,c), the major differentiation marker of nonkeratinized oral mucosa epithelium, and the basement membrane protein laminin 5 (d,e,f) in the oral mucosal equivalent based on: the collagen-ELR nanofibrous scaffold (a and d), the control collagen nanofibrous scaffold (b and e), in comparison to native oral mucosa (c and f). Immunolabelling is shown in green, cell nuclei are shown in red (x200).

As shown by the MTT assay, and by histological and immunohistological analyses, the full-thickness oral mucosal equivalent constructed by co-culture of human oral fibroblasts and epithelial cells using the nanofibrous collagen-ELR scaffold mimicked closely the native oral mucosa. It comprised a lamina propria equivalent with a pluristratified nonkeratinized epithelium expressing strongly keratin 13 and laminin 5. Fibroblasts were observed to migrate and populate the nanofibrous scaffold, and the epithelium developed on top was observed to be firmly attached to the underlying lamina propria equivalent. The presence of ELR increased the proliferation of both fibroblasts, as shown by the MTT assay, and that of epithelial cells, as shown by the thicker epithelium formed on the collagen-ELR scaffolds, compared to the one developed on the pure collagen scaffolds (the control).

CHAPTER 4

CONCLUSION

In this study, it was possible to construct a viable oral mucosa equivalent using the principles of tissue engineering. The results of histology, immunohistochemistry and transmission electron microscopy demonstrated the presence of a lamina propria equivalent with a pluristratified and nonkeratinized epithelium, mimicking very closely the native oral mucosa. Thanks to this model, it was then demonstrated that the source of fibroblasts (oral mucosa, skin, and cornea) had a significant influence on the thickness and the ultrastructure of the epithelium obtained by culture of oral epithelial cells on lamina propria, dermal and corneal stromal equivalents. Finally, in order to improve the cell adhesion properties of collagen based conventional scaffolds, a bioengineered elastin-like recombinamer (ELR) containing the cell adhesion tripeptide, RGD, was used in the production of novel, bilayer scaffolds, porous by lyophilization and covered by a nanofibrous layer created by electrospinning. Characterization of these scaffolds by mercury porosimetry, scanning electron microscopy and mechanical testing showed that the presence of ELR and the crosslinking method significantly influenced their structural and mechanical properties. *In vitro* tests revealed positive contribution of ELR on the proliferation of both fibroblasts and epithelial cells.

GLOSSARY

Allogenic: taken from different individuals of the same species

Autologous: taken from the individual himself

Basement membrane: a thin membrane upon which is posed a single layer of cells

Collagen: the principal extracellular matrix protein of the skin, tendons, cartilage, bone and connective tissue

Dermis: the connective tissue of the skin under the epithelium

Desmosome: a circular, dense body that forms the site of attachment between certain epithelial cells, especially those of stratified epithelium of the epidermis, which consist of local differentiations of the apposing cell membranes.

Elastin-like recombinamer: elastin-like recombinant polymer

Epidermis: the outermost and avascular layer of the skin, derived from the embryonic ectoderm, varying in thickness from 0.07–1.4 mm

Epithelium: the cellular covering of internal and external body surfaces, including small cavities. It consists of cells joined by small amounts of cementing substances and is classified according to the number of layers and the shape of the cells

Fibroblast: a cell found within fibrous connective tissue, varying in shape from stellate (young) to fusiform and spindle shaped. Associated with synthesis of all extracellular matrix components of connective tissue.

Keratin: an insoluble sulfur-containing protein with a high content of the amino acids tyrosine and leucine; the main component of epidermis, hair, nails, keratinized epithelium

Keratinocyte: the epidermal cell that synthesizes keratin, known in its successive stages in the layers of the skin as basal cell, prickle cell, and granular cell

Keratocyte: fibroblast of the connective tissue of cornea

Lamina propria: the connective tissue layer of mucosa

Mesenchyme: the meshwork of embryonic connective tissue in the mesoderm from which are formed the connective tissues of the body and the blood and lymphatic vessels

Scaffold: an artificial three-dimensional frame structure that serves as a mimic of extracellular matrix for cellular adhesion, migration, proliferation, and tissue regeneration in three dimensions

Stroma (Corneal): the connective tissue framework of the cornea

REFERENCES

Adams Jr S.B., Shamji M.F., Nettles D.L., Hwang P., Setton L.A. Sustained release of antibiotics from injectable and thermally responsive polypeptide depots. *J Biomed Mater Res B Appl Biomater* 2009; 90: 67-74

Alaminos M., Garzón I., Sánchez-Quevedo M.C., Moreu G., González-Andrades M., Fernández-Montoya A., et al. Time-course study of histological and genetic patterns of differentiation in human engineered oral mucosa. *J Tissue Eng Regen Med* 2007; 1: 350-9

Andrian E., Grenier D., Rouabhia M. In vitro models of tissue penetration and destruction by *Porphyromonas gingivalis*. *Infect Immun* 2004; 72: 4689-98

Augustin C., Collombel C., Damour O. Use of in vitro dermal equivalents and skin equivalent kits for evaluating cutaneous toxicity of cosmetics products. *In Vitro Toxicol* 1997; 10: 21-9

Augustin C., Collombel C., Damour O. Measurements of the protective effect of topically applied sunscreens using in vitro three-dimensional dermal and skin equivalents. *Photochem Photobiol* 1997; 66: 853-9

Auxenfans C., Fradette J., Lequeux C., Germain L., Kinikoglu B., Bechetoille N., Braye F., Auger F.A., Damour O. Evolution of three dimensional skin equivalent models reconstructed in vitro by tissue engineering. *Eur J Dermatol* 2009; 19: 107-13

Betre H., Ong S.R., Guilak F., Chilkoti A., Fermor B., Setton L.A. Chondrocytic differentiation of human adipose-derived adult stem cells in elastin-like polypeptide. *Biomaterials* 2006; 27: 91-9

Bhardwaj N. and Kundu S.C. Electrospinning: a fascinating fiber fabrication technique *Biotechnol Adv* 2010; 28: 325-47

Bhargava S., Chapple C.R., Bullock A.J., Layton C., MacNeil S. Tissue engineered buccal mucosa for substitution urethroplasty. *BJU Int* 2004; 93: 807-11

Black A., Bouez C., Perrier E., Schlotmann K., Chapuis F., Damour O. Optimization and characterization of an engineered human skin equivalent. *Tissue Eng* 2005; 11: 723-33

Blackwood K.A., McKean R., Canton I., Freeman C.O., Franklin K.L., Cole D., Brook I., Farthing P., Rimmer S., Haycock J.W., Ryan A.J., MacNeil S. Development of biodegradable electrospun scaffolds for dermal replacement. *Biomaterials* 2008; 29: 3091-104

Bodner L. and Grossman N. Autologous cultured mucosal graft to cover large intraoral mucosal defects: a clinical study. *J Oral Maxillofac Surg* 2003; 61: 169-73

Bornstein P. and Sage H. Structurally distinct collagen types. *Ann Rev Biochem* 1980; 49: 957-1003

Buckley C.T. and O'Kelly K.U. Regular scaffold fabrication techniques for investigations in tissue engineering, Trinity Centre for Bioengineering & National Centre for Biomedical Engineering Science (2004)

Builles N., Bechetoille N., Justin V., André V., Barbaro V., Di Iorio E., Auxenfans C., Hulmes D.J.S., Damour O. Development of a hemicornea from human primary cell cultures for pharmacotoxicology testing. *Cell Biol Toxicol* 2007; 23: 279-92

Carrier P., Deschambeault A., Audet C., Talbot M., Gauvin R., Giasson C.J., Auger F.A., Guérin S.L., Germain L. Impact of cell source on human cornea reconstructed by tissue engineering. *Invest Ophthalmol Vis Sci* 2009; 50: 2645-52

Chen G., Ushida T., Tateishi T. Scaffold design for tissue engineering. *Macromol Biosci* 2002; 2: 67-77

Chilkoti A., Christensen T., MacKay J.A. Stimulus responsive elastin biopolymers: Applications in medicine and biotechnology. *Curr Opin Chem Biol* 2006; 10: 652-7

Chinnathambi S., Tomanek-Chalkley A., Ludwig N., King E., DeWaard R., Johnson G., Wertz P.W., Bickenbach J.R. Recapitulation of oral mucosal tissues in long-term organotypic culture. *Anat Rec A Discov Mol Cell Evol Biol* 2003; 270: 162-74

Cho K.H., Ahn H.T., Park K.C., Chung J.H., Kim S.W., Sung M.W., *et al.* Reconstruction of human hard-palate mucosal epithelium on deepidermized dermis. *J Dermatol Sci* 2000; 22: 117-24

Clausen H., Vedtofte P., Moe D., Dabelsteen E., Sun T.T., Dale B. Differentiation-dependent expression of keratins in human oral epithelia. *J Invest Dermatol* 1986; 86: 249-54

Claveau I., Mostefaoui Y., Rouabhia M. Basement membrane protein and matrix metalloproteinase deregulation in engineered human oral mucosa following infection with *Candida albicans*. *Matrix Biol* 2004; 23: 477-86

Cleaton-Jones P. Surface characteristics of cells from different cell layers of keratinised and non-keratinised oral epithelia. *J Periodontal Res* 1975; 10: 79-87

Collombel C., Damour O., Gagnieu C., Marichy J., Poinsignon F. Biomaterials with a base of collagen, chitosan and glycosaminoglycans; process for preparing them and their application in human medicine. French patent 8708252, 1987. European patent 884101948, 1988. US patent PCT/FR/8800303, 1989.

Costa R.R., Custódio C.A., Testera A.M., Arias F.J., Rodríguez-Cabello J.C., Alves N.M., Mano J.F. Stimuli-responsive thin coatings using elastin-like polymers for biomedical applications. *Adv Funct Mater* 2009; 19: 3210-8

Cunha G.R., Shannon J.M., Taguchi O., Fujii H., Chung L.W. Mesenchymal-epithelial interactions in hormone-induced development. *J Anim Sci* 1982; 55: 14-31

Cunha G.R., Fujii H., Neubauer B.L., Shannon J.M., Sawyer L., Reese B.A. Epithelial-mesenchymal interactions in prostatic development. I. morphological observations of prostatic induction by urogenital sinus mesenchyme in epithelium of the adult rodent urinary bladder. *J Cell Biol* 1983; 96: 1662-70

Dang J.M. and Leong K.W. Natural polymers for gene delivery and tissue engineering. *Adv Drug Deliv Rev* 2006; 58: 487-99

Dohlman C.H. The function of the corneal epithelium in health and disease. *Invest Ophthalmol* 1971; 10: 383-407

Dongari-Bagtzoglou A. and Kashleva H. Development of a highly reproducible three-dimensional organotypic model of the oral mucosa. *Nat Protoc* 2006; 1: 2012-8

Duan B., Wu L., Yuan X., Hu Z., Li X., Zhang Y., Yao K., Wang M. Hybrid nanofibrous membranes of PLGA/chitosan fabricated via an electrospinning array. *J Biomed Mater Res A* 2007; 83: 868-78

El-Ghannam A., Starr L., Jones J. Laminin-5 coating enhances epithelial cell attachment, spreading, and hemidesmosome assembly on Ti-6Al-4V implant material in vitro. *J Biomed Mater Res* 1998; 41: 30-40

Elkhal A., Tunggal L., Aumailley M. Fibroblasts contribute to the deposition of laminin 5 in the extracellular matrix. *Exp Cell Res* 2004; 296: 223-30

Faraj K.A., van Kuppevelt T.H., Daamen W.F. Construction of collagen scaffolds that mimic the three-dimensional architecture of specific tissues. *Tissue Eng* 2007; 13: 2387-94

Feinberg S.E., Aghaloo T.L., Cunningham Jr. L.L. Role of tissue engineering in oral and maxillofacial reconstruction: findings of the 2005 AAOMS Research Summit. *J Oral Maxillofac Surg* 2005; 63: 1418-25

Freyman T.M., Yannas I.V., Gibson L.J. Cellular materials as porous scaffolds for tissue engineering. *Progr Mater Sci* 2001; 46: 273-82

Gallico G.G. and O'Conner N.E. Engineering a skin replacement. *Tissue Eng* 1995; 1: 231-40

Garcia Y., Hemantkumar N., Collighan R., Griffin M., Rodriguez-Cabello J.C., Pandit A. In vitro characterization of a collagen scaffold enzymatically cross-linked with a tailored elastin-like polymer. *Tissue Eng Part A* 2009; 15: 887-99

Gibbs S. and Ponec M. Intrinsic regulation of differentiation markers in human epidermis, hard palate and buccal mucosa. *Arch Oral Biol* 2000; 45: 149-58

Girotti A., Reguera J., Arias F.J., Alonso M., Testera A.M., Rodríguez-Cabello J.C. Influence of the molecular weight on the inverse temperature transition of a model genetically engineered elastin-like pH-responsive polymer. *Macromolecules* 2004; 37: 3396-400

Glowacki J. and Mizuno S. Collagen scaffolds for tissue engineering. *Biopolymers* 2008; 89: 338-44

Grossman E.S. A histometric/scanning electron microscope study of normal and loaded oral epithelium of the vervet monkey. *J Anat* 1987; 154: 81-90

Gropper S.S, Smith J.L., Groff J.L. *Advanced Nutrition and Human Metabolism*. Wadsworth Publishing, 2009

Gunatillake P.A. and Adhikari R. Biodegradable synthetic polymers for tissue engineering. *Eur Cell Mater* 2003; 5: 1-16

Han I., Shim K.J., Kim J.Y., Im S.U., Sung Y.K., Kim M., Kang I.K., Kim J.C. Effect of poly(3-hydroxybutyrate-co-3-hydroxyvalerate) nanofiber matrices cocultured with hair follicular epithelial and dermal cells for biological wound dressing. *Artif Organs* 2007; 31: 801-8

Harley B.A., Leung J.H., Silva E.C., Gibson L.J. Mechanical characterization of collagen-glycosaminoglycan scaffolds. *Acta Biomater* 2007; 3: 463-74

Harley B.A., Kim H.D., Zaman M.H., Yannas I.V., Lauffenburger D.A., Gibson L.J. Microarchitecture of three-dimensional scaffolds influences cell migration behavior via junction interactions. *Biophys J* 2008; 95: 4013-24

Hayashida Y., Nishida K., Yamato M., Watanabe K., Maeda N., Watanabe H., et al. Ocular surface reconstruction using autologous rabbit oral mucosal epithelial sheets fabricated ex vivo on a temperature-responsive culture surface. *Invest Ophthalmol Vis Sci* 2005; 46: 1632-9

Hildebrand H.C., Hakkinen L., Wiebe C.B., Larjava H.S. Characterization of organotypic keratinocyte cultures on deepithelialized bovine tongue mucosa. *Histol Histopathol* 2002; 17: 151-63

Holle J. and Kunstfeld R. The influence of fibroblasts on the differentiation of cultured epithelial cells in vitro. *Plast Reconstr Surg* 2004; 114: 599

Huang L., McMillan R.A., Apkarian R.P., Pourdeyhimi B., Conticello V.P., Chaikof E.L. Generation of synthetic elastin-mimetic small diameter fibers and fiber networks. *Macromolecules* 2000; 33: 2989-97

Igarashi T., Shimmura S., Yoshida S., Tonogi M., Shinozaki N., Yamane G.Y. Isolation of oral epithelial progenitors using collagen IV. *Oral Dis* 2008; 14: 413-8

Iida T., Takami Y., Yamaguchi R., Shimazaki S., Harii K. Development of a tissue-engineered human oral mucosa equivalent based on an acellular allogeneic dermal matrix: a preliminary report of clinical application to burn wounds. *Scand J Plast Reconstr Surg Hand Surg* 2005; 39: 138-46

Imaizumi F., Asahina I., Moriyama T., Ishii M., Omura K. Cultured mucosal cell sheet with a double layer of keratinocytes and fibroblasts on a collagen membrane. *Tissue Eng* 2004; 10: 657-64

Inatomi T., Nakamura T., Koizumi N., Sotozono C., Kinoshita S. Current progress and challenges in ocular surface reconstruction using cultivated epithelial sheet transplantation. *Med J Malaysia* 2008; 63: Suppl A:42

Izumi K., Takacs G., Terashi H., Feinberg S.E. Ex vivo development of a composite human oral mucosal equivalent. *J Oral Maxillofac Surg* 1999; 57: 571-7; discussion 577-8

Izumi K., Terashi H., Marcelo C.L., Feinberg S.E. Development and characterization of a tissue-engineered human oral mucosa equivalent produced in a serum-free culture system. *J Dent Res* 2000; 79: 798-805

Izumi K., Feinberg S.E., Iida A., Yoshizawa M. Intraoral grafting of an ex vivo produced oral mucosa equivalent: a preliminary report. *Int J Oral Maxillofac Surg* 2003; 32: 188-97

Izumi K., Tobita T., Feinberg S.E. Isolation of human oral keratinocyte progenitor/stem cells. *J Dent Res* 2007; 86: 341-6

Faraj K.A., van Kuppevelt T.H., Daamen W.F. Construction of collagen scaffolds that mimic the three-dimensional architecture of specific tissues. *Tissue Eng* 2007; 13: 2387-94

Kim G. and Kim W. Highly porous 3D nanofiber scaffold using an electrospinning technique. *J Biomed Mater Res B Appl Biomater* 2007; 81: 104-10

Kinikoglu B., Auxenfans C., Pierrillas P., Justin V., Breton P., Burillon C., Hasirci V., Damour O. Reconstruction of a full-thickness collagen-based human oral mucosal equivalent. *Biomaterials* 2009; 30: 6418-25

Kwon O.S., Chung J.H., Cho K.H., Suh D.H., Park K.C., Kim K.H., Eun H.E. Nicotine-enhanced epithelial differentiation in reconstructed human oral mucosa in vitro. *Skin Pharmacol Appl Skin Physiol* 1999; 12: 227-34

Landay M.A. and Schroeder H.E. Quantitative electron microscope analysis of the keratinizing epithelium of normal human buccal mucosa. *Cell Tissue Res* 1977; 177: 383-405

Langdon J., Williams D.M., Navsaria H., Leigh I.M. Autologous keratinocyte grafting: a new technique for intra-oral reconstruction. *Br Dent J* 1991; 171: 87-90
Lauer G. *Fundamentals of tissue engineering and regenerative medicine*, Springer, Berlin Heidelberg (2009)

de Luca M., Albanese E., Megna M., Cancedda R., Mangiante P.E., Cadoni A., Franzi A.T. Evidence that human oral epithelium reconstituted in vitro and

transplanted onto patients with defects in the oral mucosa retains properties of the original donor site. *Transplantation* 1990; 50: 454-9

Luitaud C., Laflamme C., Semlali A., Saidi S., Grenier G., Zakrzewski A., et al. Development of an engineering autologous palatal mucosa-like tissue for potential clinical applications *J Biomed Mater Res B Appl Biomater* 2007; 83: 554-61

Mackenzie I.C. and Hill M.W. Connective tissue influences on patterns of epithelial architecture and keratinization in skin and oral mucosa of the adult mouse. *Cell Tissue Res* 1984; 235: 551-9

MacNeil S. Progress and opportunities for tissue-engineered skin. *Nature* 2007; 445: 874-80

Madaghiele M., Sannino A., Yannas I.V., Spector M. Collagen-based matrices with axially oriented pores. *J Biomed Mater Res Part A* 2008; 85A: 757-67

Martín L., Alonso M., Girotti A., Arias F.J., Rodríguez-Cabello J.C. Synthesis and characterization of macroporous thermosensitive hydrogels from recombinant elastin-like polymers. *Biomacromolecules* 2009; 10: 3015-22

Martínez-Osorio H., Juárez-Campo M., Diebold Y., Girotti A., Alonso M., Arias F.J., Rodríguez-Cabello J.C., García-Vázquez C., Calonge M. Genetically engineered elastin-like polymer as a substratum to culture cells from the ocular surface. *Curr Eye Res* 2009; 34: 48-56

Masuda I. An in vitro oral mucosal model reconstructed from human normal gingival cells. *Kokubyo Gakkai Zasshi* 1996; 63: 334-53 [article in Japanese]

Matthews J.A., Wnek G.E., Simpson D.G., Bowlin G.L. Electrospinning of collagen nanofibers. *Biomacromolecules* 2002; 3: 232-8

Mcpherson D.T., Morrow C., Minehan D.S., Wu J.G., Hunter E., Urry D.W. Production and purification of a recombinant elastomeric polypeptide, G-(VPGVG)₁₉-VPGV, from *Escherichia coli*. *Biotechnol Prog* 1992; 8: 347-52

Merne M. and Syrjänen S. The mesenchymal substrate influences the epithelial phenotype in a three-dimensional cell culture. *Arch Dermatol Res* 2003; 295: 190-8

Moharamzadeh K., Brook I.M., van Noort R., Scutt A.M., Thornhill M.H. Tissue-engineered oral mucosa: a review of the scientific literature. *J Dent Res* 2007; 86: 115-24

Moharamzadeh K., Brook I.M., Van Noort R., Scutt A.M., Smith K.G., Thornhill M.H. Development, optimization and characterization of a full-thickness tissue engineered human oral mucosal model for biological assessment of dental biomaterials. *J Mater Sci Mater Med* 2008; 19: 1793-801

Moll R., Divo M., Langbein L. The human keratins: biology and pathology. *Histochem Cell Biol* 2008; 129: 705-33

Moriyama T., Asahina I., Ishii M., Oda M., Ishii Y., Enomoto S. Development of composite cultured oral mucosa utilizing collagen sponge matrix and contracted collagen gel: a preliminary study for clinical applications. *Tissue Eng* 2001; 7: 415-27

Mostefaoui Y., Claveau I., Ross G., Rouabhia M. Tissue structure, and IL-1beta, IL-8, and TNF-alpha secretions after contact by engineered human oral mucosa with dentifrices. *J Clin Periodontol* 2002; 29: 1035-41

Murakami D., Yamato M., Nishida K., Ohki T., Takagi R., Yang J., Namiki H., Okano T. Fabrication of transplantable human oral mucosal epithelial cell sheets using temperature-responsive culture inserts without feeder layer cells. *J Artif Organs* 2006; 9: 185-91

Nakamura T., Endo K., Cooper L.J., Fullwood N.J., Tanifuji N., Tsuzuki M., *et al.* The successful culture and autologous transplantation of rabbit oral mucosal epithelial cells on amniotic membrane. *Invest Ophthalmol Vis Sci* 2003; 44: 106-16

Nakanishi Y., Izumi K., Yoshizawa M., Saito C., Kawano Y., Maeda T. The expression and production of vascular endothelial growth factor in oral mucosa equivalents. *Int J Oral Maxillofac Surg* 2007; 36: 928-33

Navarro F.A., Mizuno S., Huertas J.C., Glowacki J., Orgill D.P. Perfusion of medium improves growth of human oral neomucosal tissue constructs. *Wound Repair Regen* 2001; 9: 507-12

Nettles D.L., Haider M.A., Chilkoti A., Setton L.A. Neural network analysis identifies scaffold properties necessary for in vitro chondrogenesis in elastin-like polypeptide biopolymer scaffolds. *Tissue Eng Part A* 2010; 16: 11-20

Niessen C.M. Tight junctions/adherens junctions: basic structure and function. *J Invest Dermatol* 2007; 127: 2525-32

Nisbet D.R., Forsythe J.S., Shen W., Finkelstein D.I., Horne M.K. Review paper: a review of the cellular response on electrospun nanofibers for tissue engineering. *J Biomater Appl* 2009; 24: 7-29

Noh H.K., Lee S.W., Kim J.M., Oh J.E., Kim K.H., Chung C.P., Choi S.C., Park W.H., Min B.M. Electrospinning of chitin nanofibers: degradation behavior and cellular response to normal human keratinocytes and fibroblasts. *Biomaterials* 2006; 27: 3934-44

Ohki T., Yamato M., Murakami D., Takagi R., Yang J., Namiki H., Okano T., Takasaki K. Treatment of oesophageal ulcerations using endoscopic transplantation of tissue-engineered autologous oral mucosal epithelial cell sheets in a canine model. *Gut* 2006; 55: 1704-10

Okano T., Yamada N., Sakai H., Sakurai Y. A novel recovery system for cultured cells using plasma-treated polystyrene dishes grafted with poly(N-isopropylacrylamide). *J Biomed Mater Res* 1993; 27: 1243-51

Ophof R., van Rheden R.E., Von den Hoffa J.W., Schalkwijk J., Kuijpers-Jagtman A.M. Oral keratinocytes cultured on dermal matrices form a mucosa-like tissue. *Biomaterials* 2002; 23: 3741-8

Ophof R., Maltha J.C., Kuijpers-Jagtman A.M., Von den Hoff J.W. Implantation of tissue-engineered mucosal substitutes in the dog palate. *Eur J Orthod* 2008; 30: 1-9

Ottani V., Franchi M., De Pasquale V., Leonardi L., Morocutti M., Ruggeri A. Collagen fibril arrangement and size distribution in monkey oral mucosa. *J Anat* 1998; 192: 321-8

Ozturk N., Girotti A., Kose G.T., Rodríguez-Cabello J.C., Hasirci V. Dynamic cell culturing and its application to micropatterned, elastin-like protein-modified poly(N-isopropylacrylamide) scaffolds. *Biomaterials* 2009; 30: 541726

Powell H.M., Supp D.M., Boyce S.T. Influence of electrospun collagen on wound contraction of engineered skin substitutes. *Biomaterials* 2008; 29: 834-43

Prockop D.J. and Kivirikko K.I. Collagens: molecular biology, diseases, and potentials for therapy. *Annu Rev Biochem* 1995; 64: 403-34

Raghoobar G.M., Tomson A.M., Scholma J., Blaauw E.H., Witjes M.J., Vissink A. Use of cultured mucosal grafts to cover defects caused by vestibuloplasty: an in vivo study. *J Oral Maxillofac Surg* 1995; 53: 872-8; discussion 878-9

Régnier M, Caron D, Reichert U, Schaefer H. Reconstructed human epidermis: a model to study in vitro the barrier function of the skin. *Skin Pharmacol* 1992; 5: 49-56

Rho K.S., Jeong L., Lee G., Seo B.M., Park Y.J., Hong S.D., Roh S., Cho J.J., Park W.H., Min B.M. Electrospinning of collagen nanofibers: effects on the behavior of normal human keratinocytes and early-stage wound healing. *Biomaterials* 2006; 27: 1452-61

Rodríguez-Cabello J.C., Prieto S., Reguera J., Arias F.J., Ribeiro A. Biofunctional design of elastin-like polymers for advanced applications in nanobiotechnology. *J Biomater Sci Polymer Edn* 2007; 18: 269-86

Rodríguez-Cabello J.C., Martín L., Alonso M., Arias F.J., Testera A.M. "Recombinamers" as advanced materials for the post-oil age. *Polymer* 2009; 50: 5159-69

Rouabhia M. and Deslauriers N. Production and characterization of an in vitro engineered human oral mucosa. *Biochem Cell Biol* 2002; 80: 189-95

Rowat J.S. and Squier C.A. Rates of epithelial cell proliferation in the oral mucosa and skin of the Tamarin Monkey (*Saguinus fuscicollis*). *J Dent Res* 1986; 65: 1326-31

Sahuc F., Nakazawa K., Berthod F., Collombel C., Damour O. Mesenchymal-epithelial interactions regulate gene expression of type VII collagen and kalinin in keratinocytes and dermal-epidermal junction formation in a skin equivalent model. *Wound Repair Regen* 1996; 4: 93-102

Schroeder H.E. Differentiation of human oral stratified epithelia, Karger, Basel (1981)

Schweizer J., Winter H., Hill M.W., Mackenzie I.C. The keratin polypeptide patterns in heterotypically recombined epithelia of skin and mucosa of adult mouse. *Differentiation* 1984; 26: 144-53

Shahabeddin L., Berthod F., Damour O., Collombel C. Characterization of skin reconstructed on a chitosan-cross-linked collagen-glycosaminoglycan matrix. *Skin Pharmacol* 1990; 3: 107-14

Sharpe P.M. and Ferguson M.W. Mesenchymal influences on epithelial differentiation in developing systems. *J Cell Sci Suppl* 1988; 10: 195-230

Shoulders M.D. and Raines R.T. Collagen structure and stability. *Annu Rev Biochem* 2009; 78: 929-58

Sonis S.T. The pathobiology of mucositis. *Nat Rev Cancer* 2004; 4: 277-84

Squier C.A. The permeability of oral mucosa. *Crit Rev Oral Biol Med* 1991; 2: 13-32

Squier C.A. and Kremer M.J. Biology of oral mucosa and esophagus. *J Natl Cancer Inst Monogr* 2001; 29: 7-15

Stephens P. and Genever P. Non-epithelial oral mucosal progenitor cell populations. *Oral Dis* 2007; 13: 1-10

Stewart K.J. A quantitative ultrastructural study of collagen fibrils in human skin, normal scars, and hypertrophic scars. *Clin Anat* 1995; 8: 334-8

Sundararaghavan H.G., Monteiro G.A., Lapin N.A., Chabal Y.J., Miksan J.R., Shreiber D.I. Genipin-induced changes in collagen gels: correlation of mechanical properties to fluorescence. *J Biomed Mater Res A* 2008; 87: 308-20

Susi F.R., Belt W.D., Kelly J.W. Fine structure of fibrillar complexes associated with the basement membrane in human oral mucosa. *J Cell Biol* 1967; 34: 686-90

Szpaderska A.M., Zuckerman J.D., DiPietro L.A. Differential injury responses in oral mucosal and cutaneous wounds. *J Dent Res* 2003; 82: 621-6

Tardif F., Goulet J.P., Zakrzewski A., Chauvin P., Rouabhia M. Involvement of interleukin-18 in the inflammatory response against oropharyngeal candidiasis. *Med Sci Monit* 2004; 10: 239-49

Tomakidi P., Breitzkreutz D., Fusenig N.E., Zöller J., Kohl A., Komposch G. Establishment of oral mucosa phenotype in vitro in correlation to epithelial anchorage. *Cell Tissue Res* 1998; 292: 355-66

Tunggal L., Ravaux J., Pesch M., Smola H., Krieg T., Gaill F., Sasaki T., Timpl R., Mauch C., Aumailley M. Defective laminin 5 processing in cylindroma cells. *Am J Pathol* 2002; 160: 459-68

Tuzlakoglu K. and Reis R.L. Biodegradable polymeric fiber structures in tissue engineering. *Tissue Eng Part B Rev* 2009; 15: 17-27

Ueda M. Formation of epithelial sheets by serially cultivated human mucosal cells and their applications as a graft material. *Nagoya J Med Sci* 1995; 58: 13-28

Ueda M., Tohnai I., Nakai H. Tissue engineering research in oral implant surgery. *Artif Organs* 2001; 25: 164-71

Urry D.W., Nicol A., Gowda D.C., Hoban L.D., McKee A., Williams T., Olsen D.B., Cox B.A. *Biotechnological Polymers: Medical, Pharmaceutical and Industrial Applications*, Technomic, Atlanta, GA (1993)

Urry D.W., Pattanaik A., Xu J., Woods T.C., McPherson D.T., Parker T.M. Elastic protein-based polymers in soft tissue augmentation and generation. In: *Polymers for tissue engineering*. Brill Academic Publishers, The Netherlands (1998)

Vrana N.E., Builles N., Justin V., Bednarz J., Pellegrini G., Ferrari B., Damour O., Hulmes D.J., Hasirci V. Development of a reconstructed cornea from collagen-chondroitin sulfate foams and human cell cultures. *Invest Ophthalmol Vis Sci* 2008; 49: 5325-31

Wassersug R.J. and Johnson R.K. A remarkable pyloric caecum in the evermannellid genus *Coccorella* with notes on gut structure and function in alepsisauroid fishes (Pisces, Myctophiformes). *J Zool* 1976; 179: 273-89

Weigel T., Schinkel G., Lendlein A. Design and preparation of polymeric scaffolds for tissue engineering. *Expert Rev Med Devices* 2006; 3: 835-51

Will J., Melcher R., Treul C., Travitzky N., Kneser U., Polykandriotis E., Horch R., Greil P. Porous ceramic bone scaffolds for vascularized bone tissue regeneration. *J Mater Sci Mater Med* 2008; 19: 2781-90

Winning T.A. and Townsend G.C. Oral mucosal embryology and histology. *Clin Dermatol* 2000; 18: 499-511

Xiong X., Zhao Y., Zhang W., Xie W., He S. In vitro engineering of a palatal mucosa equivalent with acellular porcine dermal matrix. *J Biomed Mater Res A* 2008; 86: 544-51

Yamada N., Okano T., Sakai H., Karikusa F., Sawasaki Y., Sakurai Y. Thermo-responsive polymeric surfaces; control of attachment and detachment of cultured cells. *Makromol Chem Rapid Commun* 1990; 11: 571-6

Yang X., Shah J.D., Wang H. Nanofiber enabled layer-by-layer approach toward three-dimensional tissue formation. *Tissue Eng Part A* 2009; 15: 945-56

Yang Y.J., Yamato M., Kohno C., Nishimoto A., Sekine H., Fukai F., Okano T. Cell sheet engineering: Recreating tissues without biodegradable scaffolds. *Biomaterials* 2005; 26: 6415-22

Yannas I.V., Lee E., Orgill D.P., Skrabut E.M., Murphy G.F. Synthesis and characterization of a model extracellular matrix that induces partial regeneration of adult mammalian skin. *Proc Natl Acad Sci USA* 1989; 86: 933-7

Yeo I.S., Oh J.E., Jeong L., Lee T.S., Lee S.J., Park W.H., Min B.M. Collagen-based biomimetic nanofibrous scaffolds: preparation and characterization of collagen/silk fibroin bicomponent nanofibrous structures. *Biomacromolecules* 2008; 9: 1106-16

Yoshizawa M., Feinberg S.E., Marcelo C.L., Elnar V.M. Ex vivo produced human conjunctiva and oral mucosa equivalents grown in a serum-free culture system. *J Oral Maxillofac Surg* 2004; 62: 980-8

Zhou Y., Yang D., Chen X., Xu Q., Lu F., Nie J. Electrospun water-soluble carboxyethyl chitosan/poly(vinyl alcohol) nanofibrous membrane as potential wound dressing for skin regeneration. *Biomacromolecules* 2008; 9: 349-54

Zhu X., Cui W., Li X., Jin Y. Electrospun fibrous mats with high porosity as potential scaffolds for skin tissue engineering. *Biomacromolecules* 2008; 9: 1795-801.

CURRICULUM VITAE

PERSONAL INFORMATION

Surname, Name: KINIKOGLU, F. Beste
Nationality: Turkish (TC)
Date and Place of Birth: 23 August 1979, Istanbul
Marital Status: Single
Phone: +33 4 72 11 07 04
Fax: +33 4 72 11 62 14
Email: bestekinik@yahoo.com

EDUCATION

Degree	Institution	Year of Graduation
MS	Bogazici University Chemical Engineering	2006
BS	METU Chemical Engineering	2003
High School/ Baccalauréat	Lycée Galatasaray	1998

TEACHING AND WORK EXPERIENCE

Enrollment	Place	Year
Teaching and Research Assistant	Bogazici Univ. Chemical Eng. Dept.	2004-2006
Intern Engineering Student	Lafarge	2001

HONORS AND FELLOWSHIPS

Ph.D. Fellowship of the French Government (2007-2010)
Ph.D. Fellowship of the Scientific and Technological Research Council of Turkey (TUBITAK) (2006-2010)
“Course Performance Award” by the Graduate School of Natural and Applied Sciences of METU (2008)
Graduated with High Honors from the Department of Chemical Engineering, METU (2003)

FOREIGN LANGUAGES

Fluent English, Fluent French, Intermediate Spanish

JOURNAL PUBLICATIONS

B. Kinikoglu, C. Auxenfans, P. Pierrillas, V. Justin, P. Breton, C. Burillon, V. Hasirci, O. Damour, Reconstruction of a full-thickness collagen-based human oral mucosal equivalent, *Biomaterials*, 30 (32): 6418-6425, 2009.

C. Auxenfans, J. Fradette, C. Lequeux, L. Germain, **B. Kinikoglu**, N. Bechetoille, F. Braye, F.A. Auger, O. Damour, Evolution of three dimensional skin equivalent models reconstructed in vitro by tissue engineering, *Eur J Dermatol*, 19 (2): 107-113, 2009.

C. Auxenfans, C. Lequeux, E. Perrusel, A. Mojallal, **B. Kinikoglu**, O. Damour, Adipose-derived stem cells (ASC) as a source of endothelial cells in the reconstruction of endothelialized skin equivalents, Submitted, 2010.

B. Kinikoglu, J.C. Rodriguez, O. Damour, V. Hasirci, A smart bilayer scaffold of elastin-like recombinamer and collagen for soft tissue engineering, Submitted, 2010.

B. Kinikoglu, M.R. Rovere, M. Haftek, V. Hasirci, O. Damour, Influence of the mesenchymal cell source on human oral epithelial development, Submitted, 2010.

B. Kinikoglu, J.C. Rodriguez, M. Haftek, O. Damour, V. Hasirci, Use of an elastin-like recombinamer in a nanofibrous bilayer scaffold for the reconstruction of full-thickness human oral mucosa , In preparation, 2010.